

# Curvature Sets Over Persistence Diagrams

Mario Gómez<sup>1</sup> and Facundo Mémoli<sup>2</sup>

<sup>1</sup>Department of Mathematics, The Ohio State University.,  
gomezflores.1@osu.edu

<sup>2</sup>Department of Mathematics and Department of Computer Science and  
Engineering, The Ohio State University., memoli@math.osu.edu

March 1, 2025

## Abstract

We study an invariant of compact metric spaces which combines the notion of *curvature sets* introduced by Gromov in the 1980s together with the notion of Vietoris-Rips *persistent homology*. For given integers  $k \geq 0$  and  $n \geq 1$  these invariants arise by considering the degree  $k$  Vietoris-Rips persistence diagrams of all subsets of a given metric space with cardinality at most  $n$ . We call these invariants *persistence sets* and denote them as  $\mathbf{D}_{n,k}^{\text{VR}}$ . We argue that computing these invariants could be significantly easier than computing the usual Vietoris-Rips persistence diagrams. We establish stability results as for these invariants and we also precisely characterize some of them in the case of spheres with geodesic and Euclidean distances. We identify a rich family of metric graphs for which  $\mathbf{D}_{4,1}^{\text{VR}}$  fully recovers their homotopy type. Along the way we prove some useful properties of Vietoris-Rips persistence diagrams.

## Contents

<b>1</b>	<b>Introduction</b>	<b>2</b>
1.1	Contributions . . . . .	6
1.2	Related work . . . . .	11
1.3	Acknowledgements . . . . .	11
<b>2</b>	<b>Background</b>	<b>12</b>
2.1	Metric geometry . . . . .	12
2.2	Metric measure spaces . . . . .	13
2.3	Simplicial complexes . . . . .	14
2.4	Persistent homology . . . . .	14
2.5	Stability . . . . .	16

<b>3</b>	<b>Curvature sets and Persistence diagrams</b>	<b>18</b>
3.1	$\mathfrak{F}$ -persistence sets . . . . .	20
3.2	$\mathfrak{F}$ -Persistence measures . . . . .	23
<b>4</b>	<b>VR-persistence sets</b>	<b>24</b>
4.1	Some properties of Vietoris-Rips complexes . . . . .	24
4.2	Computational examples . . . . .	30
<b>5</b>	<b>VR-Persistence sets of spheres</b>	<b>31</b>
5.1	Characterization of $t_b(X)$ and $t_d(X)$ for $X \subset \mathbb{S}^1$ . . . . .	32
5.2	Characterization of $\mathbf{D}_{2k+2,k}^{\text{VR}}(\mathbb{S}^1)$ for $k$ even . . . . .	34
5.3	Characterization of $\mathbf{D}_{2k+2,k}^{\text{VR}}(\mathbb{S}^1)$ for $k$ odd . . . . .	35
5.4	Characterization of $\mathbf{U}_{4,1}^{\text{VR}}(\mathbb{S}^1)$ . . . . .	38
5.5	Persistence sets of Ptolemaic spaces . . . . .	41
5.6	Persistence sets of the surface with constant curvature $\kappa$ . . . . .	43
5.7	Persistence sets of $\mathbb{S}^m$ for $m \geq 3$ . . . . .	47
<b>6</b>	<b>Concentration of persistence measures</b>	<b>51</b>
6.1	A concentration theorem . . . . .	52
<b>7</b>	<b>Coordinates</b>	<b>54</b>
<b>8</b>	<b>Persistence sets of metric graphs</b>	<b>55</b>
8.1	Split metric decompositions . . . . .	55
8.2	A family of metric graphs whose homotopy type can be characterized via $\mathbf{D}_{4,1}^{\text{VR}}$ . . . . .	60
<b>9</b>	<b>Discussion and Questions</b>	<b>68</b>

# 1 Introduction

The Gromov-Hausdorff (GH) distance, a notion of distance between compact metric spaces, was introduced by Gromov in the 1980s and was eventually adapted into data/shape analysis by the second author [Mém05, MS04, MS05] as a tool for measuring the dissimilarity between shapes/datasets.

Despite its usefulness in providing a mathematical model for shape matching procedures, [MS04, MS05, BBBK08], the Gromov-Hausdorff distance leads to NP-hard problems: [Mém12b] relates it to the well known Quadratic Assignment Problem, which is NP-hard, and Schmiedl in his PhD thesis [Sch17] (see also [AFN<sup>+</sup>18]) directly proves the NP-hardness of the computation of the Gromov-Hausdorff distance even for ultrametric spaces. Recent work has also identified certain Fixed Parameter Tractable algorithms for the GH distance between ultrametric spaces [MSW19].

These hardness results have motivated research in other directions:

- (I) finding suitable *relaxations* of the Gromov-Hausdorff distance which are more amenable to computations and
- (II) finding lower bounds for the Gromov-Hausdorff distance which are easier to compute, yet retain good discriminate power.

Related to the first thread, and based on ideas from optimal transport, the notion of Gromov-Wasserstein distance was proposed in [Mém07, Mém11]. This notion of distance leads to continuous quadratic optimization problems (as opposed to the combinatorial nature of the problems induced by the Gromov-Hausdorff distance) and, as such, it has benefited from the wealth of continuous optimization computational techniques that are available in the literature [PCS16, PC<sup>+</sup>19] and has seen a number of applications in data analysis and machine learning [VCF<sup>+</sup>20, DSS<sup>+</sup>20, AMJ18, KM21, BCM<sup>+</sup>20] in recent years.

The second thread mentioned above is that of obtaining computationally tractable lower bounds for the usual Gromov-Hausdorff distance. Several such lower bounds were identified in [Mém12b] by the second author, and then in [CM08, CM10a] and [CCSG<sup>+</sup>09] it was proved that hierarchical clustering dendrograms and *persistence diagrams* or *barcodes*, metric invariants which arose in the Applied Algebraic Topology community, provide a lower bound for the GH distance. These persistence diagrams will eventually become central to the present paper, but before reviewing them, we will describe the notion of *curvature sets* introduced by Gromov.

**Gromov’s curvature sets and curvature measures.** Given a compact metric space  $(X, d_X)$ , in the book [Gro07] Gromov identified a class of invariants of metric spaces indexed by the natural numbers that solves the classification problem for  $X$ . In more detail, Gromov defines for each  $n \in \mathbb{N}$ , the  $n$ -th *curvature set* of  $X$ , denoted by  $\mathbf{K}_n(X)$ , as the collection of all  $n \times n$  matrices that arise from restricting  $d_X$  to all possible  $n$ -tuples of points chosen from  $X$ , possibly with repetitions. The terminology curvature sets is justified by the observation that these sets contain, in particular, metric information about configurations of closely clustered points in a given metric space. This information is enough to recover the curvature of a manifold; see Figure 1.

These curvature sets have the property that  $\mathbf{K}_n(X) = \mathbf{K}_n(Y)$  for all  $n \in \mathbb{N}$  is equivalent to the statement that the compact metric spaces  $X$  and  $Y$  are isometric. Constructions similar to the curvature sets of Gromov were also identified by Peter Olver in [Olv01] in his study of invariants for curves and surfaces under different group actions (including the group of Euclidean isometries).

In [Mém12b] it is then noted that the GH distance admits lower bounds based on these curvature sets:

$$d_{\mathcal{GH}}(X, Y) \geq \widehat{d}_{\mathcal{GH}}(X, Y) := \frac{1}{2} \sup_{n \in \mathbb{N}} d_{\mathcal{H}}(\mathbf{K}_n(X), \mathbf{K}_n(Y)) \quad (1)$$

for all  $X, Y$  compact metric spaces. Here,  $d_{\mathcal{H}}$  denotes the Hausdorff distance on  $\mathbb{R}^{n \times n}$  with  $\ell^\infty$  distance. As we mentioned above, the computation of the Gromov-Hausdorff distance leads in general to NP-hard problems, whereas the lower bound in the equation above can

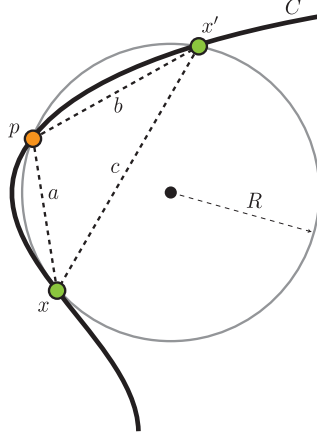


Figure 1: The curvature of a smooth curve  $C$  can be estimated as the inverse of the radius  $R$  of the circle passing through the points  $x, x'$  and  $p$ . By plane geometry results [COS<sup>+</sup>98, Theorem 2.3], this radius can be computed from the 3 interpoint distances  $a, b$ , and  $c$ , and hence from  $\mathbf{K}_3(C)$ , as  $R = R(a, b, c) = \frac{abc}{((a+b+c)(a+b-c)(a-b+c)(-a+b+c))^{1/2}}$ . In fact, Calabi et al. prove:  $R^{-1} = \kappa + \frac{1}{3}(b-a)\kappa_s + \dots$  where  $\kappa$  and  $\kappa_s$  are the curvature and its arc length derivative at the point  $p$ .

be computed in polynomial time when restricted to definite values of  $n$ . In [Mém12b] it is argued that work of Peter Olver [Olv01] and Boutin and Kemper [BK04a] leads to identifying rich classes of shapes where these lower bounds permit full discrimination.

In the category of compact mm-spaces, that is triples  $(X, d_X, \mu_X)$  where  $(X, d_X)$  is a compact metric space and  $\mu_X$  is a fully supported probability measure on  $X$ , Gromov also discusses the following parallel construction: for an mm-space  $(X, d_X, \mu_X)$  let

$$\Psi_X^{(n)} : X^{\times n} \longrightarrow \mathbb{R}^{n \times n}$$

be the map that sends the  $n$ -tuple  $(x_1, x_2, \dots, x_n)$  to the matrix  $M$  with elements  $M_{ij} = d_X(x_i, x_j)$ . Then, the  $n$ -th **curvature measure** of  $X$  is defined as

$$\mu_n(X) := \left( \Psi_X^{(n)} \right)_{\#} \mu_X^{\otimes n}.$$

Clearly, curvature measures and curvature sets are related as follows:  $\text{supp}(\mu_n(X)) = \mathbf{K}_n(X)$  for all  $n \in \mathbb{N}$ . Gromov then proves in his mm-reconstruction theorem that the collection of all curvature measures permit reconstructing any given mm-space up to isomorphism.

Similarly to (1), [MNO21] proves for each  $p \geq 1$  that

$$d_{\mathcal{G}\mathcal{W},p}(X, Y) \geq \widehat{d}_{\mathcal{G}\mathcal{W},p}(X, Y) := \frac{1}{2} \sup_{n \in \mathbb{N}} d_{\mathcal{W},p}(\mu_n(X), \mu_n(Y)), \quad (2)$$

where  $d_{\mathcal{W},p}$  denotes the  $p$ -Wasserstein distance [Vil03] on  $\mathcal{P}_1(\mathbb{R}^{n \times n})$  with  $\ell^\infty$  distance.

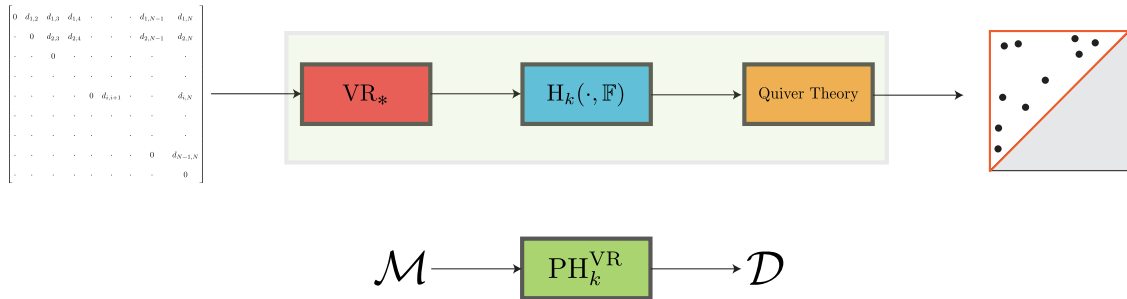


Figure 2: The pipeline to compute a persistence diagram. Starting with a distance matrix, we compute the Vietoris-Rips complex and its homology, and produce an interval decomposition. Together, we call these three steps  $PH_k^{VR}$ .

**Persistent Homology.** Ideas related to what is nowadays known as persistent homology appeared already in the late 1980s and early 1990s in the work of Patrizio Frosini [Fro90b, Fro99, Fro90a], then in the work of Vanessa Robins [Rob99], in the work of Edelsbrunner and collaborators [ELZ00], and then in the work of Carlsson and Zomorodian [ZC04]. Some excellent references for this topic are [EH10, Ghr08, Car14, Wei11].

In a nutshell, persistent homology (PH) assigns to a given compact metric space  $X$  and an integer  $k \geq 0$ , a multiset of points  $\text{dgm}_k^{VR}(X)$  in the plane, known as the  $k$ -th (Vietoris-Rips) *persistence diagram* of  $X$ . The standard PH pipeline is shown in Figure 2.

These diagrams indicate the presence of  $k$ -dimensional multi-scale topological features in the space  $X$ , and can be compared via the *bottleneck distance* (which is closely related to but is stronger than the Hausdorff distance in  $(\mathbb{R}^2, \ell^\infty)$ ).

Following work by Cohen-Steiner et al. [CSEH07], in [CCSG<sup>+</sup>09] it is proved that the maps  $X \mapsto \text{dgm}_k^{VR}(X)$  sending a given compact metric space to its  $k$ -th persistence diagrams is 2-Lipschitz under the GH and bottleneck distances.

Algorithmic work by Edelsbrunner and collaborators [ELZ00] and more recent developments [Bau19] guarantee that not only can  $\text{dgm}_k^{VR}(X)$  be computed in polynomial time (in the cardinality of  $X$ ) but also it is well known that the bottleneck distance can also be computed in polynomial time [EH10]. This means that persistence diagrams provide another source of stable invariants which would permit estimating (lower bounding) the Gromov-Hausdorff distance.

It is known that persistence diagrams are not full invariants of metric spaces. For instance, any two *tree metric spaces*, that is metric spaces satisfying the four point condition [Gro87], have trivial persistence diagrams in all degrees  $k \geq 1$ . It is also not difficult to find two finite tree metric spaces with the same degree zero persistence diagrams. See [LMO20] for more examples and [MZ19] for results about stronger invariants (i.e. *persistent homotopy groups*).

Despite the fact that persistence diagrams can be computed with effort which depends polynomially on the size of the input metric space [EH10, AW20], the computations are actually quite onerous and, as of today, it is not realistic to compute the degree 1 Vietoris-Rips persistence diagram of a finite metric space with more than a few thousand points even with state of the art implementations such as Ripser [Bau19].

**Curvature sets over persistence diagrams.** In this paper, we consider a version of the curvature set ideas which arises when combining their construction with Vietoris-Rips persistent homology.

For a compact metric space  $X$  and integers  $n \geq 1$  and  $k \geq 0$ , the  $(n, k)$ -Vietoris-Rips persistence set of  $X$  is (cf. Definition 3.9) the collection  $\mathbf{D}_{n,k}^{\text{VR}}(X)$  of all persistence diagrams in degree  $k$  of subsets of  $X$  with cardinality at most  $n$ .

In a manner similar to how the  $n$ -th curvature measure  $\mu_n(X)$  arose above, we also study the probability measure  $\mathbf{U}_{n,k}^{\text{VR}}(X)$  defined as the pushforward of  $\mu_n(X)$  under the degree  $k$  Vietoris-Rips persistence diagram map (cf. Definition 3.16). We also study a more general version wherein for any *stable* simplicial filtration functor  $\mathfrak{F}$  (cf. Definition 2.22), we consider both the persistence sets  $\mathbf{D}_{n,k}^{\mathfrak{F}}(X)$  and the persistence measures  $\mathbf{U}_{n,k}^{\mathfrak{F}}(X)$ .

## 1.1 Contributions

We provide a thorough study of persistence sets and in particular analyze the following points.

**Computational cost, parallelizability, and approximation:** One argument for considering the persistent set invariants  $\mathbf{D}_{n,k}^{\text{VR}}(X)$  as opposed to the standard degree  $k$  Vietoris-Rips persistence diagrams  $\text{dgm}_k(X)$  is that while computing the latter incurs cost  $O(|X|^{3(k+2)})$  in the worst case, computing the former incurs cost  $O(n^{3(k+2)}|X|^n)$ , which is in general (when  $n \ll |X|$ ) not only significantly smaller but also the associated computational tasks are eminently parallelizable. Furthermore, the amount of memory needed for computing persistent sets is also notably smaller than for computing persistence diagrams over the same data set. See Remark 3.15 for a detailed discussion. In fact, persistent sets are useful as an alternative paradigm for the acceleration of the computation of persistent homology based invariants; cf. Figure 3.

**Principal persistence sets, their characterization and an algorithm:** Persistence sets are defined to be sets of persistence diagrams and, although a single persistence diagram is easy to visualize, large collections of them might not be so. However, when there is a certain relation between  $n$  and  $k$  we verify in Theorem 4.4 that there can be at most one point in the degree  $k$  persistence diagram of any metric space with at most  $n$  points. This means that all persistence diagrams in the *principal persistence set*  $\mathbf{D}_{2k+2,k}^{\text{VR}}(X)$  can be *stacked* on the same axis; see Figure 4.

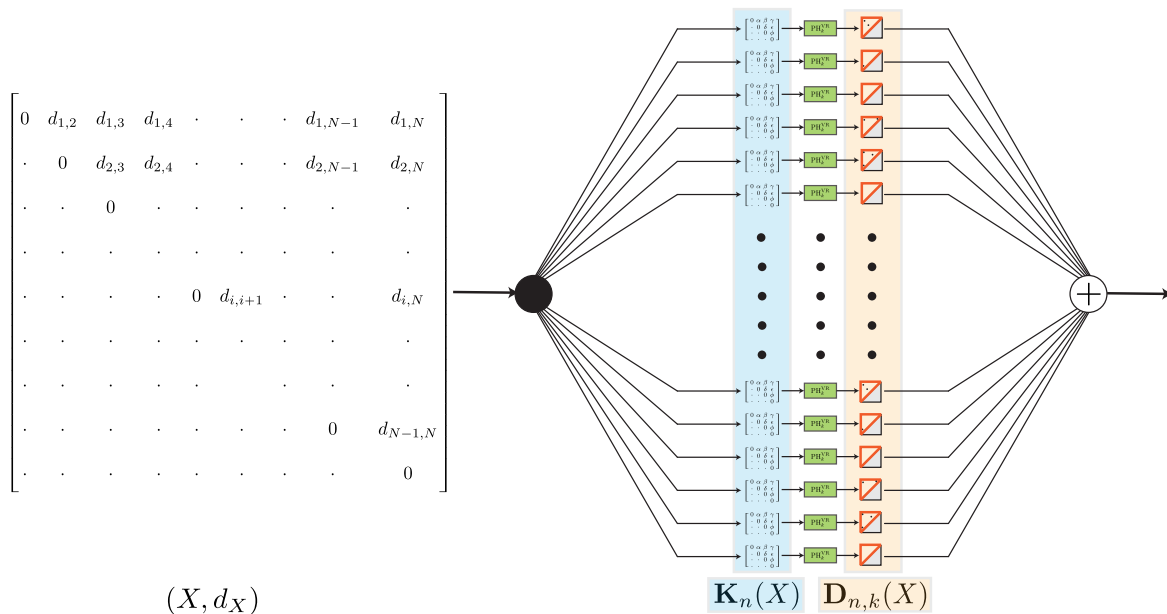


Figure 3: The pipeline to compute  $\mathbf{D}_{n,k}$ . Starting with a metric space  $(X, d_X)$ , we take samples of the distance matrix as elements of  $\mathbf{K}_n(X)$ , apply  $\text{PH}_k$  to each, and aggregate the resulting persistence diagrams. For example, Theorem 4.4 guarantees that the VR-persistence diagram in dimension  $k$  of a metric space with  $n = 2k + 2$  points only has one point. The aggregation in this case means plotting the set  $\mathbf{D}_{n,k}^{\text{VR}}(X)$  by plotting all diagrams simultaneously in one set of axes. In general, the diagrams in  $\mathbf{D}_{n,k}(X)$  have more than 1 point, so one possibility for aggregation is constructing a one-point summary or an average of a persistence diagram (for instance, a Chebyshev center or an  $\ell_\infty$  mean) and then plotting all such points simultaneously.

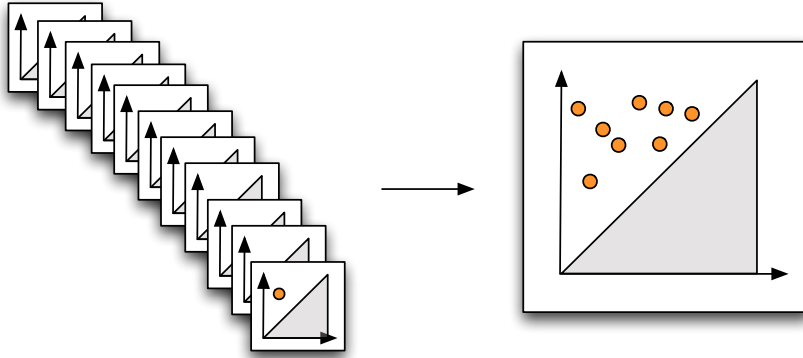


Figure 4: A graphical representation of the principal persistent sets  $\mathbf{D}_{2k+2,k}^{\text{VR}}(X)$  is obtained by overlaying the persistence diagrams of all samples  $Y \subset X$  (with  $|Y| \leq 2k + 2$ ) into *single* set of axes. This is made possible since by Theorem 4.4 these diagrams have at most one off diagonal point.

Our main result, Theorem 4.4 furthermore gives a precise representation of the unique point in the degree  $k$  persistence diagram of a metric space with at most  $n_k := 2k + 2$  points via a formula which induces an algorithm for computing the principal persistence sets. This algorithm is purely geometric in the sense that it does not rely on analyzing boundary matrices but, in contrast, directly operates at the level of distance matrices. For any  $k$ , this geometric algorithm has cost  $O(n_k^2) \approx O(k^2)$  as opposed to the much larger cost  $O(n_k^{3(k+2)}) \approx O(2^{3k} k^{3(k+2)})$  incurred by the standard persistent homology algorithms; see Remark 4.6.

**Characterization results.** We fully characterize the principal persistence sets  $\mathbf{D}_{2k+2,k}^{\text{VR}}(\mathbb{S}^1)$ . In particular, these results prove that  $\mathbf{D}_{4,1}^{\text{VR}}(\mathbb{S}^1)$  coincides with the triangle in  $\mathbb{R}^2$  with vertices  $(\frac{2\pi}{3}, \frac{2\pi}{3})$ ,  $(\frac{\pi}{2}, \pi)$ , and  $(\pi, \pi)$ ; see Figure 5. We also characterize the persistence measure  $\mathbf{U}_{4,1}^{\text{VR}}(\mathbb{S}^1)$ , which are supported on  $\mathbf{D}_{4,1}^{\text{VR}}(\mathbb{S}^1)$ , in Proposition 5.8. We show that  $\mathbf{U}_{4,1}^{\text{VR}}(\mathbb{S}^1)$  has probability density function  $f(t_b, t_d) = \frac{12}{\pi^3}(\pi - t_d)$ , for any  $(t_b, t_d)$  in the triangular region specified in Figure 5.

Propositions 5.13 and 5.17, and Corollary 5.18 provide additional information about higher dimensional spheres. Section 4.2 provides some computational examples including the case of tori.

Our characterization results are in the same spirit as results pioneered by Adamaszek and Adams related to characterizing the Vietoris-Rips persistence diagrams of circles and spheres [AA17]; see also [LMO20].

Additionally, the arguments used to characterize the Persistence Set of the sphere can be generalized to other surfaces. More precisely, we obtained:

**Theorem 5.16.** *Let  $M_\kappa$  be the 2-dimensional model space with constant sectional curvature  $\kappa$ . Then:*

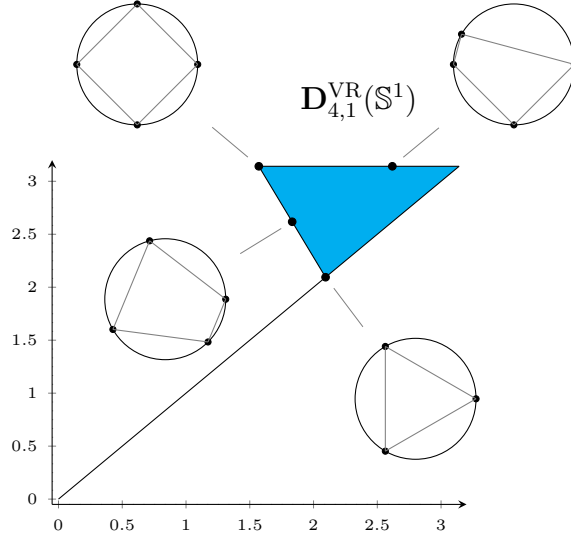


Figure 5: **Characterization of  $\mathbf{D}_{4,1}^{\text{VR}}(\mathbb{S}^1)$** : The  $(4, 1)$ -persistence set of  $\mathbb{S}^1$  (with geodesic distance) is the shaded triangular area where the top left and top right points have coordinates  $(\frac{\pi}{2}, \pi)$  and  $(\pi, \pi)$ , respectively, whereas the lowest diagonal point has coordinates  $(\frac{2\pi}{3}, \frac{2\pi}{3})$ . The figure also shows exemplary configurations  $X \subset \mathbb{S}^1$  with  $|X| \leq 4$  together with their respective persistence diagrams inside of  $\mathbf{D}_{4,1}^{\text{VR}}(\mathbb{S}^1)$ .

- If  $\kappa > 0$ ,  $\mathbf{D}_{4,1}^{\text{VR}}(M_\kappa) = \left\{ (t_b, t_d) \mid \sin\left(\frac{\sqrt{\kappa}}{2}t_d\right) \leq \sqrt{2} \sin\left(\frac{\sqrt{\kappa}}{2}t_b\right) \text{ and } 0 < t_b < t_d \leq \frac{\pi}{\sqrt{\kappa}} \right\}$ .
- If  $\kappa = 0$ ,  $\mathbf{D}_{4,1}^{\text{VR}}(M_0) = \left\{ (t_b, t_d) \mid 0 \leq t_b < t_d \leq \sqrt{2}t_b \right\}$ .
- If  $\kappa < 0$ ,  $\mathbf{D}_{4,1}^{\text{VR}}(M_\kappa) = \left\{ (t_b, t_d) \mid \sinh\left(\frac{\sqrt{-\kappa}}{2}t_d\right) \leq \sqrt{2} \sinh\left(\frac{\sqrt{-\kappa}}{2}t_b\right) \text{ and } 0 < t_b < t_d \right\}$ .

A similar result first appeared in [BHPW20]. The authors explore the question of whether persistent homology can detect the curvature of the ambient  $M_\kappa$ . They found a geometric formula to compute  $\text{dgm}_1^{\check{\text{Cech}}}(T)$  of a sample  $T \subset M_\kappa$  with *three* points, much in the same vein as our Theorem 4.4. They used it to find the logarithmic persistence  $P_a(\kappa) = t_d(T_{\kappa,a})/t_b(T_{\kappa,a})$  for an equilateral triangle  $T_{\kappa,a}$  of fixed side length  $a > 0$ , and proved that  $P_a$ , when viewed as a function of  $\kappa$ , is invertible.

The present Theorem 5.16 is in the same spirit. Instead of equilateral triangles, we can use squares with a given  $t_d$  and minimal  $t_b$  to find  $\kappa$ . Qualitatively, we can detect the sign of the curvature by looking at the boundary of  $\mathbf{D}_{4,1}^{\text{VR}}(M_\kappa)$ : it is concave up when  $\kappa > 0$ , a straight line when  $\kappa = 0$ , and concave down when  $\kappa < 0$ . See Figure 14.

Unlike us, they also detected curvature experimentally. They sampled 1000 points from a unit disk in  $M_\kappa$  and were able to approximate  $\kappa$  using the average VR death vectors in dimension 0 and average persistence landscapes in dimension 1 of 100 such samples. For example, one method consisted in finding a collection of landscapes  $L_\kappa$  labeled with a known curvature  $\kappa$ , and estimating  $\kappa_*$  for an unlabeled  $L_*$  with the average curvature of the three

nearest neighbors of  $L_*$ . They were also able to approximate  $\kappa_*$  without labeled examples by using PCA. See their paper [BHPW20] for more details.

The key ingredient in the proof of Theorem 5.16 is Ptolemy's inequality and its analogues in non-Euclidean geometries [Val70a, Val70b]. We generalize these inequalities to  $\text{CAT}(\kappa)$  spaces, albeit with some constraints when  $\kappa > 0$ . In contrast, when  $\kappa \leq 0$ , we show that the persistence set  $\mathbf{D}_{4,1}^{\text{VR}}(X)$  of a  $\text{CAT}(\kappa)$  space is contained in the persistence set  $\mathbf{D}_{4,1}^{\text{VR}}$  of the corresponding model space  $M_\kappa$ .

**Stability.** We establish the stability of persistence sets and measures under Gromov-Hausdorff and Gromov-Wasserstein distances in Theorems 3.12 and 3.17. Such results permit estimating these distances in polynomial time. As an application, we show that the Gromov-Hausdorff distance between  $\mathbb{S}^1$  and  $\mathbb{S}^m$  is bounded below by  $\frac{\pi}{15}$  when  $m = 2$  (Example 5.19) and by  $\frac{\pi}{8}$  when  $m \geq 3$  (Example 5.20). These bounds are not tight; it is known that  $d_{\mathcal{GH}}(\mathbb{S}^1, \mathbb{S}^2) = \frac{\pi}{3}$  and  $d_{\mathcal{GH}}(\mathbb{S}^1, \mathbb{S}^m) \geq \frac{1}{2} \arccos\left(\frac{-1}{m+1}\right) \geq \frac{\pi}{4}$  for  $m \geq 3$  (see [LMS21]).

**Concentration results for  $\mathbf{U}_{n,k}^{\text{VR}}$ .** Another consequence of the stability of persistence measures is the concentration of  $\mathbf{U}_{n,k}^{\mathfrak{F}}(X)$  as  $n \rightarrow \infty$ . More precisely,

**Theorem 6.3.** *Let  $(X, d_X, \mu_X)$  be an  $mm$ -space and take any stable filtration functor  $\mathfrak{F}$ . For any  $n, k \in \mathbb{N}$ , consider the random variable  $\mathbb{D}$  valued in  $\mathbf{D}_{n,k}^{\mathfrak{F}}(X)$  distributed according to  $\mathbf{U}_{n,k}^{\mathfrak{F}}(X)$ . Then:*

- For any  $\varepsilon > 0$ ,  $E_{\mathbf{U}_{n,k}^{\mathfrak{F}}(X)} [d_{\mathcal{B}}(\mathbb{D}, \text{dgm}_k^{\mathfrak{F}}(X))] < \text{diam}(X) \cdot C_X(n, \varepsilon) + \varepsilon$ .
- As a consequence, the  $mm$ -space  $\mathfrak{D}_{n,k}^{\mathfrak{F}}(X) = (\mathbf{D}_{n,k}^{\mathfrak{F}}(X), d_{\mathcal{B}}, \mathbf{U}_{n,k}^{\mathfrak{F}}(X))$  concentrates to a one-point  $mm$ -space as  $n \rightarrow \infty$ .

Similar results appear in [BGMP12] [CFL<sup>+</sup>15]. The approach in [CFL<sup>+</sup>15] is studying the average persistence landscape  $\overline{\lambda}_n^m$  of  $n$  samples  $S_1^m, \dots, S_n^m \subset X$  of size  $m$ . They show that this procedure is stable under perturbations of the Gromov-Wasserstein distance, and provide a bound on the expected  $\ell_\infty$  distance between the persistence landscape of  $X$  and  $\overline{\lambda}_n^m$ . These two results are analogous, respectively, to our Theorem 3.17 and to item 1 of 6.3 above. As for [BGMP12], the authors study the statistical robustness of persistent homology invariants. They have two results similar to ours. One is the stability of the measures  $\mathbf{U}_{n,k}^{\mathfrak{F}}(X)$  (they write  $\Phi_k^n(X)$  instead) under the Gromov-Prokhorov distance (instead of the Gromov-Hausdorff distance). Their second is a central limit theorem, where the measures  $\mathbf{U}_{n,k}^{\mathfrak{F}}(S_i)$  corresponding to an increasing sequence of finite samples  $S_1 \subset S_2 \subset \dots \subset X$  converge in probability to  $\mathbf{U}_{n,k}^{\mathfrak{F}}(X)$ .

**Persistence sets and measures capture more information than  $\text{dgm}_k^{\text{VR}}$ .** Evidently,  $\text{dgm}_k^{\mathfrak{F}}(X) \in \mathbf{D}_{n,k}^{\mathfrak{F}}(X)$  when  $n \geq |X|$ . What is interesting is that persistence sets can detect more information than the Vietoris-Rips persistent diagram. See Example 8.5 where  $G$  is a graph that consists of a cycle  $C$  with 4 edges attached such that  $\mathbf{D}_{4,1}^{\text{VR}}(G)$  contains more points than  $\mathbf{D}_{4,1}^{\text{VR}}(C)$ . As far as the Vietoris-Rips complex is concerned, though,  $\text{VR}_r(G) \simeq \text{VR}_r(C)$ .

**An application to detecting homotopy type of graphs:** In Section 8, as an application, we study a class of metric graphs for which  $\mathbf{D}_{4,1}^{\text{VR}}$ , a rather coarse invariant which is fairly easy to estimate and compute in practice, is able to characterize the homotopy type of graphs in this class. In fact,  $\mathbf{D}_{4,1}^{\text{VR}}$  detects more features than the Vietoris-Rips persistence diagram of  $G$ . See Figure 19 for an example. There,  $G$  is a cycle  $C$  with 4 edges attached and  $\mathbf{D}_{4,1}^{\text{VR}}(G)$  is different from  $\mathbf{D}_{4,1}^{\text{VR}}(C)$ . In contrast, the Vietoris-Rips complex of both graphs are homotopy equivalent.

## 1.2 Related work

The measures  $\mathbf{U}_{n,k}^{\text{VR}}$  first appeared in a paper in the work by Blumberg et al. [BGMP12] in 2012 and then in print in [BGMP14]. These measures were also exploited a couple years later by Chazal et al. in the articles [CFL<sup>+</sup>14, CFL<sup>+</sup>15] in order to devise bootstrapping methods for the estimation of persistence diagrams.

The connection to Gromov’s curvature sets and measures was not mentioned in either of these two papers. [Mém12b] studied curvature sets and their role in shape comparison and, as a natural follow up, some results regarding the persistence sets  $\mathbf{D}_{n,k}^{\text{VR}}$  and the measures  $\mathbf{U}_{n,k}^{\text{VR}}$  (as well as the more general objects  $\mathbf{D}_{n,k}^{\delta}$  and  $\mathbf{U}_{n,k}^{\delta}$ ) were first described Banff in 2012 during a conference [Mém12a] by the second author. Then, subsequent developments were described in 2013 at ACAT 2013 in Bremen [Mém13a] and Bedlewo [Mém13b], and then at IMA [Mém14a] and at SAMSI in 2014 [Mém14b]. In these presentations the second author proposed the invariants  $\mathbf{D}_{n,k}^{\text{VR}}$  as a Gromov-Hausdorff stable computationally easier alternative to the usual Vietoris-Rips persistence diagrams of metric spaces [Mém14c].

In January 2021 Bendich, et al. uploaded a paper to the arXiv [SWB21] with some ideas related to our construction of  $\mathbf{D}_{n,k}^{\delta}$ . The authors pose questions about the discriminative power of a certain labeled version of the persistent sets  $\mathbf{D}_{n,k}^{\text{VR}}$  (even though they do not call them that) and also mention some stability and computational properties similar to those mentioned in [Mém12a, Mém13a, Mém14a, Mém14b].

The second author together with Needham [MN18] has recently explored the classificatory power of  $\mu_2$  as well as that of certain *localizations* of  $\mu_2$ . In [CCM<sup>+</sup>20] the authors identify novel classes of simplicial filtrations arising from curvature sets together with suitable notions of locality. Ongoing work is exploring the classificatory power of  $\mu_n$  for general  $n$  [MNO21].

In terms of data intensive applications, the neuroscience paper [SMI<sup>+</sup>08] made use of ideas related to  $\mathbf{U}_{n,k}^{\text{VR}}$  and  $\mathbf{D}_{n,k}^{\text{VR}}$  in the context of analysis of neuroscience data.

## 1.3 Acknowledgements

We thank Henry Adams for bringing his paper [AA17] to our attention. The ideas contained therein were helpful in proving some of the results of Section 5.3.

We acknowledge funding from these sources: NSF AF 1526513, NSF DMS 1723003, NSF CCF 1740761, and and NSF CCF 1839358.

## 2 Background

For us,  $\mathcal{M}$  and  $\mathcal{M}^{\text{fin}}$  will denote, respectively, the category of compact and finite metric spaces. The morphisms in both categories will be 1-Lipschitz maps, that is, functions  $\varphi : X \rightarrow Y$  such that  $d_Y(\varphi(x), \varphi(x')) \leq d_X(x, x')$  for all  $(X, d_X), (Y, d_Y)$  in  $\mathcal{M}$  or  $\mathcal{M}^{\text{fin}}$ . We say that two metric spaces are isometric if there exists a surjective isometry  $\varphi : X \rightarrow Y$ , *i.e.* a map such that  $d_Y(\varphi(x), \varphi(x')) = d_X(x, x')$  for all  $x, x' \in X$ .

### 2.1 Metric geometry

In this section, we define the tools that we'll use to quantitatively compare metric spaces [BBI01].

**Definition 2.1.** For any subset  $A$  of a metric space  $X$ , its *diameter* is  $\mathbf{diam}_X(A) := \sup_{a, a' \in A} d_X(a, a')$ , and its *radius* is  $\mathbf{rad}_X(A) := \inf_{p \in X} \sup_{a \in A} d_X(p, a)$ . Note that  $\mathbf{rad}_X(A) \leq \mathbf{diam}_X(A)$ . The *separation* of  $X$  is  $\mathbf{sep}(X) := \inf_{x \neq x'} d_X(x, x')$ .

**Definition 2.2** (Hausdorff distance). Let  $A, B$  be subsets of a compact metric space  $(X, d_X)$ . The *Hausdorff distance* between  $A$  and  $B$  is defined as

$$d_{\mathcal{H}}^X(A, B) := \inf \{ \varepsilon > 0 \mid A \subset B^\varepsilon \text{ and } B \subset A^\varepsilon \},$$

where  $A^\varepsilon := \{x \in X \mid \inf_{a \in A} d_X(x, a) < \varepsilon\}$  is the  $\varepsilon$ -thickening of  $A$ . It is known that  $d_{\mathcal{H}}^X(A, B) = 0$  if, and only if their closures are equal:  $\bar{A} = \bar{B}$ .

We will use an alternative definition that is useful for calculations, but is not standard in the literature. It relies on the concept of a correspondence.

**Definition 2.3.** A *correspondence* between two sets  $X$  and  $Y$  is a set  $R \subset X \times Y$  such that  $\pi_1(R) = X$  and  $\pi_2(R) = Y$ , where  $\pi_i$  are projections. We will denote the set of all correspondences between  $X$  and  $Y$  as  $\mathcal{R}(X, Y)$ .

**Definition 2.4** (Proposition 2.1 of [Mém11]). For any compact metric space  $(X, d_X)$  and any  $A, B \subset X$  closed,

$$d_{\mathcal{H}}^X(A, B) := \inf_{R \in \mathcal{R}(A, B)} \sup_{(a, b) \in R} d_X(a, b).$$

The standard method for comparing two metric spaces is a generalization of the Hausdorff distance.

**Definition 2.5.** For any correspondence  $R$  between  $(X, d_X), (Y, d_Y) \in \mathcal{M}$ , we define its *distortion* as

$$\text{dis}(R) := \max \{ |d_X(x, x') - d_Y(y, y')| : (x, y), (x', y') \in R \}.$$

Then the *Gromov-Hausdorff distance* between  $X$  and  $Y$  is defined as

$$d_{\mathcal{GH}}(X, Y) := \frac{1}{2} \inf_{R \in \mathcal{R}(X, Y)} \text{dis}(R).$$

## 2.2 Metric measure spaces

To model the situation in which points are endowed with a notion of weight (signaling their trustworthiness), we will also consider finite metric spaces enriched with probability measures [Mém11]. Recall that the *support*  $\text{supp}(\nu)$  of a Borel measure  $\nu$  defined on a topological space  $Z$  is defined as the minimal closed set  $Z_0$  such that  $\nu(Z \setminus Z_0) = 0$ . If  $\varphi : Z \rightarrow X$  is a measurable map from a measure space  $(Z, \Sigma_Z, \nu)$  into the measurable space  $(X, \Sigma_X)$ , then the *pushforward measure* of  $\nu$  induced by  $\varphi$  is the measure  $\varphi_{\#}\nu$  on  $X$  defined by  $\varphi_{\#}\nu(A) = \nu(\varphi^{-1}(A))$  for all  $A \in \Sigma_X$ .

**Definition 2.6.** A *metric measure space* is a triple  $(X, d_X, \mu_X)$  where  $(X, d_X)$  is a compact metric space and  $\mu_X$  is a Borel probability measure on  $X$  with full support, *i.e.*  $\text{supp}(\mu) = X$ . Two mm-spaces  $(X, d_X, \mu_X)$  and  $(Y, d_Y, \mu_Y)$  are isomorphic if there exists an isometry  $\varphi : X \rightarrow Y$  such that  $\varphi_{\#}\mu_X = \mu_Y$ . We define the category of mm-spaces  $\mathcal{M}^w$ , where the objects are mm-spaces and the morphisms are 1-Lipschitz maps  $\varphi : X \rightarrow Y$  such that  $\varphi_{\#}\mu_X = \mu_Y$ .

Many tools in metric geometry have been adapted to study mm-spaces. Our first step is the following definition.

**Definition 2.7.** Given two measure spaces  $(X, \Sigma_X, \mu_X)$  and  $(Y, \Sigma_Y, \mu_Y)$ , a *coupling* between  $\mu_X$  and  $\mu_Y$  is a measure  $\mu$  on  $X \times Y$  such that  $\mu(A \times Y) = \mu_X(A)$  and  $\mu(X \times B) = \mu_Y(B)$  for all measurable  $A \in \Sigma_X$  and  $B \in \Sigma_Y$  (in other words,  $(\pi_1)_{\#}\mu = \mu_X$  and  $(\pi_2)_{\#}\mu = \mu_Y$ ). We denote the set of couplings between  $\mu_X$  and  $\mu_Y$  as  $\mathcal{M}(\mu_X, \mu_Y)$ .

**Remark 2.8** (The support of a coupling is a correspondence). Notice that, since  $\mu_X$  is fully supported and  $X$  is finite, then  $\mu(\pi_1^{-1}(x)) = \mu_X(\{x\}) \neq 0$  for any fixed coupling  $\mu \in \mathcal{M}(\mu_X, \mu_Y)$ . Thus, the set  $\pi_1^{-1}(x) \cap \text{supp}(\mu)$  is non-empty for every  $x \in X$ . The same argument on  $Y$  shows that  $\text{supp}(\mu)$  is a correspondence between  $X$  and  $Y$ . In that regard, couplings are a probabilistic version of correspondences.

There is also a version of the diameter that considers the measure. The *p-diameter* of a subset  $A$  of an mm-space  $X$  is defined as

$$\mathbf{diam}_{X,p}(A) := \left( \iint_{A \times A} (d_X(a, a'))^p \mu_X(a) \mu_X(a') \right)^{1/p}$$

for  $1 \leq p < \infty$ , and set  $\mathbf{diam}_{X,\infty}(A) := \mathbf{diam}_X(A)$ . We use these concepts to define a probabilistic version of the Hausdorff distance.

**Definition 2.9.** Given two probability measures  $\alpha, \beta$  on  $(Z, d_Z)$  and  $p \geq 1$ , the *Wasserstein distance* of order  $p$  is defined as [Vil03]:

$$d_{\mathcal{W},p}^Z(\alpha, \beta) := \inf_{\mu \in \mathcal{M}(\alpha, \beta)} \mathbf{diam}_{Z,p}(\text{supp}(\mu)).$$

In the same spirit, there is a generalization of Gromov-Hausdorff.

**Definition 2.10.** Given two mm-spaces  $(X, d_X, \mu_X)$  and  $(Y, d_Y, \mu_Y)$ ,  $p \geq 1$ , and  $\mu \in \mathcal{M}(\mu_X, \mu_Y)$ , we define the  $p$ -distortion of  $\mu$  as:

$$\text{dis}_p(\mu) := \left( \iint |d_X(x, x') - d_Y(y, y')|^p \mu(dx \times dy) \mu(dx' \times dy') \right)^{1/p}.$$

For  $p = \infty$  we set

$$\text{dis}_\infty(\mu) := \text{dis}(\text{supp}(\mu)).$$

Then the *Gromov-Wasserstein distance* of order  $p \in [1, \infty]$  between  $X$  and  $Y$  is defined as [Mém11]:

$$d_{\mathcal{GW}, p}(X, Y) := \frac{1}{2} \inf_{\mu \in \mathcal{M}(\mu_X, \mu_Y)} \text{dis}_p(\mu). \quad (3)$$

**Remark 2.11.** It turns out that, for each  $p \in [1, \infty]$ ,  $d_{\mathcal{GW}, p}$  defines a legitimate metric on  $\mathcal{M}^w$  modulo isomorphism of mm-spaces [Mém11].

## 2.3 Simplicial complexes

**Definition 2.12.** Let  $V$  be a set. An *abstract simplicial complex*  $K$  with vertex set  $V$  is a collection of finite subsets of  $V$  such that if  $\sigma \in K$ , then every  $\tau \subset \sigma$  is also in  $K$ . We also use  $K$  to denote its geometric realization.

A set  $\sigma \in K$  is called a  $k$ -face if  $|\sigma| = k + 1$ . A *simplicial map*  $f : K_1 \rightarrow K_2$  is a set map  $f : V_1 \rightarrow V_2$  between the vertex sets of  $K_1$  and  $K_2$  such that if  $\sigma \in K_1$ , then  $f(\sigma) \in K_2$ .

Here we define the simplicial complexes that we will focus on.

**Definition 2.13.** Let  $(X, d_X) \in \mathcal{M}$  and  $r \geq 0$ . The *Vietoris-Rips complex* of  $X$  at scale  $r$  is the simplicial complex

$$\text{VR}_r(X) := \{\sigma \subset X \text{ finite} : \mathbf{diam}_X(\sigma) \leq r\}.$$

**Definition 2.14.** Fix  $n \geq 1$ . Let  $e_i = (0, \dots, 1, \dots, 0)$  be the  $i$ -th standard basis vector in  $\mathbb{R}^n$  and  $V = \{\pm e_1, \dots, \pm e_n\}$ . Let  $\mathfrak{B}_n$  be the collection of subsets  $\sigma \subset V$  that don't contain both  $e_i$  and  $-e_i$ . This simplicial complex is called the  $n$ -th *cross-polytope*.

## 2.4 Persistent homology

The idea behind persistent homology is to construct a filtration of topological spaces  $(X_t)_{t>0}$  and compute the homology at each time  $t$ . We will adopt definitions from [Mém17].

**Definition 2.15.** A *filtration* on a finite set  $X$  is a function  $F_X : \text{pow}(X) \rightarrow \mathbb{R}$  such that  $F_X(\sigma) \leq F_X(\tau)$  whenever  $\sigma \subset \tau$ , and we call the pair  $(X, F_X)$  a *filtered set*.  $\mathcal{F}$  will denote the category of finite filtered sets, where objects are pairs  $(X, F_X)$  and the morphisms  $\varphi : (X, F_X) \rightarrow (Y, F_Y)$  are set maps  $\varphi : X \rightarrow Y$  such that  $F_Y(\varphi(\sigma)) \leq F_X(\sigma)$ .

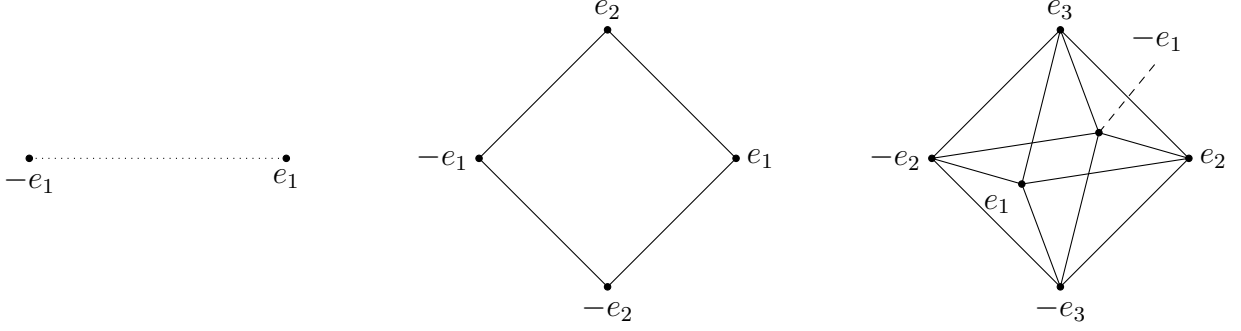


Figure 6: From left to right:  $\mathfrak{B}_1, \mathfrak{B}_2, \mathfrak{B}_3$  (there is no edge between the vertices of  $\mathfrak{B}_1$ ).

**Definition 2.16.** A *filtration functor* is any functor  $\mathfrak{F} : \mathcal{M}^{\text{fin}} \rightarrow \mathcal{F}$ .

**Remark 2.17.** Given two finite pseudometric spaces  $(X, d_X)$  and  $(Y, d_Y)$ , let  $(X, F_X) = \mathfrak{F}(X, d_X)$  and  $(Y, F_Y) = \mathfrak{F}(Y, d_Y)$ . Functoriality of  $\mathfrak{F}$  means that for any 1-Lipschitz map  $\varphi : X \rightarrow Y$ , we have  $F_Y(\varphi(\sigma)) \leq F_X(\sigma)$  for all  $\sigma \subset X$ . In particular, if  $X$  and  $Y$  are isometric,  $F_X = F_Y$  as filtrations.

**Definition 2.18.** Given  $(X, d_X) \in \mathcal{M}^{\text{fin}}$ , define the *Vietoris-Rips filtration*  $F_X^{\text{VR}}$  by setting  $F_X^{\text{VR}}(\sigma) = \text{diam}(\sigma)$  for  $\sigma \subset X$ . It is straightforward to check that this construction is functorial, so we define the *Vietoris-Rips filtration functor*  $\mathfrak{F}^{\text{VR}} : \mathcal{M}^{\text{fin}} \rightarrow \mathcal{F}$  by  $(X, d_X) \mapsto (X, F_X^{\text{VR}})$ .

Our pipeline for persistent homology starts with a filtration functor  $\mathfrak{F}$ . Given a finite (pseudo)metric space  $(X, d_X)$ , let  $(X, F_X^{\mathfrak{F}}) = \mathfrak{F}(X, d_X)$ . For every  $r > 0$ , we construct the simplicial complex  $L_r := \{\sigma \subset X : F_X^{\mathfrak{F}}(\sigma) \leq r\}$ <sup>1</sup>, and we get a nested family of simplicial complexes

$$L^{\mathfrak{F}}(X) := \{L_{r_0} \subset L_{r_1} \subset L_{r_2} \subset \cdots \subset L_{r_m}\}$$

where  $\text{range}(F_X) = \{r_0 < r_1 < r_2 < \cdots < r_m\}$ , and each  $L_{r_i}$  is, by construction, finite. Taking homology with field coefficients  $H_k(\cdot, \mathbb{F})$  of the family above gives a sequence of vector spaces and linear maps

$$\text{PH}_k^{\mathfrak{F}}(X) := \left\{ V_{r_0} \xrightarrow{v_0} V_{r_1} \xrightarrow{v_1} V_{r_2} \xrightarrow{v_2} \cdots \xrightarrow{v_{m-1}} V_{r_m} \right\}$$

which is called a *persistence vector space*. Note that each  $V_{r_i}$  is finite dimensional in our setting.

One particular type of persistent vector spaces are *interval modules*

$$\mathbb{I}[b, d] := \{0 \rightarrow \cdots \rightarrow 0 \rightarrow \mathbb{F} \rightarrow \cdots \rightarrow \mathbb{F} \rightarrow 0 \rightarrow \cdots \rightarrow 0\},$$

where the first  $\mathbb{F}$  appears at time  $b$ , and the last one, at time  $d$ . The maps between different occurrences of  $\mathbb{F}$  are identities, whereas the other maps are 0. Persistence vector spaces

<sup>1</sup>Notice that if  $\mathfrak{F} = \mathfrak{F}^{\text{VR}}$ , then  $L_r = \text{VR}_r(X)$ .

admit a classification up to isomorphism wherein a persistence vector space  $\mathbb{V}$  is decomposed as a sum of interval modules  $\mathbb{V} = \bigoplus_{\alpha \in A} \mathbb{I}[b_\alpha, d_\alpha]$  [CdS10]. These collections of intervals are sometimes referred to as *barcodes* or *persistence diagrams*, depending on the graphical representation that is adopted [EH10]. We prefer the term persistence diagrams in the present work, and denote by  $\mathcal{D}$  the collection of all finite persistence diagrams. An element  $D \in \mathcal{D}$  is multiset of points of the form

$$D = \{(b_\alpha, d_\alpha), 0 \leq b_\alpha < d_\alpha, \alpha \in A\}$$

for some (finite) index set  $A$ . In short, starting with any filtration functor  $\mathfrak{F}$ , we assign a persistence diagram to  $(X, d_X)$  via the composition  $\text{dgm}_k^{\mathfrak{F}} : \mathcal{M}^{\text{fin}} \rightarrow \mathcal{D}$  defined by

$$(X, d_X) \mapsto (X, F_X^{\mathfrak{F}}) \mapsto L^{\mathfrak{F}}(X) \mapsto \text{PH}_k^{\mathfrak{F}}(X) \mapsto \text{dgm}_k^{\mathfrak{F}}(X).$$

Notice that we could have also started with just a filtered set  $(X, F_X)$ , instead of a (pseudo)metric space, and obtain a persistence diagram. We will denote that diagram with  $\text{dgm}_k(X, F_X)$ .

## 2.5 Stability

The most useful filtration functors enjoy a property known as stability. Intuitively, it means that the persistence diagrams they produce are resistant to noise: if the input (pseudo)metric space is perturbed, the persistence diagram will not change too much. In this section, we will describe the metrics on filtrations and persistence diagrams that we use to measure stability.

We start with the bottleneck distance between persistence diagrams  $D_1, D_2 \in \mathcal{D}$ . Define the *persistence* of a point  $P = (x, y)$  with  $x \leq y$  as  $\text{pers}(P) := y - x$ . The *total persistence* of a persistence diagram  $D \in \mathcal{D}$  is the maximal persistence of its points:

$$\text{pers}(D) := \max_{P \in D} \text{pers}(P).$$

Let  $D_1 = \{P_\alpha\}_{\alpha \in A_1}$  and  $D_2 = \{Q_\alpha\}_{\alpha \in A_2}$  be two persistence diagrams indexed over the finite index sets  $A_1$  and  $A_2$  respectively. Consider subsets  $B_i \subseteq A_i$  with  $|B_1| = |B_2|$  together with a bijection  $\varphi : B_1 \rightarrow B_2$ . Define

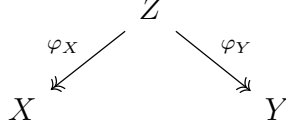
$$J(\varphi) := \max \left( \max_{\beta \in B_1} \|P_\beta - Q_{\varphi(\beta)}\|_\infty, \max_{\alpha \in A_1 \setminus B_1} \frac{1}{2} \text{pers}(P_\alpha), \max_{\alpha \in A_2 \setminus B_2} \frac{1}{2} \text{pers}(Q_\alpha) \right).$$

**Definition 2.19** ([EH10]). The *bottleneck distance* between  $D_1, D_2 \in \mathcal{D}$  is

$$d_{\mathcal{B}}(D_1, D_2) := \min_{(B_1, B_2, \varphi)} J(\varphi),$$

where  $(B_1, B_2, \varphi)$  ranges over all  $B_1 \subset A_1$ ,  $B_2 \subset A_2$ , and bijections  $\varphi : B_1 \rightarrow B_2$ . Note that for any  $D \in \mathcal{D}$  and any one-point diagram  $Q = \{(x, x)\}$ ,  $d_{\mathcal{B}}(D, Q) = \frac{1}{2} \text{pers}(D)$ .

We can also measure the difference between two finite filtered sets  $(X, F_X)$  and  $(Y, d_Y)$ . The idea is to pullback and compare the filtrations in a common set  $Z$ . To that end, we define a *tripod*, which is a triplet  $(Z, \varphi_X, \varphi_Y)$  consisting of a finite set  $Z$  and a pair of surjective maps  $\varphi_X : Z \rightarrow X$  and  $\varphi_Y : Z \rightarrow Y$  called *parametrizations*.



The *pullback filtration*  $\varphi_X^* F_X$  on  $Z$  is naturally defined as  $\varphi_X^* F_X(\tau) = F_X(\varphi(\tau))$  for every  $\tau \subset Z$  (similarly for  $\varphi_Y^* F_Y$ ).

**Definition 2.20.** The filtration distance  $d_{\mathcal{F}}$  is

$$\begin{aligned} d_{\mathcal{F}}((X, F_X), (Y, F_Y)) &:= \inf_{(Z, \varphi_X, \varphi_Y)} \|\varphi_X^* F_X - \varphi_Y^* F_Y\|_{\ell^\infty(\text{pow}(Z))} \\ &= \inf_{(Z, \varphi_X, \varphi_Y)} \max_{\tau \in \text{pow}(Z)} |\varphi_X^* F_X(\tau) - \varphi_Y^* F_Y(\tau)|, \end{aligned}$$

where the infimum ranges over all tripods  $(Z, \varphi_X, \varphi_Y)$ .

In other words, we pullback the filtrations  $F_X$  and  $F_Y$  to a common set  $Z$ , where we can compare them using the  $\ell^\infty$  norm on  $\text{pow}(Z)$ . The filtration distance is the infimum of this quantity over all choices of tripods  $(Z, \varphi_X, \varphi_Y)$ .

**Proposition 2.21** ([Mém17]).  $d_{\mathcal{F}}$  is a pseudometric on  $\mathcal{F}$ .

With these tools at hand, we define what we mean by stable functors.

**Definition 2.22** (Stable filtration functors). For a given filtration functor  $\mathfrak{F}$ , define its *Lipschitz constant*  $L(\mathfrak{F})$  as the infimal  $L > 0$  such that

$$d_{\mathcal{F}}(\mathfrak{F}(X), \mathfrak{F}(Y)) \leq L \cdot d_{\mathcal{GH}}(X, Y)$$

for all  $X, Y \in \mathcal{M}^{\text{fin}}$ . If  $L(\mathfrak{F}) < \infty$ , we say that  $\mathfrak{F}$  is *stable*. In this case, we also say that  $\mathfrak{F}$  is  $L$ -stable for all constants  $L \geq L(\mathfrak{F})$ .

[Mém17] proved the following theorem and its corollary.

**Theorem 2.23.** For all finite filtered spaces  $(X, F_X), (Y, F_Y)$  and all  $k \in \mathbb{N}$ , we have

$$d_{\mathcal{B}}(\text{dgm}_k(X, F_X), \text{dgm}_k(Y, F_Y)) \leq d_{\mathcal{F}}((X, F_X), (Y, F_Y)).$$

**Corollary 2.24.** For any stable filtration functor  $\mathfrak{F}$ ,

$$d_{\mathcal{B}}(\text{dgm}_k^{\mathfrak{F}}(X), \text{dgm}_k^{\mathfrak{F}}(Y)) \leq L(\mathfrak{F}) \cdot d_{\mathcal{GH}}(X, Y)$$

for all  $X, Y \in \mathcal{M}^{\text{fin}}$  and  $k \in \mathbb{N}$ .

**Example 2.25.** The Lipschitz constant of  $\mathfrak{F}^{\text{VR}}$  is 2. Pick any pair of finite (pseudo)metric spaces  $X$  and  $Y$  and let  $\eta > 0$  and  $R \in \mathcal{R}(X, Y)$  be such that  $\text{dis}(R) < 2\eta$ . Consider the joint parametrization  $Z = R$ ,  $\varphi_X = \pi_1$  and  $\varphi_Y = \pi_2$  of  $X$  and  $Y$ . For any  $\tau \subset Z$ ,  $d_X(\varphi_X(z, z')) \leq d_Y(\varphi_Y(z, z')) + 2\eta$ . Taking maxima over  $z, z' \in Z$  yields  $\mathbf{diam}_X(\varphi_X(\tau)) \leq \mathbf{diam}_Y(\varphi_Y(\tau)) + 2\eta$ , and the symmetric argument gives  $|F_X^{\text{VR}}(\varphi_X(\tau)) - F_Y^{\text{VR}}(\varphi_Y(\tau))| \leq 2\eta$ . This implies that  $d_{\mathcal{F}}(\mathfrak{F}^{\text{VR}}(X), \mathfrak{F}^{\text{VR}}(Y)) \leq 2\eta$  and the claim follows by taking  $\eta \rightarrow d_{\mathcal{GH}}(X, Y)$ .

The constant 2 is tight because  $X = (*, 0)$  and  $Y = \Delta_2(1)$  satisfy  $d_{\mathcal{F}}(\mathfrak{F}^{\text{VR}}(X), \mathfrak{F}^{\text{VR}}(Y)) = 2d_{\mathcal{GH}}(X, Y)$ .

### 3 Curvature sets and Persistence diagrams

Given a compact metric space  $(X, d_X)$ , Gromov identified a class of full invariants called *curvature sets* [Gro07]. Intuitively, the  $n$ -th curvature set contains the metric information of all possible samples of  $n$  points from  $X$ . In this section, we define persistence sets, an analog construction that captures the persistent homology of all  $n$ -point samples of  $X$ . We start by recalling Gromov's definition with some examples, and an analogue of the Gromov-Hausdorff distance in terms of curvature sets. We then define persistence sets and study their stability with respect to this modified Gromov-Hausdorff distance. Additionally, when dealing with metric measure spaces, we can define measures on curvature and persistence sets via the pushforward of the product measure on  $X^n$ . We also study these measures and prove an appropriate notion of stability.

**Definition 3.1.** Let  $(X, d_X)$  be a metric space. Given a positive integer  $n$ , let  $\Psi_X^{(n)} : X^n \rightarrow \mathbb{R}^{n \times n}$  be the map that sends an  $n$ -tuple  $(x_1, \dots, x_n)$  to the distance matrix  $M$ , where  $M_{ij} = d_X(x_i, x_j)$ . The  $n$ -th *curvature set* of  $X$  is  $\mathbf{K}_n(X) := \text{im}(\Psi_X^{(n)})$ , the collection of all distance matrices of  $n$  points from  $X$ .

**Remark 3.2** (Functoriality of curvature sets). Observe curvature sets are functorial in the sense that if  $X$  is isometrically embedded in  $Y$ , then  $\mathbf{K}_n(X) \subset \mathbf{K}_n(Y)$ .

**Example 3.3.**  $\mathbf{K}_2(X)$  is the set of distances of  $X$ . If  $X$  is geodesic,  $\mathbf{K}_2(X) = [0, \mathbf{diam}(X)]$ .

**Example 3.4.** Let  $X = \{p, q\}$  be a two point metric space with  $d_X(p, q) = \delta$ . Then

$$\begin{aligned} \mathbf{K}_3(X) &= \left\{ \Psi_X^{(3)}(p, p, p), \Psi_X^{(3)}(p, p, q), \Psi_X^{(3)}(p, q, p), \Psi_X^{(3)}(q, p, p), \right. \\ &\quad \left. \Psi_X^{(3)}(q, q, q), \Psi_X^{(3)}(q, q, p), \Psi_X^{(3)}(q, p, q), \Psi_X^{(3)}(p, q, q) \right\} \\ &= \left\{ \begin{pmatrix} 0 & 0 & 0 \\ 0 & 0 & 0 \\ 0 & 0 & 0 \end{pmatrix}, \begin{pmatrix} 0 & 0 & \delta \\ 0 & 0 & \delta \\ \delta & \delta & 0 \end{pmatrix}, \begin{pmatrix} 0 & \delta & 0 \\ \delta & 0 & \delta \\ 0 & \delta & 0 \end{pmatrix}, \begin{pmatrix} 0 & \delta & \delta \\ \delta & 0 & 0 \\ \delta & 0 & 0 \end{pmatrix} \right\}. \end{aligned}$$

For  $n \geq 2$  and  $0 < k < n$ , let  $x_1 = \dots = x_k = p$  and  $x_{k+1} = \dots = x_n = q$ . Define

$$M_k(\delta) := \Psi_X^{(n)}(x_1, \dots, x_n) = \left( \begin{array}{c|c} \mathbf{0}_{k \times k} & \delta \cdot \mathbf{1}_{k \times (n-k)} \\ \delta \cdot \mathbf{1}_{(n-k) \times k} & \mathbf{0}_{(n-k) \times (n-k)} \end{array} \right),$$

where  $\mathbf{1}_{r \times s}$  is the  $r \times s$  matrix with all entries equal to 1. If we make another choice of  $x_1, \dots, x_n$ , the resulting distance matrix will change only by a permutation of its rows and columns. Thus, if we define  $M_k^\Pi(\delta) := \Psi_X^{(n)}(x_1, \dots, x_n) = \Pi^T \cdot M_k(\delta) \cdot \Pi$ , for some permutation matrix  $\Pi \in S_n$ , then

$$\mathbf{K}_n(X) = \{\mathbf{0}_{n \times n}\} \cup \{M_k^\Pi(\delta) : 0 < k < n \text{ and } \Pi \in S_n\}.$$

**Example 3.5.** In this example we describe  $\mathbf{K}_3(\mathbb{S}^1)$ , where  $\mathbb{S}^1 = [0, 2\pi]/(0 \sim 2\pi)$  is equipped with the geodesic metric. Depending on the position of  $x_1, x_2, x_3$ , we need two cases. If the three points are not contained in the same semicircle, then  $d_{12} + d_{23} + d_{31} = 2\pi$ . If they are, then there exists a point, say  $x_2$ , that lies in the shortest path joining the other two so that  $d_{13} = d_{12} + d_{23} \leq \pi$ . The other possibilities are  $d_{12} = d_{13} + d_{32}$  and  $d_{23} = d_{21} + d_{13}$ .

Since  $M$  is symmetric, we only need 3 entries to characterize and plot  $\mathbf{K}_3(\mathbb{S}^1)$  (see Figure 3.5). If we label  $x = d_{12}, y = d_{23}$  and  $z = d_{31}$ , then  $\mathbf{K}_3(\mathbb{S}^1)$  is the boundary of the 3-simplex with vertices  $(0, 0, 0)$ ,  $(\pi, \pi, 0)$ ,  $(\pi, 0, \pi)$ , and  $(0, \pi, \pi)$ . Each of the cases in the previous paragraph corresponds to a face of this simplex.

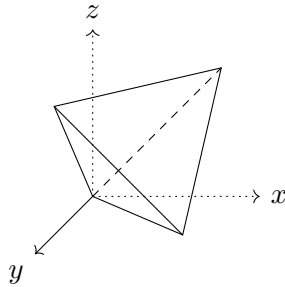


Figure 7: The curvature set  $\mathbf{K}_3(\mathbb{S}^1)$ .

As we mentioned earlier, curvature sets are a full invariant of compact metric spaces, which means that  $X \simeq Y$  if, and only if,  $\mathbf{K}_n(X) = \mathbf{K}_n(Y)$  for all  $n \geq 1$ . It makes sense to quantitatively measure the difference between two metric spaces by comparing their curvature sets. The following definition of [Mém12b] does what we need.

**Definition 3.6** ([Mém12b]). The *modified Gromov-Hausdorff* distance between  $X, Y \in \mathcal{M}$  is

$$\widehat{d}_{\mathcal{GH}}(X, Y) := \frac{1}{2} \sup_{n \in \mathbb{N}} d_{\mathcal{H}}(\mathbf{K}_n(X), \mathbf{K}_n(Y)) \quad (4)$$

Here  $d_{\mathcal{H}}$  denotes the Hausdorff distance on  $\mathbb{R}^{n \times n}$  with  $\ell^\infty$  distance.

Notice that  $\widehat{d}_{\mathcal{GH}}(X, Y) \leq d_{\mathcal{GH}}(X, Y)$ . A benefit of  $\widehat{d}_{\mathcal{GH}}$  when compared to the standard Gromov-Hausdorff distance is that the computation of the latter leads in general to NP-hard problems [Sch17], whereas computing the lower bound in the equation above on certain values of  $n$  leads to polynomial time problems. In [Mém12b] it is argued that work of Peter

Olver [Olv01] and Boutin and Kemper [BK04b] leads to identifying rich classes of shapes where these lower bounds permit full discrimination.

The analogous definitions for mm-spaces are the following.

**Definition 3.7.** Let  $(X, d_X, \mu_X)$  be an mm-space. The  $n$ -th curvature measure of  $X$  is defined as

$$\mu_n(X) := \left( \Psi_X^{(n)} \right)_{\#} \mu_X^{\otimes n}.$$

We also define the *modified Gromov-Wasserstein distance* between  $X, Y \in \mathcal{M}^w$  as

$$\widehat{d}_{\mathcal{GW},p}(X, Y) := \frac{1}{2} \sup_{n \in \mathbb{N}} d_{\mathcal{W},p}(\mu_n(X), \mu_n(Y)),$$

where  $d_{\mathcal{W},p}$  is the  $p$ -Wasserstein distance [Vil03] on  $\mathcal{P}_1(\mathbb{R}^{n \times n})$ , and  $\mathbb{R}^{n \times n}$  is equipped with the  $\ell^\infty$  distance.

Clearly,  $\text{supp}(\mu_n(X)) = \mathbf{K}_n(X)$  for all  $n \in \mathbb{N}$ , and similarly to equation (4), [MNO21] proves that  $\widehat{d}_{\mathcal{GW},p}(X, Y) \leq d_{\mathcal{GW},p}(X, Y)$ .

**Remark 3.8** (Interpretation as “*motifs*”). In network science [MP20], it is of interest to identify substructures of a dataset (network)  $X$  which appear with high frequency. The interpretation of the definitions above is that the curvature sets  $\mathbf{K}_n(X)$  for different  $n \in \mathbb{N}$  capture the information of those substructures whose cardinality is at most  $n$ , whereas the curvature measures  $\mu_n(X)$  capture their frequency of occurrence.

### 3.1 $\mathfrak{F}$ -persistence sets

The idea behind curvature sets to study a metric space by taking the distance matrix of a sample of  $n$  points. This is the inspiration for the next definition: we want to study the persistence of a compact metric space  $X$  by looking at the persistence diagrams of samples with  $n$  points.

**Definition 3.9.** Fix  $n \geq 1$  and  $k \geq 0$ . Let  $(X, d_X) \in \mathcal{M}$  and  $\mathfrak{F} : \mathcal{M}^{\text{fin}} \rightarrow \mathfrak{F}$  be any filtration functor. The  $(n, k)$ - $\mathfrak{F}$  persistence set of  $X$  is

$$\mathbf{D}_{n,k}^{\mathfrak{F}}(X) := \{ \text{dgm}_k^{\mathfrak{F}}(X') : X' \subset X \text{ such that } |X'| \leq n \},$$

and the *total  $\mathfrak{F}$ -persistence set* of  $X$  is

$$\mathbf{D}_n^{\mathfrak{F}}(X) := \{ \mathbf{D}_{n,k}^{\mathfrak{F}}(X) \}_{k \geq 0}.$$

**Remark 3.10** (Functoriality of persistence sets). Notice that, similarly to curvature sets (Cf. Remark 3.2), persistence sets are functorial. If  $X \hookrightarrow Y$  isometrically, then  $\mathbf{K}_n(X) \subset \mathbf{K}_n(Y)$ , and consequently,  $\mathbf{D}_{n,k}^{\mathfrak{F}}(X) \subset \mathbf{D}_{n,k}^{\mathfrak{F}}(Y)$  for all  $n, k \in \mathbb{N}$ .

**Remark 3.11.** Recall that filtration functors are by definition isometry invariants (see 2.17). This means that we can define the  $\mathfrak{F}$ -persistence diagram of a distance matrix as the diagram of the underlying pseudometric space. More explicitly, let  $(X, d_X) \in \mathcal{M}$ , and take  $\mathbb{X} \in X^n$  and  $M = \Psi_X^{(n)}(\mathbb{X})$ . Define  $x_i = p_i(\mathbb{X})$  and  $X' = \bigcup_{i=1}^n \{p_i(\mathbb{X})\}$ , where each  $p_i$  is the projection to the  $i$ -th coordinate. Notice that  $d_X(x_i, x_j) = M_{ij}$ . We define  $\text{dgm}_k^{\mathfrak{F}}(M) := \text{dgm}_k^{\mathfrak{F}}(X')$ . For that reason, we can view the persistence set  $\mathbf{D}_{n,k}^{\mathfrak{F}}(X)$  as the image of the map  $\text{dgm}_k^{\mathfrak{F}} : \mathbf{K}_n(X) \rightarrow \mathcal{D}$ .

$$X^n \xrightarrow{\Psi_X^{(n)}} \mathbf{K}_n(X) \xrightarrow{\text{dgm}_k^{\mathfrak{F}}} \mathbf{D}_{n,k}^{\mathfrak{F}}(X) \subset \mathcal{D}$$

$$\mathbb{X} \longmapsto M \longmapsto \text{dgm}_k^{\mathfrak{F}}(X').$$

Persistence sets inherit the stability of the filtration functor. Given their definition in terms of curvature sets, the modified Gromov-Hausdorff distance is a natural metric to use.

**Theorem 3.12.** *Let  $\mathfrak{F}$  be a stable filtration functor with Lipschitz constant  $L(\mathfrak{F})$ . Then for all compact metric spaces  $X$  and  $Y$ ,  $n \geq 1$ , and  $k \geq 0$ , one has*

$$d_{\mathcal{H}}^{\mathcal{D}}(\mathbf{D}_{n,k}^{\mathfrak{F}}(X), \mathbf{D}_{n,k}^{\mathfrak{F}}(Y)) \leq L(\mathfrak{F}) \cdot \widehat{d}_{\mathcal{G}\mathcal{H}}(X, Y),$$

where  $d_{\mathcal{H}}^{\mathcal{D}}$  denotes the Hausdorff distance between subsets of  $\mathcal{D}$ .

*Proof.* We will show that  $d_{\mathcal{H}}^{\mathcal{D}}(\mathbf{D}_{n,k}^{\mathfrak{F}}(X), \mathbf{D}_{n,k}^{\mathfrak{F}}(Y)) \leq \frac{1}{2}L(\mathfrak{F}) \cdot d_{\mathcal{H}}(\mathbf{K}_n(X), \mathbf{K}_n(Y))$  for all  $n$ . Since  $L(\mathfrak{F}) \cdot \widehat{d}_{\mathcal{G}\mathcal{H}}(X, Y)$  is an upper bound for the right-hand side, the theorem will follow.

Assume  $d_{\mathcal{H}}(\mathbf{K}_n(X), \mathbf{K}_n(Y)) < \eta$ . Pick any  $D_1 \in \mathbf{D}_{n,k}^{\mathfrak{F}}(X)$ . Let  $\mathbb{X} = (x_1, \dots, x_n) \in X^n$  such that  $\Psi_X^{(n)}(\mathbb{X}) = M_1$  and  $D_1 = \text{dgm}_k^{\mathfrak{F}}(M_1)$ . From the assumption on  $d_{\mathcal{H}}(\mathbf{K}_n(X), \mathbf{K}_n(Y))$ , there exists  $M_2 \in \mathbf{K}_n(Y)$  such that  $\|M_1 - M_2\|_{\infty} < \eta$ . As before, let  $\mathbb{Y} = (y_1, \dots, y_n)$  be such that  $M_2 = \Psi_Y^{(n)}(\mathbb{Y})$  and  $D_2 = \text{dgm}_k^{\mathfrak{F}}(M_2)$ . Let  $X' = \bigcup_{i=1}^n \{p_i(x_i)\}$  and  $Y' = \bigcup_{i=1}^n \{p_i(y_i)\}$ . The definition of  $\text{dgm}_k^{\mathfrak{F}}$  on curvature sets (see Remark 3.11) states that  $D_1 = \text{dgm}_k^{\mathfrak{F}}(X')$  and  $D_2 = \text{dgm}_k^{\mathfrak{F}}(Y')$ , so by Corollary 2.24,

$$d_{\mathcal{B}}(D_1, D_2) \leq L(\mathfrak{F}) \cdot d_{\mathcal{G}\mathcal{H}}(X', Y').$$

By taking the correspondence  $R = \{(x_i, y_i) \in X' \times Y' : i = 1, \dots, n\}$ , we can bound the  $d_{\mathcal{G}\mathcal{H}}(X', Y')$  term by

$$d_{\mathcal{G}\mathcal{H}}(X', Y') \leq \frac{1}{2} \text{dis}(R) = \frac{1}{2} \max_{i,j=1,\dots,n} |d_X(x_i, x_j) - d_Y(y_i, y_j)| = \frac{1}{2} \|M_1 - M_2\|_{\infty} < \frac{\eta}{2}.$$

In summary, for every  $D_1 \in \mathbf{D}_{n,k}^{\mathfrak{F}}(X)$ , we can find  $D_2 \in \mathbf{D}_{n,k}^{\mathfrak{F}}(Y)$  such that  $d_{\mathcal{B}}(D_1, D_2) \leq L(\mathfrak{F}) \cdot d_{\mathcal{G}\mathcal{H}}(X', Y') < L(\mathfrak{F}) \cdot \eta/2$ , and the same argument works when swapping  $X$  and  $Y$ . Thus, we let  $\eta \rightarrow d_{\mathcal{H}}(\mathbf{K}_n(X), \mathbf{K}_n(Y))$  to conclude

$$d_{\mathcal{B}}(D_1, D_2) \leq \frac{1}{2} L(\mathfrak{F}) \cdot d_{\mathcal{H}}(\mathbf{K}_n(X), \mathbf{K}_n(Y)),$$

as desired. □

**Remark 3.13** (Tightness of the bound). Let  $X = (*, 0)$  and  $Y = \Delta_2(\delta)$  with  $\delta > 0$ . Then  $\text{dgm}_0^{\text{VR}}(X) = \{[0, \infty)\}$  and  $\text{dgm}_0^{\text{VR}}(Y) = \{[0, \delta), [0, \infty)\}$ . Thus,

$$d_{\mathcal{H}}^{\mathcal{D}}(\mathbf{D}_{2,0}^{\text{VR}}(X), \mathbf{D}_{2,0}^{\text{VR}}(Y)) = d_{\mathcal{B}}(\text{dgm}_0^{\text{VR}}(X), \text{dgm}_0^{\text{VR}}(Y)) = \text{pers}(0, \delta) = \delta.$$

On the other hand, we have that  $\widehat{d}_{\mathcal{GH}}(X, Y) = \frac{\delta}{2}$ . Notice that  $\mathbf{K}_2(X) = \{(\begin{smallmatrix} 0 & 0 \\ 0 & 0 \end{smallmatrix})\}$  and  $\mathbf{K}_2(Y) = \{(\begin{smallmatrix} 0 & 0 \\ 0 & 0 \end{smallmatrix}), (\begin{smallmatrix} 0 & \delta \\ \delta & 0 \end{smallmatrix})\}$ . This gives a lower bound  $\widehat{d}_{\mathcal{GH}}(X, Y) \geq \frac{1}{2}d_{\mathcal{H}}(\mathbf{K}_2(X), \mathbf{K}_2(Y)) = \frac{\delta}{2}$ , while the upper bound is given by  $d_{\mathcal{GH}}(X, Y) = \frac{\delta}{2}$ . Thus,  $\widehat{d}_{\mathcal{GH}}(X, Y) = \frac{\delta}{2} = \frac{1}{2}d_{\mathcal{H}}^{\mathcal{D}}(\mathbf{D}_2^{\text{VR}}(X), \mathbf{D}_2^{\text{VR}}(Y))$ . This proves tightness because Example 2.25 established that  $L(\mathfrak{F}^{\text{VR}}) = 2$ .

**Remark 3.14 (Persistent sets are isometry invariant)**. Note that the persistent sets  $\mathbf{D}_{n,k}^{\mathfrak{F}}$  are themselves isometry invariants of metric spaces. As such, they can be regarded, in principle, as *signatures* that can be used to gain insight into datasets or to discriminate between different shapes.

**Remark 3.15 (Computational cost)**. One thing to keep in mind is that computing the single diagram  $\text{dgm}_1^{\text{VR}}(X)$  when  $X$  has, say, 1000 points is likely to be much more computationally expensive than computing 10,000 VR one-dimensional persistence diagrams obtained by randomly sampling points from  $X$ , i.e. approximating  $\mathbf{D}_{n,1}^{\text{VR}}(X)$  with small  $n$ . More specifically, computing the degree  $k$  VR persistence diagram of a finite metric space with  $N$  points requires knowledge of the  $k + 1$  skeleton of the full simplex over  $X$ , each of which is a subset of size  $k + 2$ , so the complexity is  $c(N, k) \approx O(N^{\omega(k+2)})$  [MMS11]. Here, we are assuming that multiplication of  $m \times m$  matrices has cost<sup>2</sup>  $O(m^\omega)$ . Since there are  $N^n$  possible  $n$ -tuples of points of  $X$ , the complexity of computing  $\mathbf{D}_{n,k}^{\text{VR}}(X)$  is bounded by  $O(c(n, k) \cdot N^n) \approx O(n^{\omega(k+2)} N^n)$ . For example, when  $n = 4$  and  $k = 1$ , the comparison boils down to  $O(N^{3\omega}) \approx O(N^{7.11})$  versus  $O(N^4)$ . When  $k = 2$  and  $n = 6$  one needs to compare  $O(N^{9.49})$  versus  $O(N^6)$ .

Another point which lends flexibility to the approximate computation of persistence sets is that one can actually easily cap the number of  $n$ -tuples to be considered by a parameter  $M_{\max}$ , and in this case the complexity associated to estimating  $\mathbf{D}_{n,k}^{\text{VR}}$  will be  $O(n^{\omega(k+2)} M_{\max})$ . One can then easily select random  $n$ -tuples from the dataset up to an upper limit  $M_{\max}$  – this is the pragmatic approach we have followed in the experiments reported in this paper and in the code on our github repository [GM21].

Furthermore, these calculations are of course eminently parallelizable. Furthermore, for  $n \ll N$ , the memory requirements for computing an estimate to  $\mathbf{D}_{n,k}^{\text{VR}}(X)$  are substantially more modest than what computing  $\text{dgm}_k^{\text{VR}}(X)$  would require since the boundary matrices that one needs to store in memory are several orders of magnitude smaller.

Finally, if one is only interested in the principal persistence set, a much faster geometric algorithm is available, cf. Remark 4.6.

See our github repository [GM21] for a `parfor` based Matlab implementation.

---

<sup>2</sup>Currently, the best known constant is  $\omega \approx 2.37286$ . [AW20]

## 3.2 $\mathfrak{F}$ -Persistence measures

Much in the same way as curvature measures define probability measures supported over curvature sets, one can consider measures supported on  $\mathcal{D}$ , called *persistence measures*, which encode the way mass is distributed on persistence sets.

**Definition 3.16.** For each filtration functor  $\mathfrak{F}$ , integers  $n \geq 1, k \geq 0$ , and  $X \in \mathcal{M}^w$ , define the  $(n, k)$ -persistence measure of  $X$  as (cf. Def. 3.7)

$$\mathbf{U}_{n,k}^{\mathfrak{F}}(X) := (\mathrm{dgm}_k^{\mathfrak{F}})_{\#} \mu_n(X).$$

We also have a stability result for these measures in terms of the Gromov-Wasserstein distance.

**Theorem 3.17.** *Let  $\mathfrak{F}$  be a given filtration functor with Lipschitz constant  $L(\mathfrak{F})$ . For all  $X, Y \in \mathcal{M}^w$  and integers  $n \geq 1$  and  $k \geq 0$ ,*

$$d_{\mathcal{W},p}^{\mathcal{D}}(\mathbf{U}_{n,k}^{\mathfrak{F}}(X), \mathbf{U}_{n,k}^{\mathfrak{F}}(Y)) \leq \frac{L(\mathfrak{F})}{2} \cdot d_{\mathcal{W},p}(\mu_n(X), \mu_n(Y))$$

and, in consequence,

$$d_{\mathcal{W},p}^{\mathcal{D}}(\mathbf{U}_{n,k}^{\mathfrak{F}}(X), \mathbf{U}_{n,k}^{\mathfrak{F}}(Y)) \leq L(\mathfrak{F}) \cdot \widehat{d}_{\mathcal{GW},p}(X, Y).$$

*Proof.* This proof follows roughly the same outline as that of (3.12). Let  $\eta > d_{\mathcal{W},p}(\mu_n(X), \mu_n(Y))$ . Choose a coupling  $\mu \in \mathcal{M}(\mu_n(X), \mu_n(Y))$  such that

$$[d_{\mathcal{W},p}(\mu_n(X), \mu_n(Y))]^p \leq \iint_{\mathbf{K}_n(X) \times \mathbf{K}_n(Y)} \|M - M'\|_{\infty}^p \mu(dM \times dM') < \eta^p,$$

where  $\|\cdot\|_{\infty}$  denotes the  $\ell^{\infty}$  norm on  $\mathbb{R}^{n \times n}$ . It's a basic fact of measure theory that the pushforward  $\nu = (\mathrm{dgm}_k^{\mathfrak{F}} \times \mathrm{dgm}_k^{\mathfrak{F}})_{\#} \mu$  of the coupling  $\mu$  is a coupling of the pushforwards  $(\mathrm{dgm}_k^{\mathfrak{F}})_{\#} \mu_n(X) = \mathbf{U}_{n,k}^{\mathfrak{F}}(X)$  and  $(\mathrm{dgm}_k^{\mathfrak{F}})_{\#} \mu_n(Y) = \mathbf{U}_{n,k}^{\mathfrak{F}}(Y)$ . Thus, a change of variables gives

$$\begin{aligned} [d_{\mathcal{W},p}^{\mathcal{D}}(\mathbf{U}_{n,k}^{\mathfrak{F}}(X), \mathbf{U}_{n,k}^{\mathfrak{F}}(Y))]^p &\leq \iint_{\mathbf{D}_{n,k}^{\mathfrak{F}}(X) \times \mathbf{D}_{n,k}^{\mathfrak{F}}(Y)} [d_{\mathcal{B}}(D, D')]^p \nu(dD \times dD') \\ &= \iint_{\mathbf{K}_n(X) \times \mathbf{K}_n(Y)} [d_{\mathcal{B}}(\mathrm{dgm}_k^{\mathfrak{F}}(M), \mathrm{dgm}_k^{\mathfrak{F}}(M'))]^p \mu(dM \times dM'). \end{aligned}$$

Recall from the proof of Theorem 3.12 that  $d_{\mathcal{B}}(\mathrm{dgm}_k^{\mathfrak{F}}(M), \mathrm{dgm}_k^{\mathfrak{F}}(M')) \leq \frac{L(\mathfrak{F})}{2} \|M - M'\|_{\infty}$ . Thus, the previous integral is bounded above by

$$\begin{aligned} \iint_{\mathbf{K}_n(X) \times \mathbf{K}_n(Y)} \left[ \frac{L(\mathfrak{F})}{2} \|M - M'\|_{\infty} \right]^p \mu(dM \times dM') \\ = \left( \frac{L(\mathfrak{F})}{2} \right)^p \iint_{\mathbf{K}_n(X) \times \mathbf{K}_n(Y)} \|M - M'\|_{\infty}^p \mu(dM \times dM') \\ < \left( \frac{L(\mathfrak{F})}{2} \right)^p \eta^p. \end{aligned}$$

Taking the  $p$ -th root and letting  $\eta \searrow d_{\mathcal{W},p}(\mu_n(X), \mu_n(Y))$  gives

$$d_{\mathcal{W},p}^{\mathcal{D}}(\mathbf{U}_{n,k}^{\mathfrak{F}}(X), \mathbf{U}_{n,k}^{\mathfrak{F}}(Y)) \leq \frac{L(\mathfrak{F})}{2} \cdot d_{\mathcal{W},p}(\mu_n(X), \mu_n(Y)) \leq L(\mathfrak{F}) \cdot \widehat{d}_{\mathcal{G}\mathcal{W},p}(X, Y).$$

□

## 4 VR-persistence sets

From this point on, we focus on the Vietoris-Rips persistence sets  $\mathbf{D}_{n,k}^{\text{VR}}$  with  $n = 2k + 2$ . The reason to do so is Theorem 4.4, which states that the  $k$ -dimensional persistence diagram of  $\text{VR}_*(X)$  is empty if  $|X| < 2k + 2$  and has at most one point if  $|X| = 2k + 2$ . What this means for persistence sets  $\mathbf{D}_{n,k}^{\text{VR}}(X)$  is that given a fixed  $k$ , the first interesting choice of  $n$  is  $n = 2k + 2$ . We prove this fact in Section 4.1 and then use it to construct a graphical representation of  $\mathbf{D}_{2k+2,k}^{\text{VR}}(X)$ . Section 4.2 presents computational examples.

### 4.1 Some properties of Vietoris-Rips complexes

Let  $X$  be a finite metric space with  $n$  points. The highest dimensional simplex of  $\text{VR}_*(X)$  has dimension  $n$ , but even if  $\text{VR}_*(X)$  contains  $k$ -dimensional simplices, it won't necessarily produce persistent homology in dimension  $k$ . A good example is  $n = 3$  and  $k = 1$ . The only simplicial 1-cycle in a triangle is the union of its three edges. In order for  $\text{VR}_r(X)$  to contain all three edges, we must have  $r \geq d_X(x_i, x_j)$  for all  $i \neq j$ . However, this condition is equivalent to  $r \geq \mathbf{diam}(X)$ , which makes  $\text{VR}_r(X)$  isomorphic to the 2-simplex, a contractible complex. In other words, either  $\text{VR}_r(X)$  doesn't contain any 1-cycle (when  $r < \mathbf{diam}(X)$ ) or it is contractible (when  $r \geq \mathbf{diam}(X)$ ), so the persistence module  $\text{PH}_1^{\text{VR}}(X)$  is 0. Among other things,  $X$  needs more points to produce persistent homology in dimension 1.

The first definition of this section is inspired by the structure of the cross-polytope  $\mathfrak{B}_m$ ; see Figure 6. Recall that a set  $\sigma \subset V = \{\pm e_1, \dots, \pm e_m\}$  is a face if it doesn't contain both  $e_i$  and  $-e_i$ . In particular, there is an edge between  $e_i$  and every other vertex except  $-e_i$ . The next definition tries to emulate this phenomenon in  $\text{VR}_*(X)$ .

**Definition 4.1.** Let  $(X, d_X)$  be a finite metric space,  $A \subset X$ , and let  $x_0 \in X$  fixed. Find  $x_1, x_2 \in A$  such that

$$d_X(x_0, x_1) \geq d_X(x_0, x_2) \geq d_X(x_0, a) \text{ for all } a \in A \setminus \{x_1, x_2\}.$$

Define

$$t_d(x_0, A) := d_X(x_0, x_1)$$

and

$$t_b(x_0, A) := d_X(x_0, x_2).$$

We set  $v_d(x_0, A) := x_1$  if  $x_1$  is unique. When  $A = X$  and there is no risk of confusion, we will denote  $t_b(x_0, X), t_d(x_0, X)$ , and  $v_d(x_0, X)$  simply as  $t_b(x_0), t_d(x_0)$ , and  $v_d(x_0)$ , respectively. Also define

$$t_b(X) := \max_{x \in X} t_b(x, X)$$

and

$$t_d(X) := \min_{x \in X} t_d(x, X).$$

In a few words,  $t_d(x) \geq t_b(x)$  are the two largest distances between  $x$  and any other point of  $X$ . The motivation behind these choices is that if  $r$  satisfies  $t_b(x) \leq r < t_d(x)$ , then  $\text{VR}_r(X)$  contains all edges between  $x$  and all other points of  $X$ , except for  $v_d(x)$ . If this holds for all  $x \in X$ , then  $\text{VR}_r(X)$  is isomorphic to a cross-polytope. Also, note that  $t_d(x)$  is the *radius*  $\mathbf{rad}(X)$  of  $X$ , cf. Definition 2.1. Also note that according to [LMO20, Proposition 9.6], the death time of *any* interval in  $\text{dgm}_*(X)$  is bounded by  $\mathbf{rad}(X)$ .

Of course, as defined above,  $v_d(x)$  is not unique in general, but it is well defined in the case that interests us, as we see next.

**Lemma 4.2.** *Let  $(X, d_X)$  be a finite metric space and suppose that  $t_b(X) < t_d(X)$ . Then  $v_d : X \rightarrow X$  is well defined and  $v_d \circ v_d = \text{id}$ .*

*Proof.* Given a point  $x \in X$ , suppose there exist  $x_1 \neq x_2 \in X$  such that  $d_X(x, x_1) = d_X(x, x_2) \geq d_X(x, x')$  for all  $x' \in X$ . Since  $t_b(x)$  and  $t_d(x)$  are the two largest distances between  $x$  and any  $x' \in X$ , we have  $t_b(x) = t_d(x)$ . However, this implies  $t_d(X) \leq t_d(x) = t_b(x) \leq t_b(X)$ , which contradicts the hypothesis  $t_b(X) < t_d(X)$ . Thus, we have a unique choice of  $v_d(x)$  for every  $x \in X$ .

For the second claim, suppose that  $v_d^2(x) := v_d(v_d(x)) \neq x$ . Since  $t_d(v_d(x))$  is the largest distance between  $v_d(x)$  and any other point of  $X$ ,  $t_d(v_d(x)) = d_X(v_d(x), v_d^2(x)) \geq d_X(v_d(x), x)$ . Hence, the second largest distance  $t_b(v_d(x))$  is at least  $d_X(x, v_d(x))$ . However,

$$t_d(X) \leq t_d(x) = d_X(x, v_d(x)) \leq t_b(v_d(x)) \leq t_b(X),$$

which is, again, a contradiction. Thus,  $v_d^2(x) = x$ . □

Once  $v_d$  is well defined, we can produce the desired isomorphism between  $\text{VR}_r(X)$  and a cross-polytope.

**Proposition 4.3.** *Let  $(X, d_X)$  be a metric space with  $|X| = n$ , where  $n \geq 2$  is even, and suppose that  $t_b(X) < t_d(X)$ . Let  $k = \frac{n}{2} - 1$ . Then  $\text{VR}_r(X)$  is isomorphic, as a simplicial complex, to the cross-polytope  $\mathfrak{B}_{k+1}$  for all  $r \in [t_b(X), t_d(X))$ .*

*Proof.* Let  $r \in [t_b(X), t_d(X))$ . Lemma 4.2 implies that we can partition  $X$  into  $k + 1$  pairs  $\{x_i^+, x_i^-\}$  such that  $x_i^- = v_d(x_i^+)$ , so define  $f : \{\pm e_1, \dots, \pm e_k\} \rightarrow X$  as  $f(\varepsilon \cdot e_i) = x_i^\varepsilon$ , for  $\varepsilon = \pm 1$ . Both cross-polytopes and Vietoris-Rips complexes are flag complexes, so it's enough to verify that  $f$  induces an isomorphism of their 1-skeleta. Indeed, for any  $i = 1, \dots, k + 1$ ,  $\varepsilon = \pm 1$ , and  $x \neq x_i^\varepsilon$ , we have  $d_X(x_i^\varepsilon, x) \leq t_b(x_i^\varepsilon) \leq t_b(X) \leq r < t_d(X) \leq t_d(x_i^\varepsilon) =$

$d_X(x_i^+, x_i^-)$ . Thus,  $\text{VR}_r(X)$  contains the edges  $[x_i^\varepsilon, x]$  for  $x \neq x_i^{-\varepsilon}$ , but not  $[x_i^+, x_i^-]$ . Since  $f(\varepsilon \cdot e_i) = x_i^\varepsilon$ ,  $f$  sends the simplices  $[\varepsilon \cdot e_i, v]$  to the simplices  $[x_i^\varepsilon, f(v)]$  and the non-simplex  $[e_i, -e_i]$  to the non-simplex  $[x_i^+, x_i^-]$ .  $\square$

A consequence of the previous proposition is that  $H_k(\text{VR}_r(X)) \simeq H_k(\mathfrak{B}_{k+1}) = \mathbb{F}$  for  $r \in [t_b(X), t_d(X))$ . It turns out that  $n = 2k + 2$  is the minimum number of points that  $X$  needs to have in order to produce persistent homology in dimension  $k$ , which is what we prove next. The proof is inspired by the use of the Mayer-Vietoris sequence to find  $H_k(\mathbb{S}^k)$  by splitting  $\mathbb{S}^k$  into two hemispheres that intersect in an equator  $\mathbb{S}^{k-1}$ . Since the hemispheres are contractible, the Mayer-Vietoris sequence produces an isomorphism  $H_k(\mathbb{S}^k) \simeq H_{k-1}(\mathbb{S}^{k-1})$ . We emulate this by splitting  $\text{VR}_r(X)$  into two halves which, under the right circumstances, are contractible and find the  $k$ -th persistent homology of  $\text{VR}_*(X)$  in terms of the  $(k - 1)$ -dimensional persistent homology of a subcomplex.

Two related results appear in [Kah09, Ada14, CCR13]. Case (1) in our Theorem 4.4 is a consequence of Lemma 5.3 in [Kah09] and Proposition 5.4 in [Ada14], and the decomposition  $\text{VR}_r(X) = \text{VR}_r(B_0) \cup \text{VR}_r(B_1)$  (see the proof for the definition of  $B_0$  and  $B_1$ ) already appears as Proposition 2.2 in the appendix of [CCR13]. The novelty in the next Theorem is the characterization of the persistent module  $\text{PH}_k^{\text{VR}}(X)$  in terms of  $t_b(X)$  and  $t_d(X)$ .

**Theorem 4.4.** *Let  $(X, d_X)$  be a metric space with  $n$  points. Here,  $\text{PH}_k^{\text{VR}}(X)$  denotes the reduced homology of the VR-complex:  $\tilde{H}_k(\text{VR}_*(X))$ . Then:*

1. For all integers  $k > \frac{n}{2} - 1$ ,  $\text{PH}_k^{\text{VR}}(X) = 0$ .
2. If  $n$  is even and  $k = \frac{n}{2} - 1$ , then

$$\text{PH}_k^{\text{VR}}(X) = \begin{cases} \mathbb{I}[t_b(X), t_d(X)) & \text{if and only if } t_b(X) < t_d(X), \\ 0 & \text{otherwise.} \end{cases}$$

**Example 4.5.**

Let us consider the case  $k = 1$  and  $n = 4$ . Let  $X = \{x_1, x_2, x_3, x_4\}$  as shown in Figure 8. In order for  $\text{PH}_1^{\text{VR}}(X)$  to be non-zero,  $\text{VR}_r(X)$  has to contain all the ‘‘outer edges’’ and none of the ‘‘diagonals’’. That is, there exists  $r > 0$  such that

$$d_{12}, d_{23}, d_{34}, d_{41} \leq r < d_{13}, d_{24}.$$

In other words, we require that  $\max(d_{12}, d_{23}, d_{34}, d_{41}) < \min(d_{13}, d_{24})$  and, in that case,  $\text{PH}_1^{\text{VR}}(X) = [\max(d_{12}, d_{23}, d_{34}, d_{41}), \min(d_{13}, d_{24}))$ . In our language, we have:

	$t_b$	$t_d$
$x_1$	$\max(d_{41}, d_{12})$	$d_{13}$
$x_2$	$\max(d_{12}, d_{23})$	$d_{24}$
$x_3$	$\max(d_{23}, d_{34})$	$d_{13}$
$x_4$	$\max(d_{34}, d_{41})$	$d_{24}$

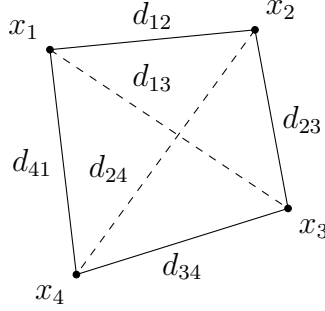


Figure 8: A generic metric space with 4 points. In order for  $\text{PH}_1^{\text{VR}}(X)$  to be non-zero, the two “diagonals”  $d_{13}, d_{24}$  should be larger than the outer edges  $d_{12}, d_{23}, d_{34}, d_{41}$ .

From these, we get  $t_b(X) = \max(d_{12}, d_{23}, d_{34}, d_{41})$ ,  $t_d(X) = \min(d_{13}, d_{24})$ , and  $\text{PH}_1(X) = \mathbb{I}[t_b(X), t_d(X))$ . We also have  $v_d(x_1) = x_3$ ,  $v_d(x_2) = x_4$ , and  $v_d \circ v_d = \text{id}$ .

However, if we had  $d_{12}, d_{23}, d_{34} < d_{24} < d_{41} < d_{13}$  for example, then the 2-simplex  $[x_2, x_3, x_4]$  appears before the would-be generator  $[x_1, x_2] + [x_2, x_3] + [x_3, x_4] + [x_4, x_1]$ , and  $\text{PH}_1^{\text{VR}}(X) = 0$ . In this case,

	$t_b$	$t_d$
$x_1$	$d_{41}$	$d_{13}$
$x_2$	$\max(d_{12}, d_{23})$	$d_{24}$
$x_3$	$\max(d_{23}, d_{34})$	$d_{13}$
$x_4$	$d_{24}$	$d_{41}$

Thus,  $t_b(X) = d_{41} > d_{24} = t_d(X)$ , and  $v_d(x_2) = x_4$  but  $v_d(x_4) = x_1 \neq x_2$ .

In general, we want to partition  $X$  into pairs of “opposite” points, that is pairs  $x, y$  such that  $v_d(x) = y$  and  $v_d(y) = x$ . Intuitively, this says that the diagonals are larger than every other edge. If not, as in the second case, then no persistence is produced. As for  $k = 1$  and  $n = 4$ , we will generally label the points as  $x_1, x_2, x_3, x_4$  in such a way that

$$t_b(X) = \max(d_{12}, d_{23}, d_{34}, d_{41}) \text{ and}$$

$$t_d(X) = \min(d_{13}, d_{24}).$$

*Proof of Theorem 4.4.* The proof is by induction on  $n$ . If  $n = 1$ ,  $\text{VR}_r(X)$  is contractible for all  $r$ , and so  $\text{PH}_k^{\text{VR}}(X) = 0$  for all  $k \geq 0 > \frac{n}{2} - 1$ . If  $n = 2$ , let  $X = \{x_0, x_1\}$ . The space  $\text{VR}_r(X)$  is two discrete points when  $r \in [0, \mathbf{diam}(X))$  and an interval when  $r \geq \mathbf{diam}(X)$ . Then  $\text{PH}_k^{\text{VR}}(X) = 0$  for all  $k \geq 1 > \frac{n}{2} - 1$ , and  $\text{PH}_0^{\text{VR}}(X) = \mathbb{I}[0, \mathbf{diam}(X))$ . Furthermore, this interval module equals  $\mathbb{I}[t_b(X), t_d(X))$  because  $d_X(x_0, x_1) > d_X(x_0, x_0) = 0$ , so  $t_b(x_0) = 0$  and  $t_d(x_0) = d_X(x_0, x_1)$ . The same holds for  $x_1$ , so  $t_b(X) = 0$  and  $t_d(X) = d_X(x_0, x_1) = \mathbf{diam}(X)$ .

For the inductive step, assume that the proposition holds for every metric space with less than  $n$  points. Fix  $X$  with  $|X| = n$  and an integer  $k \geq \frac{n}{2} - 1$ .  $\text{VR}_r(X)$  is contractible when  $r \geq \mathbf{diam}(X)$ , so let  $r < \mathbf{diam}(X)$  and choose any pair  $x_0, x_1 \in X$  such that  $d_X(x_0, x_1) =$



Since  $\partial_*$  in (4.1) is also an injection,  $\tilde{H}_k(\text{VR}_r(X)) = 0$  for  $r \in [t_b(A), b)$ . Next, if  $r < t_b(A)$  or  $t_d(A) \leq r < \mathbf{diam}(X)$ ,  $\tilde{H}_k(\text{VR}_r(A)) = 0$ , so  $\tilde{H}_k(\text{VR}_r(X)) = 0$  from the Mayer-Vietoris sequence. Lastly, if  $r \geq \mathbf{diam}(X)$ , then  $\text{VR}_r(X)$  is contractible. Altogether, these cases give  $\text{PH}_k^{\text{VR}}(X) = \mathbb{I}[b, t_d(A)]$ . If, on the other hand,  $b \geq t_d(A)$ , we obtain  $\text{PH}_k^{\text{VR}}(X) = 0$  by using the above cases for  $r \in [0, t_b(A))$ ,  $r \in [t_b(A), b)$  (if  $t_b(A) < b$ ), and  $r \in [t_d(A), \infty)$ .

The last thing left to check is that  $\text{VR}_*(X)$  produces persistent homology precisely when  $t_b(X) < t_d(X)$ . So far we have  $\text{PH}_k^{\text{VR}}(X) = \mathbb{I}[b, t_d(A)]$  if, and only if,  $b < t_d(A)$ , so now we show that  $t_b(X) < t_d(X)$  is equivalent to  $b < t_d(A)$ . First, suppose that  $b < t_d(A)$ . For every  $a \in A$  and  $j = 0, 1$ , we have  $d_X(a, x_j) \leq b < t_d(A) \leq t_d(a, A)$  by definition of  $b$ . Also, for every  $a' \neq v_d(a, A)$  we have  $d_X(a, a') \leq t_b(a, A) < t_d(a, A)$ . In other words, for every  $x \in X \setminus \{v_d(a, A)\}$ ,  $d_X(a, x) < t_d(a, A)$ , which means that the point in  $X$  furthest away from  $a$  is still  $v_d(a, A) \in A$ . Thus,  $t_d(a, X) = t_d(a, A)$  and  $t_b(a, X) = \max[t_b(a, A), d_X(a, x_0), d_X(a, x_1)]$ . Additionally,  $d_X(x_0, x_1) = \mathbf{diam}(X)$ , so clearly  $v_d(x_0, X) = x_1$  and  $t_b(x_j, X) = \max_{a \in A} d_X(x_j, a)$ . Thus,

$$t_d(X) = \min \left\{ t_d(x_0, X), t_d(x_1, X), \min_{a \in A} t_d(a, X) \right\} = \min \left\{ \mathbf{diam}(X), \min_{a \in A} t_d(a, A) \right\} = t_d(A),$$

and

$$\begin{aligned} b &= \max \left[ t_b(A), \max_{a \in A} d_X(x_0, a), \max_{a \in A} d_X(x_1, a) \right] \\ &= \max \left[ \max_{a \in A} t_b(a, A), \max_{a \in A} d_X(x_0, a), \max_{a \in A} d_X(x_1, a) \right] \\ &= \max \left[ \max_{a \in A} t_b(a, X), t_b(x_0, X), t_b(x_1, X) \right] \\ &= t_b(X). \end{aligned}$$

In conclusion,  $t_b(X) = b < t_d(A) = t_d(X)$ , and  $\text{PH}_k^{\text{VR}}(X) = \mathbb{I}[t_b(X), t_d(X)]$ .

Now suppose  $b \geq t_d(A)$ . Let  $a_0 \in A$  such that  $t_d(A) = t_d(a_0, A)$ . Notice that  $t_d(a_0, X)$  can differ from  $t_d(a_0, A)$  if  $d_X(a_0, x_j) \geq d_X(a_0, v_d(a_0, A))$  for some  $j = 0, 1$ . However, we have  $b \geq d_X(a_0, x_j)$  by definition, so  $b$  would still be greater than  $t_d(a_0, X)$  even if  $t_d(a_0, X) \neq t_d(a_0, A)$ . With this in mind, we have two cases depending on whether  $b = t_b(A)$  or not. If they are equal, notice that  $t_b(a, A) \leq t_b(a, X)$  for every  $a \in A$  because  $t_b(a, X)$  takes the maximum over a larger set than  $t_b(a, A)$  does. Then

$$t_b(X) \geq t_b(A) = b \geq t_d(a_0, X) \geq t_d(X).$$

If  $b > t_b(A)$  instead, write  $b = d_X(a_1, x_j)$ , where  $a_1 \in A$  and  $j$  is either 0 or 1. Observe that  $t_d(x_j, X) = \mathbf{diam}(X) \geq d_X(a_1, x_j)$ , so  $t_b(x_j, X) \geq d_X(a_1, x_j)$ . Then

$$t_b(X) \geq t_b(x_j, X) \geq d_X(a_1, x_j) = b \geq t_d(a_2, X) \geq t_d(X).$$

In either case,  $t_b(X) \geq t_d(X)$ , as desired. This completes the proof.  $\square$

**Remark 4.6 (A geometric algorithm for computing  $\text{PH}_k^{\text{VR}}(X)$  when  $|X| = n$  and  $k = \frac{n}{2} - 1$ ).** Recall that  $t_b(x)$  and  $t_d(x)$  are the two greatest distances from  $x$  to every other point in  $X$ . Both can be found in at most  $(n - 1) + (n - 2) = 2n - 3$  steps because finding a maximum takes as many steps as the number of entries. We compute both quantities for each of the  $n$  points in  $X$ , and then find  $t_b(X) = \min_{x \in X} t_b(x)$  and  $t_d(X) = \min_{x \in X} t_d(x)$  in  $n$  steps each. After comparing  $t_b(X)$  and  $t_d(X)$ , we are able to determine whether  $\text{PH}_k^{\text{VR}}(X)$  is equal to  $\mathbb{I}[t_b(X), t_d(X))$  or to 0 in at most  $n(2n - 3) + 2n + 1 = 2n^2 - n + 1 = O(n^2)$  steps. This is a significant improvement from the bound  $O(n^{\omega(k+2)})$  given in [MMS11] (cf. Remark 3.15). Indeed, using  $n = 2k + 2$ , our custom tailored algorithm incurs a cost  $O(k^2)$  whereas the standard algorithm incurs the much larger cost  $\approx O((2k)^{\omega(k+2)})$ . You can see a `parfor` based Matlab implementation in our github repository [GM21].

## 4.2 Computational examples

Theorem 4.4 has two consequences for VR-persistence sets. The first is the following corollary.

**Corollary 4.7.** *Let  $X$  be any metric space and  $k \geq 0$ .  $\mathbf{D}_{n,k}^{\text{VR}}(X)$  is empty for all  $n < 2k + 2$ .*

This means that the first interesting choice of  $n$  is  $n = 2k + 2$ , and in that case, any sample  $Y \subset X$  with  $|Y| = n$  will produce at most one point in its persistence diagram. What's more, this allows us to visualize  $\mathbf{D}_{2k+2,k}^{\text{VR}}(X)$  by taking all possible such samples  $Y \subset X$  and plotting their persistence diagrams in the same axis; see Figure 4. In other words, we plot  $\mathbf{D}_{2k+2,k}^{\text{VR}}(X)$  as a subset of  $\mathbb{R}^2$  where each point  $(t_b, t_d) \in \mathbf{D}_{2k+2,k}^{\text{VR}}(X)$  corresponds to a possibly non-unique  $n$ -point sample  $Y \subset X$  such that  $\text{dgm}_k^{\text{VR}}(Y) = \{(t_b, t_d)\}$ ; see Figure 5 for an example. We can take this one step further and color the graph according to the density of the points to obtain a plot of the persistence measure  $\mathbf{U}_{4,1}^{\text{VR}}(X)$ . For these reasons, we give a name to this particular persistence set.

**Notation:**  $\mathbf{D}_{2k+2,k}^{\text{VR}}(X)$  and  $\mathbf{U}_{2k+2,k}^{\text{VR}}(X)$  are called, respectively, the *principal persistence set* and the *principal persistence measure* of  $X$  in dimension  $k$ .

Figure 9 shows computational approximations to the principal persistence measure  $\mathbf{U}_{4,1}^{\text{VR}}$  of  $\mathbb{S}^1$ ,  $\mathbb{S}^2$ , and  $\mathbb{T}^2 = \mathbb{S}^1 \times \mathbb{S}^1$ . The spheres are equipped with their usual Riemannian metrics  $d_{\mathbb{S}^1}$  and  $d_{\mathbb{S}^2}$  respectively. As for the torus, we used the  $\ell^2$  product metric defined as

$$d_{\mathbb{T}^2}((\theta_1, \theta_2), (\theta'_1, \theta'_2)) := \sqrt{(d_{\mathbb{S}^1}(\theta_1, \theta'_1))^2 + (d_{\mathbb{S}^1}(\theta_2, \theta'_2))^2},$$

for all  $(\theta_1, \theta_2), (\theta'_1, \theta'_2) \in \mathbb{T}^2$ . The diagrams were computed using a MATLAB wrapper<sup>3</sup> for Ripser [Bau19] developed by C. Tralie using over 1,000,000 random 4-tuples of points. It should be noted that only about 12% of those configurations generated a non-diagonal point.

We can observe the functoriality property  $\mathbf{D}_{n,k}^{\text{VR}}(X) \subset \mathbf{D}_{n,k}^{\text{VR}}(Y)$  whenever  $X \hookrightarrow Y$  in these

<sup>3</sup>The MATLAB wrapper was adapted from the one found in <https://github.com/ctralie/Math412S2017>.

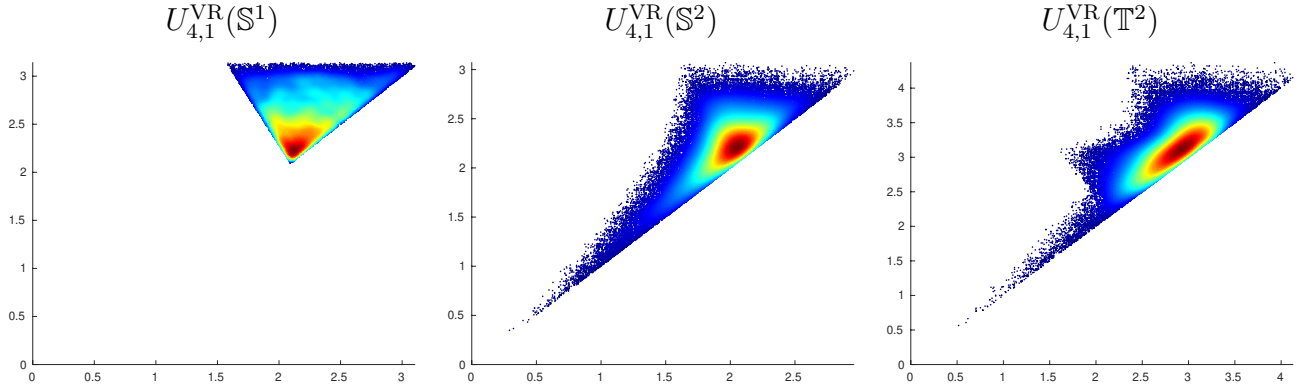


Figure 9: From left to right: computational approximations to the 1-dimensional persistence measures  $U_{4,1}^{\text{VR}}(\mathbb{S}^1)$ ,  $U_{4,1}^{\text{VR}}(\mathbb{S}^2)$ , and  $U_{4,1}^{\text{VR}}(\mathbb{T}^2)$ . The colors represent the density of points in the diagram. The support of each measure (that is, the colored region) is the persistence set  $\mathbf{D}_{4,1}^{\text{VR}}$  of the corresponding metric space. Notice how these results agree with the functoriality property (cf. Remark 3.10): namely, that the persistence set of  $\mathbb{S}^1$  is a subset of the respective persistence sets of  $\mathbb{S}^2$  and  $\mathbb{T}^2$ .

graphs. Notice that  $\mathbb{S}^1$  embeds into  $\mathbb{S}^2$  as the equator, and as slices  $\mathbb{S}^1 \times \{x_0\}$  and  $\{x_0\} \times \mathbb{S}^1$  in  $\mathbb{T}^2$ . The effect on the persistence sets is that a copy of  $\mathbf{D}_{4,1}^{\text{VR}}(\mathbb{S}^1)$  appears in both  $\mathbf{D}_{4,1}^{\text{VR}}(\mathbb{S}^2)$  and  $\mathbf{D}_{4,1}^{\text{VR}}(\mathbb{T}^2)$ .

## 5 VR-Persistence sets of spheres

In this section, we will describe the principal persistence sets  $\mathbf{D}_{2k+2,k}^{\text{VR}}(\mathbb{S}^1)$  for all  $k \geq 0$ . After that, we will take advantage of functoriality to find some of the persistence sets of the higher dimensional spheres  $\mathbb{S}^m$ ,  $m \geq 2$ , and describe the limitations (if any) to obtain higher principal persistence sets. We begin with a general technical lemma.

**Lemma 5.1.** *Let  $k \geq 0$  and  $n = 2k + 2$ . Let  $(X, d_X)$  be a metric space with  $n$  points. Then:*

1.  $t_d(X) \leq 2t_b(X)$ .
2.  $\text{pers}(\text{dgm}_k^{\text{VR}}(X)) = t_d(X) - t_b(X) \leq \mathbf{sep}(X)$ .
3. *If  $X$  can be isometrically embedded on an interval, then  $t_b(X) \geq t_d(X)$ .*

*Proof.*

1. If  $t_b(X) \geq t_d(X)$ , then  $\text{pers}(\text{dgm}_k^{\text{VR}}(X)) = 0$  and items 1 and 2 are trivially true. Suppose, then,  $t_b(X) < t_d(X)$ . Choose any  $x_0, x \in X$  such that  $x \neq x_0, v_d(x_0)$ . By definition of  $v_d(x_0)$ , we have  $d_X(x_0, x) \leq t_b(x_0)$  and  $d_X(x, v_d(x_0)) \leq t_b(v_d(x_0))$ . Then

$$\begin{aligned}
 d_X(x_0, x) &\geq d_X(x_0, v_d(x_0)) - d_X(x, v_d(x_0)) \\
 &\geq t_d(x_0) - t_b(v_d(x_0)) \\
 &\geq t_d(X) - t_b(X).
 \end{aligned}$$

Since  $d_X(x_0, x) \leq t_b(X)$ , we get the coarse bound  $t_d(X) \leq 2t_b(X)$ .

2. The finer bound  $\mathbf{sep}(X) \geq t_d(X) - t_b(X) = \text{pers}(\text{dgm}_k^{\text{VR}}(X))$  follows by taking the minimum of  $d_X(x_0, x)$  over  $x_0$  and  $x$ .

3 Suppose, without loss of generality, that  $X \subset \mathbb{R}$  and that  $x_1 < x_2 < \dots < x_n$ . Notice that  $t_d(x_k) = \max(x_k - x_1, x_n - x_k)$  and, in particular,  $t_d(x_1) = t_d(x_n) = x_n - x_1$ . If  $k \neq 1, n$ , then  $t_b(x_1) \geq x_k - x_1$  and  $t_b(x_n) \geq x_n - x_k$ . Then

$$t_b(X) \geq \max(t_b(x_1), t_b(x_n)) \geq \max(x_k - x_1, x_n - x_k) = t_d(x_k) \geq t_d(X).$$

□

## 5.1 Characterization of $t_b(X)$ and $t_d(X)$ for $X \subset \mathbb{S}^1$

Now we focus on subsets of the circle. We model  $\mathbb{S}^1$  as the quotient  $[0, 2\pi]/0 \sim 2\pi$  equipped with the geodesic distance, *i.e.*

$$d_{\mathbb{S}^1}(x, y) = \min(|x - y|, 2\pi - |x - y|).$$

We define a *cyclic order*  $\prec$  on  $\mathbb{S}^1$  by saying that  $x \prec y \prec z$  if, when viewing  $x, y, z$  as elements of  $[0, 2\pi]$ , we have one of the three choices of  $0 \leq x < y < z$ ,  $x < 2\pi$  and  $0 \leq y < z$ , or  $x < y < 2\pi$  and  $0 \leq z$ . In other words, if we define counter-clockwise to be the increasing direction in  $[0, 2\pi]$ , then  $x \prec y \prec z$  means that the counter-clockwise path starting at  $x$  meets  $y$  before reaching  $z$ . We also use  $\preceq$  to allow the points to be equal.

Throughout this section,  $k \geq 1$  and  $n = 2k + 2$  will be fixed. Let  $X = \{x_1, x_2, \dots, x_n\} \subset \mathbb{S}^1$  such that  $x_i \prec x_{i+1} \prec x_{i+2}$  for all  $i$  (addition is done modulo  $n$ ). Write  $d_{ij} = d_{\mathbb{S}^1}(x_i, x_j)$  for the distances, and assume  $t_b(X) < t_d(X)$ .

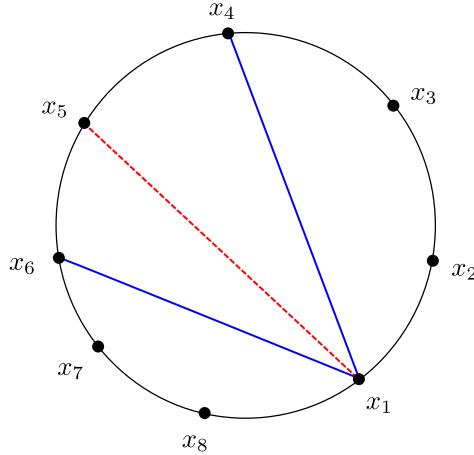


Figure 10: This configuration shows the edges that realize  $t_b(x_1) = \max(d_{1,1+3}, d_{1,1-3})$  and  $t_d(x_1) = d_{1,1+3+1}$  in the case  $k = 3$  and  $n = 8$ . In this figure, the shortest path between  $x_1$  and  $x_5$  contains  $x_8, x_7, x_6$ , so when  $r > d_{15}$ ,  $\text{VR}_r(X)$  will contain a 4-simplex. These ideas were inspired by [Kat91].

**Lemma 5.2.**

1. For any  $i$ , and  $t_b(x_i) = \max(d_{i,i+k}, d_{i,i-k})$  and  $t_d(x_i) = d_{i,i+k+1}$ .
2. For any  $X \subset \mathbb{S}^1$  with  $|X| = 2k + 2$ ,

$$t_b(X) = \max_{i=1,\dots,n} d_{i,i+k}$$

and

$$t_d(X) = \min_{i=1,\dots,n} d_{i,i+k+1}.$$

3. For all  $i$ ,  $d_{i,i+k} = d_{i,i+1} + d_{i+1,i+2} + \dots + d_{i+k-1,i+k}$ .
4.  $t_b(X) \geq \frac{k}{k+1}\pi$ .

*Proof.* 1 Let  $r \in [t_b(X), t_d(X)]$ . By Proposition 4.3,  $\text{VR}_r(X)$  is a cross-polytope with  $n$  points. In particular,  $\text{VR}_r(X)$  contains no simplices of dimension  $k + 1$ . We claim that this forces  $t_d(x_i) = d_{i,i+k+1}$  for all  $i$ . Indeed, the shortest path between  $x_i$  and  $x_{i+k+1}$  contains either the set  $\{x_{i+1}, \dots, x_{i+k-1}\}$  or the set  $\{x_{i+k+2}, \dots, x_{i-1}\}$  (see Figure 10). For any  $x_j$  in that shortest path,  $d_{i,j} \leq d_{i,i+k+1}$ , so if we had  $d_{i,i+k+1} \leq r$ ,  $\text{VR}_r(X)$  would contain a  $k + 1$  simplex, either  $[x_i, x_{i+1}, \dots, x_{i+k+1}]$  or  $[x_{i+k+1}, x_{i+k+2}, \dots, x_i]$ . Thus,  $r < d_{i,i+k+1}$  for all  $i$ .

In particular,  $\text{VR}_r(X)$  doesn't contain the edge  $[x_i, x_{i+k+1}]$ . According to definition 2.14, cross-polytopes contain all edges incident on a fixed point  $x_i$  except one, so  $[x_i, x_j] \in \text{VR}_r(X)$  for all  $j \neq i+k+1$ . In consequence,  $d_{i,j} \leq r < d_{i,i+k+1}$  for all  $j \neq i+k+1$ , so  $t_d(x_i) = d_{i,i+k+1}$  and  $t_b(x_i) = \max_{j \neq i+k+1} d_{i,j}$ . Additionally, the shortest path between  $x_i$  and  $x_{i+k}$  contains the set  $\{x_{i+1}, \dots, x_{i+k-1}\}$  rather than  $\{x_{i+k+2}, \dots, x_{i-1}\}$ , so  $d_{i,i+j} \leq d_{i,i+k}$  for  $j = 1, \dots, k-1$  (otherwise,  $\text{VR}_r(X)$  would contain the  $k + 2$  simplex  $[x_{i+k}, x_{i+k+1}, \dots, x_i]$ ). The analogous statement  $d_{i,i-j} \leq d_{i,i-k}$  holds for  $j = 1, 2, \dots, k-1$ . Thus,  $t_b(x_i) = \max(d_{i,i+k}, d_{i,i-k})$ .

2. These equations follow by taking the maximum (resp. minimum) over all  $i$  of the above expression for  $t_b(x_i)$  (resp.  $t_d(x_i)$ ), as per Definition 4.1.

3. As we saw in the proof of item 1, the shortest path from  $x_i$  to  $x_{i+k}$  contains the set  $\{x_{i+1}, \dots, x_{i+k-1}\}$ . The length of this path is  $d_{i,i+k} = d_{i,i+1} + \dots + d_{i+k-1,i+k}$ .

4. By items 2 and 3,

$$nt_b(X) \geq \sum_{i=1}^n d_{i,i+k} = \sum_{i=1}^n \sum_{j=1}^k d_{i+j-1,i+j} = \sum_{j=1}^k \sum_{i=1}^n d_{i+j-1,i+j} = k \cdot 2\pi.$$

Thus,  $t_b(X) \geq \frac{2k}{n}\pi = \frac{k}{k+1}\pi$ .

□

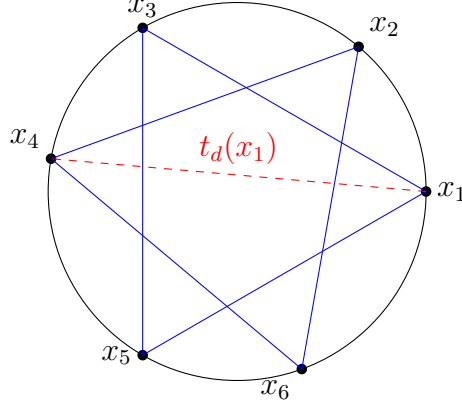


Figure 11: Example of a critical configuration for  $k = 2$ . The solid blue lines all have length  $t_b(X) = 2\pi/3$ , while the dotted red line has length  $t_d(X)$ . Notice that two regular  $(k + 1)$ -gons are formed.

## 5.2 Characterization of $\mathbf{D}_{2k+2,k}^{\text{VR}}(\mathbb{S}^1)$ for $k$ even

Lemma 5.2 shows that every configuration has  $t_b(X) \geq \frac{k}{k+1}\pi$ . The converse holds in the case that  $k$  is even. We obtain the proof by exhibiting configurations such that  $t_b(X) = t_b$  and  $t_d(X) = t_d$  for every pair of values  $t_b, t_d$  with  $\frac{k}{k+1}\pi \leq t_b < t_d \leq \pi$ .

**Theorem 5.3.**  $\mathbf{D}_{2k+2,k}^{\text{VR}}(\mathbb{S}^1) = \left\{ (t_b, t_d) : \frac{k}{k+1}\pi \leq t_b < t_d \leq \pi \right\}$ .

*Proof.* We will first construct what we call the critical configurations, those where  $t_b(X) = \frac{k}{k+1}\pi$  and  $t_d(X) = t_d \in (t_b(X), \pi]$ . Consider the points

$$x_i = \begin{cases} \frac{\pi}{k+1} \cdot (i-1), & i \text{ odd} \\ \frac{\pi}{k+1} \cdot (i-1) - (\pi - t_d), & i \text{ even,} \end{cases}$$

for  $i = 1, \dots, n$ . If  $i$  is odd, clearly  $x_{i-1} < x_i$ . If  $i$  is even,  $x_i - x_{i-1} = -\frac{k\pi}{k+1} + t_d > 0$  because of Lemma 5.2 item 4 and the assumption that  $t_d > t_b$ . Thus,  $x_1 < x_2 < \dots < x_n$ . Additionally, since  $t_d \leq \text{diam}(\mathbb{S}^1)$ , we have  $x_{2k+2} = \frac{k\pi}{k+1} + t_d \leq \frac{(2k+1)\pi}{k+1} < 2\pi$ , so we also have  $x_i < x_{i+1} < x_{i+2}$  for all  $i$ .

Since  $k$  is even,  $i$  and  $i+k$  have the same parity,

$$d_{i,i+k} = |x_{i+k} - x_i| = \frac{\pi}{k+1} [(i+k-1) - (i-1)] = \frac{k\pi}{k+1}.$$

Thus,  $t_b(X) = \max_i d_{i,i+k} = \frac{k}{k+1}\pi$ . To find  $t_d(X) = \min_i d_{i,i+k+1}$ , we have two cases depending on the parity of  $i$ . If  $i \leq k+1$  is odd (and  $i+k+1 \leq 2k+2$  even),

$$d_{i,i+k+1} = |x_{i+k+1} - x_i| = \frac{1}{k+1}\pi [(i+k) - (i-1)] - (\pi - t_d) = t_d,$$

and if  $i \leq k + 1$  is even,

$$d_{i,i+k+1} = 2\pi - |x_{i+k+1} - x_i| = 2\pi - \left| \frac{1}{k+1}\pi[(i+k) - (i-1)] + (\pi - t_d) \right| = t_d.$$

Thus,  $t_d(X) = t_d$ .

Lastly, we can use these critical configurations to construct  $X'$  such that  $t_b(X') = t_b > \frac{k}{k+1}\pi$ . Let  $\varepsilon := t_b - \frac{k}{k+1}\pi > 0$ , and take  $x'_{k+1} = x_{k+1} + \varepsilon$  and  $x'_i = x_i$  for  $i \neq k+1$ . Write  $d'_{ij} = d_{\mathbb{S}^1}(x'_i, x'_j)$ . Since  $t_b < t_d$ , we have  $d_{\mathbb{S}^1}(x_{k+1}, x'_{k+1}) = \varepsilon < t_d - \frac{k\pi}{k+1} = d_{\mathbb{S}^1}(x_{k+1}, x'_{k+2})$ , so  $x'_k = x_k \prec x_{k+1} \prec x'_{k+1} \prec x'_{k+2}$ . As for  $t_b(x'_{k+1})$  and  $t_d(x'_{k+1})$ , we have

$$\begin{aligned} d'_{k+1,1} &= d_{k+1,1} + \varepsilon = \frac{k}{k+1}\pi + \varepsilon = t_b, \\ d'_{k+1,2k+1} &= d_{k+1,2k+1} - \varepsilon = \frac{k}{k+1}\pi - \varepsilon < t_b, \text{ and} \\ d'_{k+1,2k+2} &= d_{k+1,2k+2} + \varepsilon = t_d + \varepsilon > t_d. \end{aligned}$$

Thus,  $t_b(X') = \max d'_{i,i+k} = t_b$  and  $t_d(X') = \min d'_{i,i+k+1} = t_d$ , as desired.  $\square$

### 5.3 Characterization of $\mathbf{D}_{2k+2,k}^{\text{VR}}(\mathbb{S}^1)$ for $k$ odd

An important difference between even and odd  $k$  is that only for even  $k$  can we find configurations that have the minimal possible birth time  $t_b(X) = \frac{k}{k+1}\pi$  given any  $t_d \in (t_b(X), \pi]$ . The difference is that sequences of the form  $x_i, x_{i+k}, x_{i+2k}, \dots$  eventually reach all points when  $k$  is odd, but only half of them when  $k$  is even (see Figure 11). This allows us to separate  $X \subset \mathbb{S}^1$  into two regular  $(k+1)$ -gons with fixed  $t_b(X)$  and it still allows control on  $t_d(X)$ , as shown in Proposition 5.3. For odd  $k$ , we will instead use an idea from Proposition 5.4 of [AA17]. We won't need the result in its full generality, so we only use part of its argument to provide a bound for  $t_b(X)$  in terms of  $t_d(X)$ .

**Theorem 5.4.** *Let  $k$  be an odd positive integer. Then  $t_d(X) \geq (k+1)(\pi - t_b(X))$ .*

*Proof.* Fix  $i \in \{1, \dots, n\}$ . Let  $r \geq \frac{k}{k+1}\pi$  and  $\delta = r - \frac{k-1}{k}\pi$ . Notice that  $k^2 = \frac{1}{2}(k-1) \cdot n + 1$ , so the path that passes through the points  $x_i, x_{i+k}, \dots, x_{i+k \cdot k}$  makes  $\frac{1}{2}(k-1)$  revolutions around the circle and stops at  $x_{i+k^2} = x_{i+1}$ . At the same time,  $d_{\ell, \ell+k} \leq t_b(X)$ . These facts give:

$$\frac{1}{2}(k-1) \cdot 2\pi + d_{i,i+1} = \sum_{j=1}^k d_{i+(j-1)k, i+jk} \leq kt_b(X).$$

Thus,  $(k-1)\pi + \max_{i=1, \dots, n} d_{i,i+1} \leq kt_b(X)$ .

By Lemma 5.2, there exists an  $\ell$  for which  $d_{\ell, \ell+k+1} = t_d(X)$ . Let  $\gamma$  be the path between  $x_\ell$  and  $x_{\ell+k+1}$  such that  $d_{\ell, \ell+k+1} + |\gamma| = 2\pi$ . Assume, without loss of generality, that  $\gamma$  contains  $x_{\ell+1}$ . This means that  $|\gamma| = d_{\ell, \ell+1} + d_{\ell+1, \ell+k+1}$ , so

$$d_{\ell, \ell+1} = |\gamma| - d_{\ell+1, \ell+k+1} = 2\pi - t_d(X) - d_{\ell+1, \ell+k+1} \geq 2\pi - t_d(X) - t_b(X).$$

Thus,  $kt_b(X) \geq (k-1)\pi + \max_{i=1, \dots, n} d_{i,i+1} \geq (k+1)\pi - t_d(X) - t_b(X)$ . Solving this inequality for  $t_d(X)$  gives the result.  $\square$

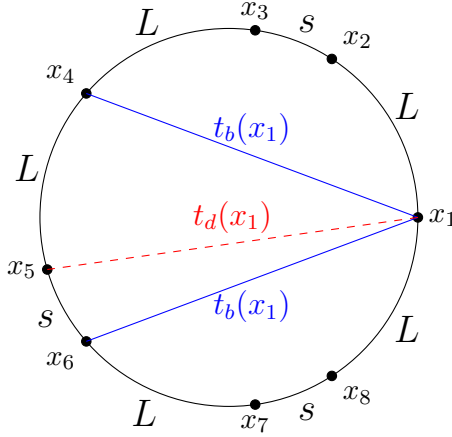


Figure 12: Example of a critical configuration for  $k = 3$ . Notice that  $t_b(X) = 2L + s$  and  $t_d(X) = 2L + 2s$ .

The critical configurations are easier to describe in terms of the distances between consecutive points. Given  $0 < t_b < t_d \leq \pi$  such that  $t_d = (k+1)(\pi - t_b)$ , let  $L = kt_b - (k-1)\pi$  and  $s = -(k+2)t_b + (k+1)\pi$ . Set  $x_1 = 0$  and define

$$x_{i+1} = \begin{cases} x_i + L, & i \leq k \text{ odd or } i > k \text{ even,} \\ x_i + s, & i < k \text{ even or } i > k \text{ odd} \end{cases}$$

for  $i = 1, \dots, 2k+2$ . In this setup,  $d_{12} = L, d_{23} = s, \dots, d_{k,k+1} = L$ , then  $d_{k+1,k+2} = L$ , and the pattern resumes after the repetition:  $d_{k+2,k+3} = s, d_{k+3,k+4} = L, \dots, d_{2k+1,2k+2} = s$ . Notice that  $x_{2k+2} = (k+1)L + ks = 2\pi - L$ , so  $d_{2k+2,1} = L$ .

Now we verify  $t_b(X) = t_b$  and  $t_d(X) = t_d$ . Recall that  $d_{i,i+k} = d_{i,i+1} + \dots + d_{i+k-1,i+k}$  from Lemma 5.2 item 3. It can then be shown that  $d_{i,i+k} = (\frac{k+1}{2})L + (\frac{k-1}{2})s$  when  $i \neq k+2$ , and  $d_{k+2,2k+2} = (\frac{k-1}{2})L + (\frac{k+1}{2})s$ . Since  $s \leq L$ ,  $t_b(X) = (\frac{k+1}{2})L + (\frac{k-1}{2})s = t_b$ . To find  $t_d(X)$ , let  $\gamma_i$  be the path from  $x_i$  to  $x_{i+k+1}$  that passes through  $x_{i+1}$ . The distance  $d_{i,i+k+1}$  is then the minimum of  $|\gamma_i| = d_{i,i+1} + \dots + d_{i+k,i+k+1}$  and  $|\gamma_{i+k+1}| = d_{i+k+1,i+k+2} + \dots + d_{i-1,i}$ . It can be verified that

$$|\gamma_i| = \begin{cases} (\frac{k+3}{2})L + (\frac{k-1}{2})s, & i < k+1 \text{ odd or } i > k+1 \text{ even,} \\ (\frac{k+1}{2})L + (\frac{k+1}{2})s, & i \leq k+1 \text{ even or } i > k+1 \text{ odd.} \end{cases}$$

Recall that  $k$  is odd, so regardless of the parity of  $i$ , we have

$$\begin{aligned} d_{i,i+k+1} &= \min\{|\gamma_i|, |\gamma_{i+k+1}|\} \\ &= \min\{(\frac{k+3}{2})L + (\frac{k-1}{2})s, (\frac{k+1}{2})L + (\frac{k+1}{2})s\} \\ &= (\frac{k+1}{2})L + (\frac{k+1}{2})s \\ &= (k+1)(\pi - t_b(X)). \end{aligned}$$

Thus,  $t_d(X) = (k+1)(\pi - t_b(X))$ .

**Theorem 5.5.** *For odd  $k$ ,*

$$\mathbf{D}_{2k+2,k}^{\text{VR}}(\mathbb{S}^1) = \{(t_b, t_d) : (k+1)(\pi - t_b) \leq t_d \leq \pi \text{ and } t_b \leq t_d\}.$$

*Proof.* We got the inequality  $(k+1)(\pi - t_b) \leq t_d$  in Theorem 5.4 and showed that equality can be achieved in the preceding paragraph. To get a configuration where  $(k+1)(\pi - t_b) < t_d$ , construct the set  $X$  as above so that  $t_d(X) = t_d$  and  $t_b(X) = \pi - \frac{1}{k+1}t_d(X)$  is the smallest birth time possible with death time  $t_d(X)$ . Pick any  $t_b$  such that  $t_b(X) < t_b < t_d(X)$ , and let  $\varepsilon = t_b - t_b(X)$ . Define  $x'_1 = x_1 + \varepsilon$ ,  $x'_{k+2} = x_{k+2} + \varepsilon$ , and  $x'_i = x_i$  for  $i \neq 1, k+2$ . By Lemma 5.2,  $\varepsilon = t_b - t_b(X) < t_d(X) - t_b(X) = \text{pers}(\text{dgm}_k^{\text{VR}}(X)) \leq \mathbf{sep}(X)$ . Because of this,  $x'_1 = x_1 + \varepsilon < x_1 + \mathbf{sep}(X) \leq x_2 = x'_2$ , so  $x_1 \prec x'_1 \prec x'_2$ . Analogously,  $x_{k+2} \prec x'_{k+2} \prec x'_{k+3}$ , and the cyclic ordering is maintained. As for the distances, we have

$$\begin{aligned} d'_{1,1+k} &= d_{1,1+k} - \varepsilon \\ d'_{1,1-k} &= d_{1,1-k} + \varepsilon \\ d'_{k+2,(k+2)+k} &= d_{k+2,(k+2)+k} - \varepsilon \\ d'_{k+2,(k+2)-k} &= d_{k+2,(k+2)-k} + \varepsilon \end{aligned}$$

and  $d'_{1,k+2} = d_{1,k+2}$ . Thus,  $t_b(X') = t_b(x'_1) = d_{1,1-k} + \varepsilon = t_b(X) + \varepsilon = t_b$ , and  $t_d(X') = t_d(X) = t_d$ .  $\square$

**Remark 5.6.** The persistence sets of a circle  $\frac{\lambda}{\pi} \cdot \mathbb{S}^1$  with diameter  $\lambda$  are obtained by rescaling the results of this section. For example,  $\mathbf{D}_{4,1}^{\text{VR}}(\frac{\lambda}{\pi} \cdot \mathbb{S}^1)$  is the set bounded by  $2(\lambda - t_b) \leq t_d$  and  $t_b < t_d \leq \lambda$ .

In general, there are multiple configurations with the same persistence diagram, even among those that minimize the death time. The exception is the configuration that has the minimal birth time, as the following lemma shows.

**Proposition 5.7.** *For any  $k \geq 0$ , let  $n = 2k + 2$ . If  $X \subset \mathbb{S}^1$  has  $n$  points and satisfies  $t_b(X) = \frac{k}{k+1}\pi$  and  $t_d(X) = \pi$ , then  $X$  is a regular  $n$ -gon. As a consequence, the configuration  $X$  with  $n$  points such that  $\text{dgm}_k^{\text{VR}}(X) = \{(\frac{k}{k+1}\pi, \pi)\}$  is unique up to rotations.*

*Proof.* An application of Lemma 5.2 item 3 and the triangle inequality gives:

$$\begin{aligned}
\frac{k}{k+1}\pi = t_b(X) &= \max(d_{i,i+k}) \geq \frac{1}{2k+2} \sum_{i=1}^{2k+2} d_{i,i+k} = \frac{1}{2k+2} \sum_{i=1}^{2k+2} \sum_{j=1}^k d_{i+j-1,i+j} \\
&= \frac{1}{2k+2} \sum_{j=1}^k \sum_{i=1}^{2k+2} d_{i+j-1,i+j} \\
&= \frac{1}{2k+2} \sum_{j=1}^k \left[ \sum_{i=1}^{k+1} d_{i+j-1,i+j} + \sum_{i=k+2}^{2k+2} d_{i+j-1,i+j} \right] \\
&\geq \frac{1}{2k+2} \sum_{j=1}^k [d_{j,j+k+1} + d_{j+k+1,j}] \\
&\geq \frac{1}{2k+2} \sum_{j=1}^k [2t_d(X)] \\
&= \frac{k}{k+1}\pi.
\end{aligned}$$

Thus, all intermediate inequalities become equalities, most notably,  $d_{i,i+k} = \frac{k}{k+1}\pi$  for all  $i$ , and  $d_{j,j+k+1} = \sum_{i=1}^{k+1} d_{i+j-1,i+j} = \pi$  for all  $j$ . Then

$$d_{i,i+1} = d_{i-k,i+1} - d_{i-k,i} = \pi - \frac{k}{k+1}\pi = \frac{2\pi}{2k+2}.$$

In other words,  $X$  is a regular  $n$ -gon. □

## 5.4 Characterization of $\mathbf{U}_{4,1}^{\text{VR}}(\mathbb{S}^1)$

The case of  $k = 1$  in Theorem 5.5 allows us to find a probability density function for  $\mathbf{U}_{4,1}^{\text{VR}}(\mathbb{S}^1)$  with respect to the Lebesgue measure.

**Proposition 5.8.** *Consider  $(\mathbb{S}^1, d_{\mathbb{S}^1}, \mu_{\mathbb{S}^1})$  as an mm-space where  $\mu_{\mathbb{S}^1}$  is the uniform measure. Then, the measure  $\mathbf{U}_{4,1}^{\text{VR}}(\mathbb{S}^1)$  has probability density function*

$$f(t_b, t_d) = \frac{12}{\pi^3} (\pi - t_d)$$

with respect to the Lebesgue measure in  $\mathbb{R}^2$ . Here, we view  $\mathbf{D}_{4,1}^{\text{VR}}(\mathbb{S}^1) \subset \mathbb{R}^2$ .

*Proof.* Recall that we are modeling  $\mathbb{S}^1$  as the quotient  $[0, 2\pi]/0 \sim 2\pi$ . Consider a set  $X = \{x_1, x_2, x_3, x_4\} \subset [0, 2\pi]$  of four points chosen uniformly at random. Relabel  $x_i$  as  $x^{(j)} \in [0, 2\pi]$  so that  $x^{(1)} < x^{(2)} < x^{(3)} < x^{(4)}$ . Consider the image of  $x^{(j)}$  under the quotient map  $[0, 2\pi] \rightarrow \mathbb{S}^1$ , and let  $\gamma_i$  be the path between  $x^{(i)}$  and  $x^{(i+1)}$  that doesn't contain any other

point  $x^{(j)}$ . Set  $y_i = |\gamma_i|$ . It can be shown that the pushforward of the uniform measure on  $[0, 2\pi]^4$  into the set

$$\{(x^{(1)}, x^{(2)}, x^{(3)}, x^{(4)}) \in [0, 2\pi]^4 : x^{(1)} < x^{(2)} < x^{(3)} < x^{(4)}\}$$

is the uniform measure, and the pushforward of this measure under the map

$$(x^{(1)}, x^{(2)}, x^{(3)}, x^{(4)}) \mapsto (y_1, y_2, y_3)$$

onto

$$\Delta_3(2\pi) := \{(y_1, y_2, y_3) \in [0, 2\pi]^3 : y_1 + y_2 + y_3 \leq 2\pi\}$$

is also the uniform measure. Thus, we will model a configuration of four points in  $\mathbb{S}^1$  as the set of distances  $y_1, y_2, y_3, y_4$  instead.

We will first find the cumulative distribution function of  $\mathbf{U}_{4,1}^{\text{VR}}(\mathbb{S}^1)$ . To do that, we fix a point  $(t_b, t_d) \in \mathbf{D}_{4,1}^{\text{VR}}(\mathbb{S}^1)$ . According to Lemma 5.2,

$$t_b(X) = \max_{i=1,\dots,4} y_i$$

$$t_d(X) = \min_{i=1,\dots,4} y_i + y_{i+1}.$$

Since  $\Delta_3(2\pi)$  has the uniform measure, the probability that  $t_b \leq t_b(X) < t_d(X) \leq t_d$  is the volume of the set

$$R(t_b, t_d) := \{(y_1, y_2, y_3) \in \Delta_3(2\pi) : t_b \leq t_b(X) < t_d(X) \leq t_d\}$$

divided by  $\text{Vol}(\Delta_3(2\pi)) = \frac{(2\pi)^3}{3!}$ . We will find  $\text{Vol}(R(t_b, t_d))$  using an integral with a suitable parametrization of  $y_1, y_2, y_3$ .

Assume that  $t_b(X) = y_1$ . There are four choices for  $t_d(X)$ , but to start, let  $t_d(X) = y_1 + y_2$ . Since  $y_3 \leq y_1$  by definition of  $t_b(X)$ , we have  $y_3 + y_2 \leq y_1 + y_2$ , but since  $y_1 + y_2 = t_d(X)$ , we actually have an equality  $t_d(X) = y_1 + y_2 = y_3 + y_2$ . Thus, this case is a subset of the case when  $t_d(X) = y_2 + y_3$ . Similarly, the case  $t_d(X) = y_1 + y_4$  implies  $t_d(X) = y_3 + y_4$ . Hence, we only have two possible choices for  $t_d(X)$ . Since they are symmetric, we can choose one of them and account for the symmetry later. Thus, set  $t_d(X) = y_2 + y_3$ .

The condition  $t_b(X) = y_1$  is equivalent to having  $y_i \leq y_1$  for  $i = 2, 3, 4$ . Also,  $t_d(X) = y_2 + y_3$  gives  $y_2 + y_3 \leq y_3 + y_4$ , and so  $y_2 \leq y_4$ . It can be verified that the set of inequalities

$$y_2 \leq y_4 \leq y_1 \tag{6}$$

$$y_3 \leq y_1 \tag{7}$$

is equivalent to  $t_b(X) = y_1$  and  $t_d(X) = y_2 + y_3$ . By rewriting  $y_4$  as  $2\pi - y_1 - y_2 - y_3$ , the inequalities in (6) become

$$2y_2 + y_3 \leq 2\pi - y_1, \tag{8}$$

$$2\pi - 2y_1 \leq y_2 + y_3, \tag{9}$$

and (7) is equivalent to

$$(y_2 + y_3) - y_1 \leq y_2. \quad (10)$$

Since we are assuming that  $t_b(X) < t_d(X)$ , we also have  $y_1 < y_2 + y_3$ . If we make the substitution  $s = y_2 + y_3$ , we find that (8)-(10) are equivalent to the following system of inequalities:

$$\begin{aligned} t_b &\leq y_1 \leq t_d \\ \max(2\pi - 2y_1, y_1) &< s \leq t_d \\ s - y_1 &\leq y_2 \leq 2\pi - s - y_1. \end{aligned}$$

Call the region defined by this system of inequalities  $R'(t_b, t_d)$ . Notice that the Jacobian  $\left| \frac{\partial(y_1, y_2, y_3)}{\partial(y_1, y_2, s)} \right|$  is 1. Also, there were four choices for  $t_b(X)$  (all four  $y_i$ ) and for each, two choices for  $t_d(X)$  ( $y_2 + y_3$  and  $y_3 + y_4$  in our case). Thus, there were 8 possible choices for  $t_b(X)$  and  $t_d(X)$ , so

$$\text{Vol}(R(t_b, t_d)) = 8 \text{Vol}(R'(t_b, t_d)) = 8 \iiint_{R'(t_b, t_d)} 1 \, dy_2 \, ds \, dy_1.$$

To find this integral, notice that  $2\pi - 2y_1 \leq y_1$  when  $\frac{2\pi}{3} \leq y_1$ . Thus, for  $t_b \geq \frac{2\pi}{3}$ , we have

$$\begin{aligned} \text{Vol}(R(t_b, t_d)) &= 8 \int_{t_b}^{t_d} \int_{y_1}^{t_d} \int_{s-y_1}^{2\pi-s-y_1} 1 \, dy_2 \, ds \, dy_1 \\ &= -\frac{16}{3}t_d^3 + 8(\pi + t_b)t_d^2 - (16\pi t_b)t_d + \left( -\frac{8}{3}t_b^3 + 8\pi t_b^2 \right). \end{aligned} \quad (11)$$

In particular,  $\text{Vol}(R(\frac{2\pi}{3}, t_d)) = -\frac{16}{3}t_d^3 + \frac{40}{3}\pi t_d^2 - \frac{32}{3}\pi^2 t_d + \frac{224}{81}\pi^3$ . In order to calculate the volume of  $R(t_b, t_d)$  when  $t_b \leq \frac{2\pi}{3}$ , we split the integral into two pieces where  $t_b \leq y_1 \leq \frac{2\pi}{3}$  and  $\frac{2\pi}{3} \leq y_1 < t_d$ , respectively. The second case was calculated above, and in the first, we have  $\max(2\pi - 2y_1, y_1) = 2\pi - 2y_1$ . Thus:

$$\begin{aligned} \text{Vol}(R(t_b, t_d)) &= \text{Vol}(R(2\pi/3, t_d)) + 8 \int_{t_b}^{2\pi/3} \int_{2\pi-2y_1}^{t_d} \int_{s-y_1}^{2\pi-s-y_1} 1 \, dy_2 \, ds \, dy_1 \\ &= -\frac{16}{3}t_d^3 + 8(\pi + t_b)t_d^2 - (16\pi t_b)t_d + \left( -\frac{32}{3}t_b^3 + 16\pi t_b^2 - \frac{32}{27}\pi^3 \right). \end{aligned} \quad (12)$$

Now, let  $f$  be the probability density function of  $\mathbf{U}_{4,1}^{\text{VR}}(\mathbb{S}^1)$ . Since the probability of  $t_b \leq t_b(X) < t_d(X) \leq t_d$  is  $\text{Vol}(R(t_b, t_d)) / \text{Vol}(\Delta_3(2\pi))$ , we have

$$\frac{\text{Vol}(R(t_b, t_d))}{\text{Vol}(\Delta_3(2\pi))} = \int_{t_b}^{t_d} \int_{\max(2(\pi-\tau_b), \tau_b)}^{t_d} f(\tau_b, \tau_d) \, d\tau_d \, d\tau_b.$$

The lower bound on  $\tau_d$  comes from Theorem 5.5, which in the case  $k = 1$  gives  $t_d \geq 2(\pi - t_b)$ . Thus,

$$f(t_b, t_d) = \frac{\partial}{\partial t_d} \left( -\frac{\partial}{\partial t_b} \frac{\text{Vol}(R(t_b, t_d))}{\text{Vol}(\Delta_3(2\pi))} \right).$$

The mixed derivatives  $\frac{\partial}{\partial t_d} \left( -\frac{\partial}{\partial t_b} \right)$  of both (11) and (12) are  $16(\pi - t_d)$ , so

$$f(t_b, t_d) = \frac{16(\pi - t_d)}{(2\pi)^3/3!} = \frac{12}{\pi^3}(\pi - t_d),$$

regardless of whether  $t_b \leq \frac{2\pi}{3}$  or not. This is the desired probability density function of  $\mathbf{U}_{4,1}^{\text{VR}}(\mathbb{S}^1)$ .  $\square$

**Example 5.9.** Equation (12) gives

$$\frac{\text{Vol}(R(\pi/2, \pi))}{\text{Vol}(\Delta_3(2\pi))} = \frac{4\pi^3/27}{(2\pi)^3/3!} = \frac{1}{9} \approx 11\%.$$

This is the probability that a set  $\{x_1, x_2, x_3, x_4\} \subset \mathbb{S}^1$  chosen uniformly at random produces persistent homology at all in dimension 1. This is consistent with the 10.98% success rate obtained in the simulations; *cf.* Section 4.2.

## 5.5 Persistence sets of Ptolemaic spaces

Example 4.5 showed that in a metric space with four points, the birth time of its one-dimensional persistent homology is given by the length of the largest side and the death time, by that of the smaller diagonal. In this section, we use Ptolemy's inequality, which relates the lengths of the diagonals and sides of Euclidean quadrilaterals, to bound the first persistence set  $\mathbf{D}_{4,1}^{\text{VR}}$  of several spaces and show examples where the bound is attained.

**Definition 5.10.** A metric space  $(X, d_X)$  is called *Ptolemaic* if for any  $x_1, x_2, x_3, x_4 \in X$ ,

$$d_X(x_1, x_3) \cdot d_X(x_2, x_4) \leq d_X(x_1, x_2) \cdot d_X(x_3, x_4) + d_X(x_1, x_4) \cdot d_X(x_2, x_3).$$

It should be noted that the inequality holds for any permutation of  $x_1, x_2, x_3, x_4$ . Examples of Ptolemaic metric spaces include the Euclidean spaces  $\mathbb{R}^n$  and CAT(0) spaces; see [BFW09] for a more complete list of references. The basic result of this section is the following.

**Proposition 5.11.** *Let  $(X, d_X)$  be a Ptolemaic metric space. For any  $(t_b, t_d) \in \mathbf{D}_{4,1}^{\text{VR}}(X)$  where  $t_b < t_d$ ,*

$$t_d \leq \sqrt{2}t_b.$$

*Proof.* Let  $X' = \{x_1, x_2, x_3, x_4\} \subset X$  be such that  $t_b(X') < t_d(X')$ . As per Example 4.5, relabel the points so that  $t_b(X') = \max(d_{12}, d_{23}, d_{34}, d_{41})$  and  $t_d(X') = \min(d_{13}, d_{24})$ . Then, Ptolemy's inequality gives

$$\begin{aligned} (t_d(X))^2 &= (\min(d_{13}, d_{24}))^2 \\ &\leq d_{13} \cdot d_{24} \\ &\leq d_{12} \cdot d_{34} + d_{23} \cdot d_{14} \\ &\leq 2(\max(d_{12}, d_{23}, d_{34}, d_{41}))^2 \\ &= 2(t_b(X))^2. \end{aligned}$$

Taking square root gives the result.  $\square$

Another way to phrase the above proposition is to say that  $\mathbf{D}_{4,1}^{\text{VR}}(X)$  is contained in the set

$$\left\{ (t_b, t_d) \mid 0 \leq t_b < t_d \leq \min(\sqrt{2}t_b, \mathbf{diam}(X)) \right\}.$$

A key example where the containment is strict is the following.

**Proposition 5.12.** *Let  $\mathbb{S}_E^1$  denote the unit circle in  $\mathbb{R}^2$  equipped with the Euclidean metric. Then*

$$\mathbf{D}_{4,1}^{\text{VR}}(\mathbb{S}_E^1) = \left\{ (t_b, t_d) \mid 2t_b\sqrt{1 - \frac{t_b^2}{4}} \leq t_d, \text{ and } \sqrt{2} \leq t_b < t_d \leq 2 \right\}.$$

*Proof.* Observe that the Euclidean distance  $d_E$  between two points in  $\mathbb{S}^1$  is related to their geodesic distance  $d$  by  $d_E = f_E(d) = 2 \sin(d/2)$ . Since  $f_E$  is increasing on  $[-\pi, \pi]$ , an interval that contains all possible distances between points in  $\mathbb{S}^1$ , a configuration  $X = \{x_1, x_2, x_3, x_4\} \subset \mathbb{S}^1$  produces non-zero persistence if, and only if, its Euclidean counterpart  $X_E \subset \mathbb{S}_E^1$  does. For this reason,  $\mathbf{D}_{4,1}^{\text{VR}}(\mathbb{S}_E^1) = f_E(\mathbf{D}_{4,1}^{\text{VR}}(\mathbb{S}^1))$ .

From Theorem 5.5,

$$\mathbf{D}_{4,1}^{\text{VR}}(\mathbb{S}^1) = \{(t_b, t_d) \mid 2(\pi - t_b) \leq t_d \leq \pi \text{ and } \pi/2 \leq t_b < t_d \leq \pi\}.$$

Applying  $f_E$  to the bound  $t_d \geq 2(\pi - t_b)$  gives

$$\begin{aligned} t_{d,E} &= 2 \sin(t_d/2) \geq 2 \sin(\pi - t_b) = 2 \sin(t_b) = 2 \sin(2 \arcsin(t_{b,E}/2)) \\ &= 4 \sin(\arcsin(t_{b,E}/2)) \cos(\arcsin(t_{b,E}/2)) = 2t_{b,E} \sqrt{1 - t_{b,E}^2/4}, \end{aligned}$$

while the image of the bound  $\pi/2 \leq t_b < t_d \leq \pi$  under  $f_E$  is  $\sqrt{2} \leq t_{b,E} < t_{d,E} \leq 2$ .  $\square$

Even though  $\mathbf{D}_{4,1}^{\text{VR}}(\mathbb{S}_E^1)$  doesn't attain equality in the bound given by Proposition 5.11, it can be used to show that other spaces do. Two examples are  $\mathbb{S}^2$  and  $\mathbb{R}^2$ .

**Proposition 5.13.**

$$\begin{aligned} \mathbf{D}_{4,1}^{\text{VR}}(\mathbb{R}^2) &= \left\{ (t_b, t_d) \mid 0 < t_b < t_d \leq \sqrt{2}t_b \right\}, \text{ and} \\ \mathbf{D}_{4,1}^{\text{VR}}(\mathbb{S}_E^2) &= \left\{ (t_b, t_d) \mid 0 < t_b < t_d \leq \min(\sqrt{2}t_b, 2) \right\}. \end{aligned}$$

*Proof.* Let  $P_D = \{(t_b, t_d) \mid 0 < t_b < t_d \leq \min(\sqrt{2}t_b, D)\}$ . Both  $\mathbb{R}^2$  and  $\mathbb{S}_E^2 \subset \mathbb{R}^3$  are Ptolemaic spaces, so Proposition 5.11 gives  $\mathbf{D}_{4,1}^{\text{VR}}(\mathbb{R}^2) \subset P_\infty$  and  $\mathbf{D}_{4,1}^{\text{VR}}(\mathbb{S}_E^2) \subset P_2$ . To show the other direction, notice that  $\mathbb{R}^2$  contains circles  $R \cdot \mathbb{S}_E^1$  of any radius  $R > 0$ . By functoriality of persistence sets (Remark 3.10),  $\mathbf{D}_{4,1}^{\text{VR}}(R \cdot \mathbb{S}_E^1) \subset \mathbf{D}_{4,1}^{\text{VR}}(\mathbb{R}^2)$  so, in particular,  $\mathbf{D}_{4,1}^{\text{VR}}(\mathbb{R}^2)$  contains the line  $[\sqrt{2}R, 2R) \times 2R$  that bounds  $\mathbf{D}_{4,1}^{\text{VR}}(R \cdot \mathbb{S}_E^1)$  from above (see Figure 13). The inequality  $t_b < t_d \leq \sqrt{2}t_b$  can be rearranged to  $\frac{\sqrt{2}}{2}t_d \leq t_b < t_d$ , so given any point  $(t_b, t_d) \in P_\infty$ , taking  $R = t_d/2$  gives  $(t_b, t_d) \in [\sqrt{2}R, 2R) \times 2R \subset \mathbf{D}_{4,1}^{\text{VR}}(\mathbb{R}^2)$ . Thus,  $P_\infty \subset \mathbf{D}_{4,1}^{\text{VR}}(\mathbb{R}^2)$ . The same argument with the added restriction of  $R \leq 1$  shows that  $P_2 \subset \mathbf{D}_{4,1}^{\text{VR}}(\mathbb{S}_E^2)$ .  $\square$

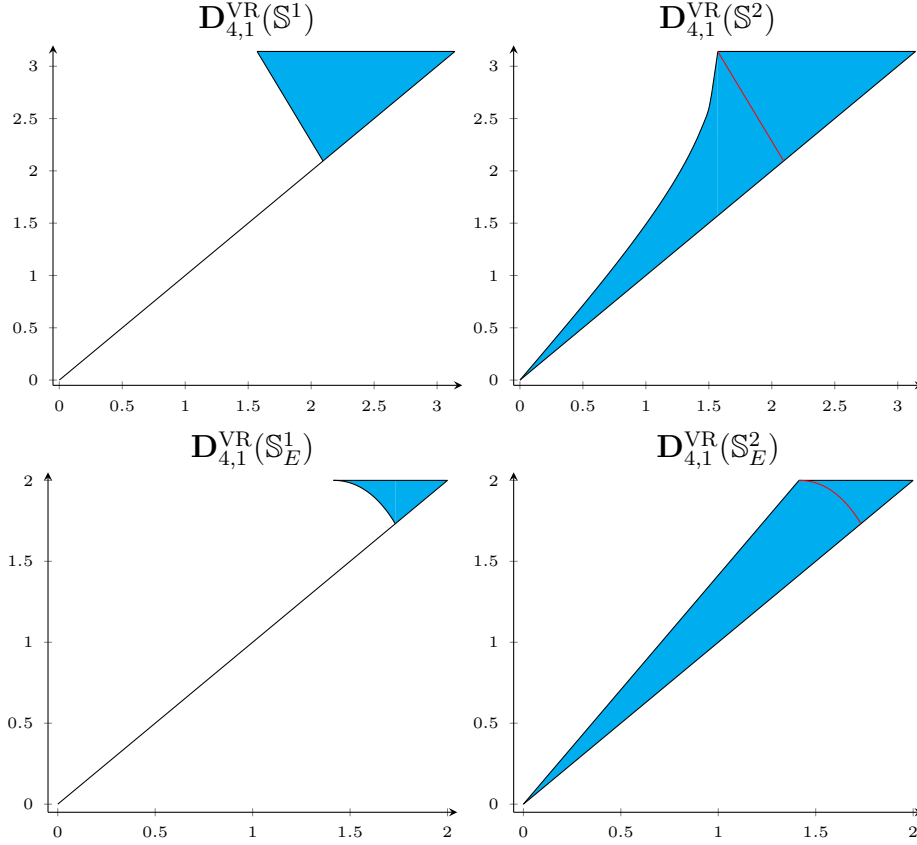


Figure 13: Top left:  $\mathbf{D}_{4,1}^{\text{VR}}(\mathbb{S}^1)$ . Top right:  $\mathbf{D}_{4,1}^{\text{VR}}(\mathbb{S}^2)$ . Bottom left:  $\mathbf{D}_{4,1}^{\text{VR}}(\mathbb{S}_E^1)$ . Bottom right:  $\mathbf{D}_{4,1}^{\text{VR}}(\mathbb{S}_E^2)$ . Notice that  $\mathbf{D}_{4,1}^{\text{VR}}(\mathbb{S}^1) \subset \mathbf{D}_{4,1}^{\text{VR}}(\mathbb{S}^2)$ , as indicated by the red line in the top right diagram. The analogous statement holds for  $\mathbb{S}_E^1 \subset \mathbb{S}_E^2$ .

Two observations summarize the proof of Proposition 5.13: Ptolemy's inequality gives a region  $P_\infty$  that contains  $\mathbf{D}_{4,1}^{\text{VR}}(\mathbb{R}^2)$ , while the circles in  $\mathbb{R}^2$  produce enough points to fill  $P_\infty$ . It turns out that this technique can be generalized to other spaces, provided that we have a suitable analogue of Ptolemy's inequality. This is explored in the next section.

## 5.6 Persistence sets of the surface with constant curvature $\kappa$

Consider the model space  $M_\kappa$  with constant sectional curvature  $\kappa$ . In this section, we will characterize  $\mathbf{D}_{4,1}^{\text{VR}}(M_\kappa)$ . Proposition 5.13 already has the case  $\kappa = 0$ , so now we deal with  $\kappa \neq 0$ . To fix notation, let  $x, y \in \mathbb{R}^3$ . Define

$$\begin{aligned} \langle x, y \rangle &= x_1y_1 + x_2y_2 + x_3y_3, \text{ and} \\ \langle x|y \rangle &= -x_1y_1 + x_2y_2 + x_3y_3. \end{aligned}$$

We model  $M_\kappa$  as

$$M_\kappa = \left\{ x \in \mathbb{R}^3 \mid \langle x, x \rangle = \frac{1}{\kappa} \right\}, \text{ if } \kappa > 0, \text{ and}$$

$$M_\kappa = \left\{ x \in \mathbb{R}^3 \mid \langle x|x \rangle = \frac{1}{\kappa} \text{ and } x_1 > 0 \right\}, \text{ if } \kappa < 0.$$

In other words,  $M_\kappa$  is the sphere of radius  $1/\sqrt{\kappa}$  if  $\kappa > 0$ , and the hyperbolic plane of constant curvature  $\kappa < 0$  with the hyperboloid model. The geodesic distance in  $M_\kappa$  is given by

$$d_{M_\kappa}(x, y) = \begin{cases} \frac{1}{\sqrt{+\kappa}} \arccos(\kappa \langle x, y \rangle), & \text{if } \kappa > 0, \\ \frac{1}{\sqrt{-\kappa}} \operatorname{arccosh}(\kappa \langle x|y \rangle), & \text{if } \kappa < 0. \end{cases} \quad (13)$$

To use the same technique as in Proposition 5.13, we use a version of Ptolemy's inequality for spaces of non-zero curvature.

**Lemma 5.14** (Spherical Ptolemy's inequality, [Val70a]).

For  $\kappa > 0$ , let  $x_1, x_2, x_3, x_4 \in M_\kappa$ , and  $d_{ij} = d_{M_\kappa}(x_i, x_j)$ . The determinant

$$C_\kappa = \left| \sin^2 \left( \frac{\sqrt{\kappa}}{2} d_{ij} \right) \right| \quad (14)$$

is non-positive. In particular,

$$\sin \left( \frac{\sqrt{\kappa}}{2} d_{13} \right) \sin \left( \frac{\sqrt{\kappa}}{2} d_{24} \right) \leq \sin \left( \frac{\sqrt{\kappa}}{2} d_{12} \right) \sin \left( \frac{\sqrt{\kappa}}{2} d_{34} \right) + \sin \left( \frac{\sqrt{\kappa}}{2} d_{14} \right) \sin \left( \frac{\sqrt{\kappa}}{2} d_{23} \right). \quad (15)$$

*Proof.* [Val70a] proved that the determinant (14) is non-positive when  $\kappa = 1$ ; we obtain the general version by rescaling the distances as follows. Let  $x_i \in M_\kappa$  for  $i = 1, 2, 3, 4$ ; define  $y_i = \sqrt{\kappa}x_i$ , and  $d'_{ij} = d_{M_1}(y_i, y_j)$ . Notice that  $\langle y_i, y_i \rangle = \kappa \langle x_i, x_i \rangle = 1$ , so  $y_i \in M_1$  and, by (13),

$$\frac{\sqrt{\kappa}}{2} d_{ij} = \frac{1}{2} \arccos(\kappa \langle x_i, x_j \rangle) = \frac{1}{2} \arccos(\langle y_i, y_j \rangle) = \frac{1}{2} d'_{ij}.$$

Then, the determinant

$$C_\kappa(x_1, x_2, x_3, x_4) = \left| \sin^2 \left( \frac{\sqrt{\kappa}}{2} d_{ij} \right) \right| = \left| \sin^2 \left( \frac{d'_{ij}}{2} \right) \right| = C_1(y_1, y_2, y_3, y_4)$$

is non-positive by Theorem 3.1 of [Val70a] and, by the Corollary following that, we get (15).  $\square$

Valentine also generalized this result to hyperbolic geometry. The rescaling is analogous to the one in the previous lemma, so we omit the proof.

**Lemma 5.15** (Hyperbolic Ptolemy's inequality, [Val70b]).

If  $\kappa < 0$ , let  $x_1, x_2, x_3, x_4 \in M_\kappa$ , and  $d_{ij} = d_{M_\kappa}(x_i, x_j)$ . Then the determinant

$$K_\kappa = \left| \sinh^2 \left( \frac{\sqrt{-\kappa}}{2} d_{ij} \right) \right| \quad (16)$$

is non-positive. In particular,

$$\sinh \left( \frac{\sqrt{-\kappa}}{2} d_{13} \right) \sinh \left( \frac{\sqrt{-\kappa}}{2} d_{24} \right) \leq \sinh \left( \frac{\sqrt{-\kappa}}{2} d_{12} \right) \sinh \left( \frac{\sqrt{-\kappa}}{2} d_{34} \right) + \sinh \left( \frac{\sqrt{-\kappa}}{2} d_{14} \right) \sinh \left( \frac{\sqrt{-\kappa}}{2} d_{23} \right). \quad (17)$$

With these tools, we are ready to prove the main theorem of this section.

**Theorem 5.16.** Let  $M_\kappa$  be the 2-dimensional model space with constant sectional curvature  $\kappa$ . Then:

- If  $\kappa > 0$ ,  $\mathbf{D}_{4,1}^{\text{VR}}(M_\kappa) = \left\{ (t_b, t_d) \mid \sin \left( \frac{\sqrt{\kappa}}{2} t_d \right) \leq \sqrt{2} \sin \left( \frac{\sqrt{\kappa}}{2} t_b \right) \text{ and } 0 < t_b < t_d \leq \frac{\pi}{\sqrt{\kappa}} \right\}$ .
- If  $\kappa = 0$ ,  $\mathbf{D}_{4,1}^{\text{VR}}(M_0) = \left\{ (t_b, t_d) \mid 0 \leq t_b < t_d \leq \sqrt{2} t_b \right\}$ .
- If  $\kappa < 0$ ,  $\mathbf{D}_{4,1}^{\text{VR}}(M_\kappa) = \left\{ (t_b, t_d) \mid \sinh \left( \frac{\sqrt{-\kappa}}{2} t_d \right) \leq \sqrt{2} \sinh \left( \frac{\sqrt{-\kappa}}{2} t_b \right) \text{ and } 0 < t_b < t_d \right\}$ .

*Proof.* The case  $\kappa = 0$  was already done in Proposition 5.13. For  $\kappa > 0$ , let

$$P = \left\{ (t_b, t_d) \mid \sin \left( \frac{\sqrt{\kappa}}{2} t_d \right) \leq \sqrt{2} \sin \left( \frac{\sqrt{\kappa}}{2} t_b \right) \text{ and } 0 < t_b < t_d \leq \frac{\pi}{\sqrt{\kappa}} \right\}.$$

Let  $X = \{x_1, x_2, x_3, x_4\} \subset M_\kappa$  and  $d_{ij} = d_{M_\kappa}(x_i, x_j)$ . Suppose that  $t_b(X) < t_d(X)$  and label the  $x_i$  so that  $t_b(X) = \max(d_{12}, d_{23}, d_{34}, d_{41})$  and  $t_d(X) = \min(d_{13}, d_{24})$ . Let  $s_{ij} := \sin \left( \frac{\sqrt{\kappa}}{2} d_{ij} \right)$ . By (15),

$$s_{13}s_{24} \leq s_{12}s_{34} + s_{14}s_{23},$$

and, since  $\sin \left( \frac{\sqrt{\kappa}}{2} t \right)$  is increasing when  $\frac{\sqrt{\kappa}}{2} t \in \left[ 0, \frac{\sqrt{\kappa}}{2} \mathbf{diam}(M_\kappa) \right] = \left[ 0, \frac{\pi}{2} \right]$ , we get

$$\begin{aligned} \sin^2 \left( \frac{\sqrt{\kappa}}{2} t_d(X) \right) &= (\min(s_{13}, s_{24}))^2 \\ &\leq s_{13}s_{24} \\ &\leq s_{12}s_{34} + s_{14}s_{23} \\ &\leq 2 \sin^2 \left( \frac{\sqrt{\kappa}}{2} t_b(X) \right). \end{aligned}$$

Thus,

$$\sin \left( \frac{\sqrt{\kappa}}{2} t_d \right) \leq \sqrt{2} \sin \left( \frac{\sqrt{\kappa}}{2} t_b \right). \quad (18)$$

This shows that  $\mathbf{D}_{4,1}^{\text{VR}}(M_\kappa) \subset P$ . For the other direction, let  $0 < t \leq 1$  and  $s \in [0, \pi/2]$ , and consider  $X = \{x_1, x_2, x_3, x_4\}$  where

$$\begin{aligned} x_1 &= \left( \frac{1}{\sqrt{\kappa}} \sqrt{1-t^2}, \frac{t}{\sqrt{\kappa}}, 0 \right) \\ x_2 &= \left( \frac{1}{\sqrt{\kappa}} \sqrt{1-t^2}, \frac{t}{\sqrt{\kappa}} \sin(s), \frac{t}{\sqrt{\kappa}} \cos(s) \right) \\ x_3 &= \left( \frac{1}{\sqrt{\kappa}} \sqrt{1-t^2}, -\frac{t}{\sqrt{\kappa}}, 0 \right) \\ x_4 &= \left( \frac{1}{\sqrt{\kappa}} \sqrt{1-t^2}, -\frac{t}{\sqrt{\kappa}} \sin(s), -\frac{t}{\sqrt{\kappa}} \cos(s) \right) \end{aligned}$$

It can be checked that:

- $x_i \in M_\kappa$ ,
- $\langle x_1, x_3 \rangle = \langle x_2, x_4 \rangle = \frac{1}{\kappa}(1 - 2t^2)$ ,
- $\langle x_1, x_2 \rangle = \langle x_3, x_4 \rangle = \frac{1}{\kappa}(1 - t^2(1 - \sin(s)))$ , and
- $\langle x_1, x_4 \rangle = \langle x_2, x_3 \rangle = \frac{1}{\kappa}(1 - t^2(1 + \sin(s)))$ .

Since  $\arccos(t)$  is decreasing, we have

$$\begin{aligned} t_b(X) &= \frac{1}{\sqrt{\kappa}} \arccos(\kappa \langle x_1, x_4 \rangle) = \frac{1}{\sqrt{\kappa}} \arccos(1 - t^2(1 + \sin(s))), \text{ and} \\ t_d(X) &= \frac{1}{\sqrt{\kappa}} \arccos(\kappa \langle x_1, x_3 \rangle) = \frac{1}{\sqrt{\kappa}} \arccos(1 - 2t^2). \end{aligned}$$

Notice that for a fixed  $t$ ,  $t_b(X)$  is minimized at  $s = 0$  and the equality in (18) is achieved. Also,  $t_d(X)$  is maximized at  $t = 1$ , at which point  $t_d(X) = \frac{\pi}{\sqrt{\kappa}}$ . Now, let  $(t_b, t_d) \in P$  be arbitrary. If we set  $t_b(X) = t_b$  and  $t_d(X) = t_d$ , we can solve the equations above to get

$$\begin{aligned} t &= \sqrt{\frac{1 - \cos(\sqrt{\kappa} t_d)}{2}}, \text{ and} \\ \sin(s) &= 2 \cdot \frac{1 - \cos(\sqrt{\kappa} t_b)}{1 - \cos(\sqrt{\kappa} t_d)} - 1. \end{aligned}$$

Such a  $t$  exists because  $\cos(\sqrt{\kappa} t_d) \leq 1$ . As for  $s$ , the half-angle identity  $1 - \cos(x) = 2 \sin^2(x/2)$  gives the equivalent expression

$$\sin(s) = 2 \cdot \frac{\sin^2(\sqrt{\kappa} t_b/2)}{\sin^2(\sqrt{\kappa} t_d/2)} - 1.$$

Since  $(t_b, t_d)$  satisfies (18), the right side is bounded below by 0 and, since  $t_b < t_d \leq \frac{\pi}{\sqrt{\kappa}}$ , it is also bounded above by 1. Thus, there exists an  $s \in [0, \pi/2]$  that satisfies the equality. This

finishes the proof of  $P \subset \mathbf{D}_{4,1}^{\text{VR}}(M_\kappa)$ .

The proof for  $\kappa < 0$  proceeds in much the same way. The only major change is in the definition of the points  $x_i$  when showing  $P \subset \mathbf{D}_{4,1}^{\text{VR}}(M_\kappa)$ :

$$\begin{aligned} x_1 &= \left( \frac{1}{\sqrt{-\kappa}} \sqrt{1+t^2}, \frac{t}{\sqrt{-\kappa}}, 0 \right) \\ x_2 &= \left( \frac{1}{\sqrt{-\kappa}} \sqrt{1+t^2}, \frac{t}{\sqrt{-\kappa}} \sin(s), \frac{t}{\sqrt{-\kappa}} \cos(s) \right) \\ x_3 &= \left( \frac{1}{\sqrt{-\kappa}} \sqrt{1+t^2}, -\frac{t}{\sqrt{-\kappa}}, 0 \right) \\ x_4 &= \left( \frac{1}{\sqrt{-\kappa}} \sqrt{1+t^2}, -\frac{t}{\sqrt{-\kappa}} \sin(s), -\frac{t}{\sqrt{-\kappa}} \cos(s) \right) \end{aligned}$$

Other than that, and the fact that  $M_\kappa$  is unbounded when  $\kappa < 0$ , the proof is completely analogous.  $\square$

A related result appears in [BHPW20]. The authors explore the question of whether persistent homology can detect the curvature of the ambient  $M_\kappa$ . On the theoretical side, they found a geometric formula to compute  $\text{dgm}_1^{\text{Cech}}(T)$  of a sample  $T \subset M_\kappa$  with *three* points, much in the same vein as our Theorem 4.4. They used it to find the logarithmic persistence  $P_a(\kappa) = t_d(T_{\kappa,a})/t_b(T_{\kappa,a})$  for an equilateral triangle  $T_{\kappa,a}$  of fixed side length  $a > 0$ , and proved that  $P_a$ , when viewed as a function of  $\kappa$ , is invertible. On the experimental side, they sampled 1000 points from a unit disk in  $M_\kappa$  and were able to approximate  $\kappa$  using the average VR death vectors in dimension 0 and average persistence landscapes in dimension 1 of 100 such samples. For example, one method consisted in finding a collection of landscapes  $L_\kappa$  labeled with a known curvature  $\kappa$ , and estimating  $\kappa_*$  for an unlabeled  $L_*$  with the average curvature of the three nearest neighbors of  $L_*$ . They were also able to approximate  $\kappa_*$  without labeled examples by using PCA. See their paper [BHPW20] for more details.

Our Theorem 5.16 is in the same spirit. The curvature  $\kappa$  determines the boundary of  $\mathbf{D}_{4,1}^{\text{VR}}(M_\kappa)$ , and instead of triangles, we could use squares with a given  $t_d$  and minimal  $t_b$  to find  $\kappa$ . Additionally, we can qualitatively detect the sign of the curvature by looking at the boundary of  $\mathbf{D}_{4,1}^{\text{VR}}(M_\kappa)$ : it is concave up when  $\kappa > 0$ , a straight line when  $\kappa = 0$ , and concave down when  $\kappa < 0$ . See Figure 14.

## 5.7 Persistence sets of $\mathbb{S}^m$ for $m \geq 3$

General spheres are another example where our strategy provides a characterization of their persistence sets. The next proposition is inspired by the equality condition in Ptolemy's theorem, that is, equality occurs when the four points lie on a circle. We can generalize that argument to higher dimensional spheres.

**Proposition 5.17.** *For all  $m \geq n - 1$  and all  $k \geq 0$ ,  $\mathbf{D}_{n,k}^{\text{VR}}(\mathbb{S}_E^m) = \bigcup_{\lambda \in [0,1]} \lambda \cdot \mathbf{D}_{n,k}^{\text{VR}}(\mathbb{S}_E^{n-2})$ .*

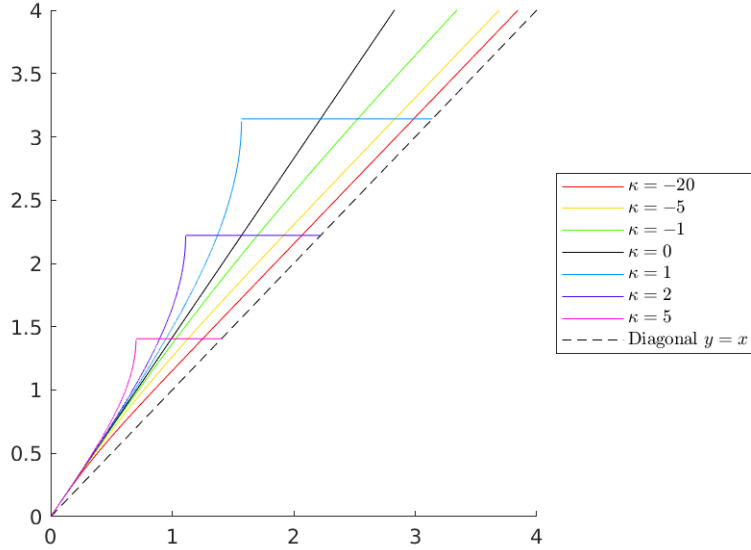


Figure 14: The boundary of  $\mathbf{D}_{4,1}^{\text{VR}}(M_{\kappa})$  for multiple  $\kappa$ . Observe this set is bounded only when  $\kappa > 0$ , and that the left boundary of these persistence sets is concave up when  $\kappa > 0$ , a straight line when  $\kappa = 0$ , and concave down when  $\kappa < 0$ .

*Proof.*  $\mathbb{S}_E^m$  contains copies of  $\lambda \cdot \mathbb{S}_E^{n-2}$  for  $\lambda \in [0, 1]$ , so  $\bigcup_{\lambda \in [0,1]} \lambda \cdot \mathbf{D}_{n,k}^{\text{VR}}(\mathbb{S}_E^{n-2}) \subset \mathbf{D}_{n,k}^{\text{VR}}(\mathbb{S}_E^m)$ . For the other direction, notice that a set  $X \subset \mathbb{S}_E^m \subset \mathbb{R}^{m+1}$  with  $n$  points generates an  $(n-1)$ -hyperplane which intersects  $\mathbb{S}_E^m$  on a  $(n-2)$ -dimensional sphere of radius  $\lambda \leq 1$ . Thus,  $X \subset \lambda \cdot \mathbb{S}_E^{n-2}$ , so  $\mathbf{D}_{n,k}^{\text{VR}}(\mathbb{S}_E^m) \subset \bigcup_{\lambda \in [0,1]} \lambda \cdot \mathbf{D}_{n,k}^{\text{VR}}(\mathbb{S}_E^{n-2})$ .  $\square$

In particular, this gives a description of the first principal persistence set of all spheres with the Euclidean metric.

**Corollary 5.18.** *For all  $m \geq 2$ ,  $\mathbf{D}_{4,1}^{\text{VR}}(\mathbb{S}_E^m) = \{(t_b, t_d) \mid 0 \leq t_b < t_d \leq \min(\sqrt{2}t_b, \pi)\}$ .*

*Proof.* By Proposition 5.17, for every  $m \geq 3$ ,

$$\mathbf{D}_{4,1}^{\text{VR}}(\mathbb{S}_E^m) = \bigcup_{\lambda \in [0,1]} \lambda \cdot \mathbf{D}_{4,1}^{\text{VR}}(\mathbb{S}_E^2).$$

However, it is clear that  $\lambda \cdot \mathbf{D}_{4,1}^{\text{VR}}(\mathbb{S}_E^2) \subset \mathbf{D}_{4,1}^{\text{VR}}(\mathbb{S}_E^2)$ , as the latter is convex. Thus,

$$\bigcup_{\lambda \in [0,1]} \lambda \cdot \mathbf{D}_{4,1}^{\text{VR}}(\mathbb{S}_E^2) = \mathbf{D}_{4,1}^{\text{VR}}(\mathbb{S}_E^2),$$

and now, Proposition 5.13 gives the result.  $\square$

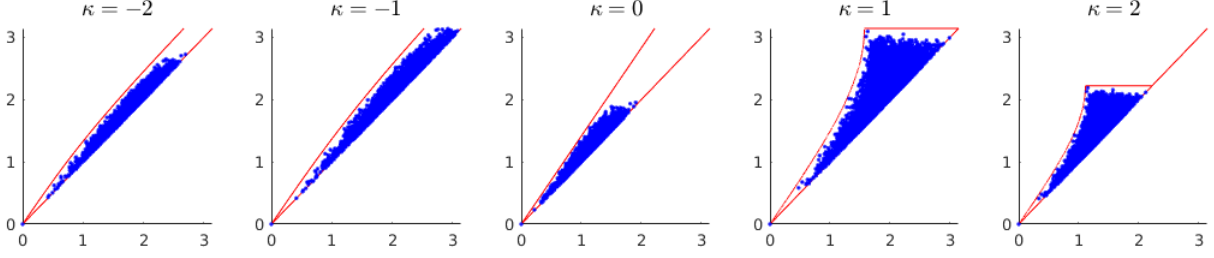


Figure 15: The diagrams  $\mathbf{D}_{4,1}^{\text{VR}}(D_\kappa)$  for disks  $D_\kappa \subset M_\kappa$  of radius  $R = \pi/\sqrt{|\kappa|}$  for various  $\kappa \neq 0$ . Also shown is  $\mathbf{D}_{4,1}^{\text{VR}}(D_0)$  for  $D_0 \subset M_0$ , a disk of radius 1.

Given that we know several persistence sets of spheres, we can use them, together with the stability in Theorem 3.12, to find lower bounds for the Gromov-Hausdorff distance between the circle and other spheres.

**Example 5.19.** Since  $\mathbf{D}_{4,1}^{\text{VR}}(\mathbb{S}^1) \subset \mathbf{D}_{4,1}^{\text{VR}}(\mathbb{S}^2)$ ,

$$d_{\mathcal{H}}^{\mathcal{D}}(\mathbf{D}_{4,1}^{\text{VR}}(\mathbb{S}^1), \mathbf{D}_{4,1}^{\text{VR}}(\mathbb{S}^2)) = \sup_{D_2 \in \mathbf{D}_{4,1}^{\text{VR}}(\mathbb{S}^2)} \inf_{D_1 \in \mathbf{D}_{4,1}^{\text{VR}}(\mathbb{S}^1)} d_{\mathcal{B}}(D_1, D_2).$$

Fix a diagram  $D_2 = (x_2, y_2) \in \mathbf{D}_{4,1}^{\text{VR}}(\mathbb{S}^2) \setminus \mathbf{D}_{4,1}^{\text{VR}}(\mathbb{S}^1)$  and take  $D_1 = (x_1, y_1) \in \mathbf{D}_{4,1}^{\text{VR}}(\mathbb{S}^1)$  arbitrary. The distance  $d_{\mathcal{B}}(D_1, D_2)$  can be realized by either the  $\ell^\infty$  distance between  $D_1$  and  $D_2$  or by half the persistence of either diagram (Definition 2.19), so in order to minimize  $d_{\mathcal{B}}(D_1, D_2)$ , let's start by finding the minimum of  $\|D_1 - D_2\|_\infty = \max(|x_1 - x_2|, |y_1 - y_2|)$ .

Clearly, this distance is smallest when  $D_1$  is on the line  $\ell$  with equation  $y = 2(\pi - x)$  (case  $k = 1$  in Theorem 5.4). Additionally, the maximum is minimized when  $|x_1 - x_2| = |y_1 - y_2|$ . If both conditions can be achieved, we will have minimized the  $\ell^\infty$  distance. The only possibility, though, is  $x_2 \leq x_1$  and  $y_2 \leq y_1$  (if either inequality is reversed, the  $\ell^\infty$  distance would be larger because  $\ell$  has negative slope). In that case, the solutions to the system of equations  $x_1 - x_2 = y_1 - y_2$  and  $y_1 = 2(\pi - x_1)$  are  $x_1 = \frac{1}{3}(2\pi + x_2 - y_2)$  and  $y_1 = \frac{2}{3}(\pi - x_2 + y_2)$ . Thus,

$$d_{\ell^\infty}(D_2, \ell) = \frac{1}{3}(2\pi - 2x_2 - y_2).$$

This quantity is positive because  $x_2, y_2$  is below  $\ell$ , that is,  $y_2 \leq 2\pi - 2x_2$ .

Now fix  $D_1$  as the solution described in the previous paragraph and let  $D_2$  vary. The distance  $d_{\mathcal{B}}(D_1, D_2)$  can be equal to  $\frac{1}{2}\text{pers}(D_i)$  if that quantity is larger than  $d_{\ell^\infty}(D_2, \ell)$  for either  $i = 1, 2$ . Notice, also, that  $\text{pers}(D_1) = \text{pers}(D_2)$  because  $x_1 - x_2 = y_1 - y_2$ . If we can find  $D_2$  such that

$$\frac{1}{2}\text{pers}(D_2) = d_{\ell^\infty}(D_2, \ell), \tag{19}$$

then the maximum will have been achieved. Equation (19) can be simplified to  $y_2 = -\frac{1}{5}x_2 + \frac{4\pi}{5}$ . The point  $D_2 = (x_2, y_2)$  that realizes the Hausdorff distance will be in the intersection of this line and  $\mathbf{D}_{4,1}^{\text{VR}}(\mathbb{S}^2)$  and have maximal persistence. That is achieved in the intersection

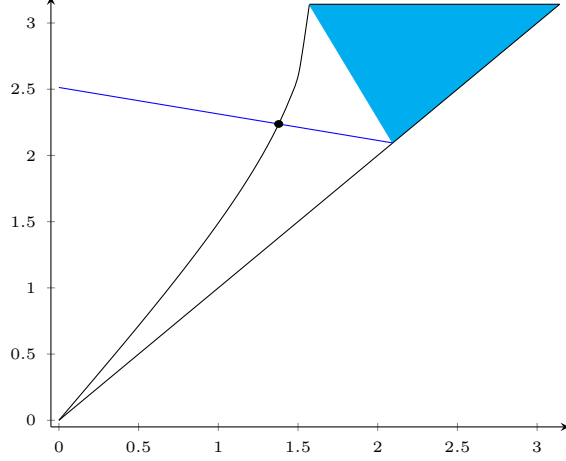


Figure 16: The point  $D_2$  that realizes the Hausdorff distance between  $\mathbf{D}_{4,1}^{\text{VR}}(\mathbb{S}^1)$  and  $\mathbf{D}_{4,1}^{\text{VR}}(\mathbb{S}^2)$  with respect to the bottleneck distance. The shaded region is  $\mathbf{D}_{4,1}^{\text{VR}}(\mathbb{S}^1)$  and the black lines outline  $\mathbf{D}_{4,1}^{\text{VR}}(\mathbb{S}^2)$ . The blue line is  $y_2 = -\frac{1}{5}x_2 + \frac{4\pi}{5}$ , the region where  $\frac{1}{2}\text{pers}(D_2) = d_{\ell^\infty}(D_2, \ell)$ , and  $\ell$  is the line  $y = 2(\pi - x) \subset \partial(\mathbf{D}_{4,1}^{\text{VR}}(\mathbb{S}^1))$ .

with the left boundary, the curve  $x = 2 \arcsin\left(\frac{1}{\sqrt{2}} \sin\left(\frac{y}{2}\right)\right)$  (use  $\kappa = 1$  in Theorem 5.16). That point is  $x_2 \approx 1.3788, y_2 = 2.2375$  (see Figure 16) and will give  $d_{\mathcal{H}}^{\mathcal{D}}(\mathbf{D}_{4,1}^{\text{VR}}(\mathbb{S}^1), \mathbf{D}_{4,1}^{\text{VR}}(\mathbb{S}^2)) \approx 0.4293$ . Thus,

$$d_{\mathcal{G}\mathcal{H}}(\mathbb{S}^1, \mathbb{S}^2) \geq \frac{1}{2} d_{\mathcal{H}}^{\mathcal{D}}(\mathbf{D}_{4,1}^{\text{VR}}(\mathbb{S}^1), \mathbf{D}_{4,1}^{\text{VR}}(\mathbb{S}^2)) \approx 0.2147 \approx \frac{\pi}{14.6344}.$$

In the case of  $k \geq 3$ , we can obtain a better bound.

**Example 5.20.** Let  $n = 2k + 2$ ; we seek lower bound for  $d_{\mathcal{G}\mathcal{H}}(\mathbb{S}^1, \mathbb{S}^k)$  for  $k \geq 3$ . First, similarly to Example 5.19, we have

$$d_{\mathcal{H}}^{\mathcal{D}}(\mathbf{D}_{n,k}^{\text{VR}}(\mathbb{S}^1), \mathbf{D}_{n,k}^{\text{VR}}(\mathbb{S}^k)) = \sup_{D_2 \in \mathbf{D}_{n,k}^{\text{VR}}(\mathbb{S}^k)} \inf_{D_1 \in \mathbf{D}_{n,k}^{\text{VR}}(\mathbb{S}^1)} d_{\mathcal{B}}(D_1, D_2).$$

We now exhibit a configuration, more specifically, a cross-polytope  $X \subset \mathbb{S}^k$ , in order to fix a specific diagram  $D_2$ . Let  $X = \{\pm e_1, \dots, \pm e_{k+1}\} \subset \mathbb{R}^{k+1}$ , where  $e_i$  is the  $i$ -th standard basis vector. Notice that  $d_{\mathbb{S}^k}(\pm e_i, \pm e_j) = \frac{\pi}{2}$  if  $j \neq i$ , and  $d_{\mathbb{S}^k}(e_i, -e_i) = \pi$ . Then  $t_b(e_i) = t_b(-e_i) = \frac{\pi}{2}$  and  $t_d(e_i) = t_d(-e_i) = \pi$ , so  $t_b(X) = \frac{\pi}{2}$  and  $t_d(X) = \pi$ . Since  $X$  has  $2k + 2 = n$  points, we just proved that  $D_2 = (\frac{\pi}{2}, \pi) \in \mathbf{D}_{n,k}^{\text{VR}}(\mathbb{S}^k)$ . Then

$$d_{\mathcal{H}}^{\mathcal{D}}(\mathbf{D}_{n,k}^{\text{VR}}(\mathbb{S}^1), \mathbf{D}_{n,k}^{\text{VR}}(\mathbb{S}^k)) \geq \inf_{D_1 \in \mathbf{D}_{n,k}^{\text{VR}}(\mathbb{S}^1)} d_{\mathcal{B}}(D_1, D_2).$$

For concreteness, write  $D_1 = \{(x, y)\}$ . Let  $\varphi : D_1 \rightarrow D_2$  be the unique bijection. By Lemma 5.2,  $x \geq \frac{k}{k+1}\pi$ , so

$$J(\varphi) = \left\| \left( \frac{\pi}{2}, \pi \right) - (x, y) \right\|_{\infty} \geq x - \frac{\pi}{2} \geq \frac{k-1}{2(k+1)}\pi.$$

On the other hand, since  $y \leq \pi$ ,  $\text{pers}(D_1) = y - x \leq \frac{\pi}{k+1}$ . Thus, for the empty matching  $\emptyset : \emptyset \rightarrow \emptyset$ , we have

$$J(\emptyset) = \max \left( \frac{1}{2} \text{pers}(D_1), \frac{1}{2} \text{pers}(D_2) \right) = \frac{1}{2} \text{pers}(D_2) = \frac{\pi}{4}.$$

Since  $\frac{\pi}{4} \leq \frac{k-1}{2(k+1)}\pi$  whenever  $k \geq 3$ , we have  $d_{\mathcal{B}}(D_1, D_2) = \min_{\varphi} J(\varphi) = \frac{\pi}{4}$  for all  $D_1 \in \mathbf{D}_{n,k}^{\text{VR}}(\mathbb{S}^1)$ . Thus, by Theorem 3.12,

$$d_{\mathcal{GH}}(\mathbb{S}^1, \mathbb{S}^k) \geq \frac{1}{2} d_{\mathcal{H}}^{\mathcal{D}}(\mathbf{D}_{n,k}^{\text{VR}}(\mathbb{S}^1), \mathbf{D}_{n,k}^{\text{VR}}(\mathbb{S}^k)) \geq \frac{1}{2} \inf_{D_1 \in \mathbf{D}_{n,k}^{\text{VR}}(\mathbb{S}^1)} d_{\mathcal{B}}(D_1, D_2) = \frac{\pi}{8}.$$

## 6 Concentration of persistence measures

By paring  $\mathbf{D}_{n,k}^{\mathfrak{F}}(X)$  with the persistence measure  $\mathbf{U}_{n,k}^{\mathfrak{F}}(X)$ , we can view persistence sets as an mm-space

$$\mathfrak{D}_{n,k}^{\mathfrak{F}}(X) := (\mathbf{D}_{n,k}^{\mathfrak{F}}(X), d_{\mathcal{B}}, \mathbf{U}_{n,k}^{\mathfrak{F}}(X)) \in \mathcal{M}^w,$$

where  $d_{\mathcal{B}}$  is restricted to pairs in  $\mathbf{D}_{n,k}^{\mathfrak{F}}(X) \times \mathbf{D}_{n,k}^{\mathfrak{F}}(X)$ .

The main result in this section is that  $\mathfrak{D}_{n,k}^{\mathfrak{F}}(X)$  *concentrates* to a one-point mm-space  $*$  as  $n \rightarrow \infty$ . Since  $*$  is generic, we also prove that the expected bottleneck distance between a random diagram  $\mathbb{D} \in \mathbf{D}_{n,k}^{\mathfrak{F}}(X)$  and  $\text{dgm}_k^{\mathfrak{F}}(X)$ , the degree- $k$  persistence diagram of the space  $X$ , goes to 0 as  $n \rightarrow \infty$ , effectively showing that  $\mathfrak{D}_{n,k}^{\mathfrak{F}}(X)$  concentrates to  $\text{dgm}_k^{\mathfrak{F}}(X)$  when the latter is viewed as a one-point mm-space equipped with the trivial choices of metric and probability measure.

**Example 6.1** (The case of an mm-space with two points). Let  $X = \{x_1, x_2\}$  be a metric space with two points at distance  $\varepsilon$  and mass  $\mu_X(x_1) = \alpha$ ,  $\mu_X(x_2) = 1 - \alpha$  for some  $\alpha \in (0, 1)$ . For each  $n \in \mathbb{N}$ , the matrices in  $K_n(X)$  are of the form  $M_0 = \mathbf{0} \in \mathbb{R}_+^{n \times n}$  or  $M_{\Pi} = \Pi^T M_1 \Pi$  for some  $\Pi \in S_n$ , where

$$M_1 := \begin{pmatrix} 0 & \varepsilon & 0 & \cdots & 0 \\ \varepsilon & 0 & 0 & \cdots & 0 \\ & \vdots & & \ddots & \vdots \\ 0 & 0 & 0 & \cdots & 0 \end{pmatrix} \in \mathbb{R}_+^{n \times n}.$$

For the curvature measure  $\mu_n$  on  $K_n(X)$ , we have  $w_n := \mu_n(M_0) = \alpha^n + (1 - \alpha)^n$ . This comes from choosing either all  $n$  points to be  $x_1$  or all to be  $x_2$ . The rest of the mass is distributed among the non-zero matrices of  $K_n(X)$ . Notice that  $w_n \rightarrow 0$  as  $n \rightarrow \infty$ .

As for the persistence sets  $\mathfrak{D}_{n,k}^{\text{VR}}(X)$ , the only interesting case is at  $k = 0$ . Here,  $\mathbf{U}_{n,0}^{\text{VR}}$  is supported on the two point set  $\mathbf{D}_{n,0}^{\text{VR}}(X) = \{\mathbf{0}_{\mathcal{D}}, (0, \varepsilon)\}$ , where  $\mathbf{0}_{\mathcal{D}}$  is the empty diagram of  $\mathcal{D}$ . From the computations above,  $\mathbf{U}_{n,0}^{\text{VR}}(\mathbf{0}_{\mathcal{D}}) = w_n$  and  $\mathbf{U}_{n,0}^{\text{VR}}((0, \varepsilon)) = 1 - w_n$ .

The fact that  $w_n \rightarrow 0$  as  $n \rightarrow \infty$  means that the mass concentrates on  $(0, \varepsilon)$ , so, as an mm-space,  $\mathfrak{D}_{n,0}^{\text{VR}}(X)$  is converging to the 1-point mm-space

$$(\{(0, \varepsilon)\}, 0, \delta_{(0,\varepsilon)}),$$

where  $\delta_{(0,\varepsilon)}$  is the Dirac delta measure concentrated on  $\delta_{(0,\varepsilon)}$ . This is the persistence diagram  $\text{dgm}_0^{\text{VR}}(X)$  viewed as a 1-point mm-space.

We now generalize this result.

## 6.1 A concentration theorem

Let  $(X, d_X, \mu_X)$  be an mm-space. Using terminology from [CM10b, Section 5.3], we define the functions  $f_X : \mathbb{R}^+ \rightarrow \mathbb{R}^+$  given by  $\varepsilon \mapsto \inf_{x \in X} \mu_X(B_\varepsilon(x))$ . Note that  $f_X(\varepsilon) > 0$  for every  $\varepsilon > 0$  since  $\text{supp}(\mu_X) = X$  is compact. Define also

$$C_X : \mathbb{N} \times \mathbb{R}_+ \rightarrow \mathbb{R}_+$$

given by

$$(n, \varepsilon) \mapsto \frac{e^{-nf_X(\varepsilon/4)}}{f_X(\varepsilon/4)}.$$

The relevant result from that paper is the following:

**Theorem 6.2** (Covering theorem [CM10b, Theorem 34]). *Let  $(X, d_X, \mu_X)$  be an mm-space. For a given  $n \in \mathbb{N}$  and  $\varepsilon > 0$  consider the set*

$$Q_X(n, \varepsilon) := \{(x_1, \dots, x_n) \in X^n \mid d_{\mathcal{H}}^X(\{x_i\}_{i=1}^n, X) > \varepsilon\}.$$

Then

$$\mu_X^{\otimes n}(Q_X(n, \varepsilon)) \leq C_X(n, \varepsilon).$$

We now prove our concentration result.

**Theorem 6.3.** *Let  $(X, d_X, \mu_X)$  be an mm-space and take any stable filtration functor  $\mathfrak{F}$ . For any  $n, k \in \mathbb{N}$ , consider the random variable  $\mathbb{D}$  valued in  $\mathbf{D}_{n,k}^{\mathfrak{F}}(X)$  distributed according to  $\mathbf{U}_{n,k}^{\mathfrak{F}}(X)$ . Then:*

- For any  $\varepsilon > 0$ ,  $E_{\mathbf{U}_{n,k}^{\mathfrak{F}}(X)} [d_{\mathcal{B}}(\mathbb{D}, \text{dgm}_k^{\mathfrak{F}}(X))] < \mathbf{diam}(X) \cdot C_X(n, \varepsilon) + \varepsilon$ .
- As a consequence, the mm-space  $\mathfrak{D}_{n,k}^{\mathfrak{F}}(X) = (\mathbf{D}_{n,k}^{\mathfrak{F}}(X), d_{\mathcal{B}}, \mathbf{U}_{n,k}^{\mathfrak{F}}(X))$  concentrates to a one-point mm-space as  $n \rightarrow \infty$ .

*Proof.* Fix  $\varepsilon > 0$ . Let  $\mathbb{X} = (x_1, \dots, x_n) \in X^n$  be a random variable distributed according to  $\mu_X^{\otimes n}$ . Since  $\mathbf{U}_{n,k}^{\mathfrak{F}}(X)$  is the push-forward of the product measure  $\mu_X^{\otimes n}$  under the map

$\text{dgm}_k^{\mathfrak{F}} \circ \Psi_X^{(n)} : X^n \rightarrow K_n(X) \rightarrow \mathcal{D}$ , we have  $\mathbb{D} = \text{dgm}_k^{\mathfrak{F}}(\Psi_X^{(n)}(\mathbb{X}))$ . Then, we can make a change of variables to rewrite the expected value of  $d_{\mathcal{B}}(\mathbb{D}, \text{dgm}_k^{\mathfrak{F}}(X))$  as follows:

$$\begin{aligned} E_{\mathbf{U}_{n,k}^{\mathfrak{F}}(X)} [d_{\mathcal{B}}(\mathbb{D}, \text{dgm}_k^{\mathfrak{F}}(X))] &= E_{\mu_X^{\otimes n}} \left[ d_{\mathcal{B}} \left( \text{dgm}_k^{\mathfrak{F}} \left[ \Psi_X^{(n)}(\mathbb{X}) \right], \text{dgm}_k^{\mathfrak{F}}(X) \right) \right] \\ &= \int_{X^n} d_{\mathcal{B}} \left( \text{dgm}_k^{\mathfrak{F}} \left[ \Psi_X^{(n)}(\mathbb{X}) \right], \text{dgm}_k^{\mathfrak{F}}(X) \right) \mu_X^{\otimes n}(d\mathbb{X}). \end{aligned}$$

By stability of  $\mathfrak{F}$ , the last integral is bounded above by

$$L(\mathfrak{F}) \int_{X^n} d_{\mathcal{H}}(\mathbb{X}, X) \mu_X^{\otimes n}(d\mathbb{X}) \leq L(\mathfrak{F}) \int_{X^n} d_{\mathcal{H}}(\mathbb{X}, X) \mu_X^{\otimes n}(d\mathbb{X}),$$

where, by abuse of notation, we see  $\mathbb{X}$  as a sub-metric space of  $X$ . In that case,  $d_{\mathcal{H}}(\mathbb{X}, X) = \mathbf{rad}_X(\mathbb{X}) \leq \mathbf{diam}(X)$ , so we split the above integral into the sets  $Q_X(n, \varepsilon)$  and  $X^n \setminus Q_X(n, \varepsilon)$ :

$$\begin{aligned} \int_{X^n} d_{\mathcal{H}}(\mathbb{X}, X) \mu_X^{\otimes n}(d\mathbb{X}) &= \int_{X^n} \mathbf{rad}_X(\mathbb{X}) \mu_X^{\otimes n}(d\mathbb{X}) \\ &= \int_{Q_X(n, \varepsilon)} \mathbf{rad}_X(\mathbb{X}) \mu_X^{\otimes n}(d\mathbb{X}) + \int_{X^n \setminus Q_X(n, \varepsilon)} \mathbf{rad}_X(\mathbb{X}) \mu_X^{\otimes n}(d\mathbb{X}) \\ &\leq \int_{Q_X(n, \varepsilon)} \mathbf{diam}(X) \mu_X^{\otimes n}(d\mathbb{X}) + \int_{X^n} \varepsilon \mu_X^{\otimes n}(d\mathbb{X}) \\ &= \mathbf{diam}(X) \cdot \mu_X^{\otimes n}(Q_X(n, \varepsilon)) + \varepsilon \\ &< \mathbf{diam}(X) \cdot C_X(n, \varepsilon) + \varepsilon. \end{aligned}$$

This proves the first claim.

To show that  $\mathfrak{D}_{n,k}^{\mathfrak{F}}(X)$  concentrates for a point, we will show that  $d_{\mathcal{GW},1}(\mathfrak{D}_{n,k}^{\mathfrak{F}}(X), *) \rightarrow 0$ . For any mm-space  $(Z, d_Z, \mu_Z)$ ,

$$d_{\mathcal{GW},1}(Z, *) = \frac{1}{2} \iint_{Z \times Z} d_X(z, z') \mu_Z(dz) \mu_Z(dz').$$

Then, using the triangle inequality,

$$\begin{aligned} d_{\mathcal{GW},1}(\mathfrak{D}_{n,k}^{\mathfrak{F}}(X), *) &= \frac{1}{2} \iint_{\mathbf{D}_{n,k}^{\mathfrak{F}}(X) \times \mathbf{D}_{n,k}^{\mathfrak{F}}(X)} d_{\mathcal{B}}(D, D') \mathbf{U}_{n,k}^{\mathfrak{F}}(dD) \mathbf{U}_{n,k}^{\mathfrak{F}}(dD') \\ &\leq \frac{1}{2} \iint_{\mathbf{D}_{n,k}^{\mathfrak{F}}(X) \times \mathbf{D}_{n,k}^{\mathfrak{F}}(X)} [d_{\mathcal{B}}(D, \text{dgm}_k^{\mathfrak{F}}(X)) + d_{\mathcal{B}}(\text{dgm}_k^{\mathfrak{F}}(X), D')] \mathbf{U}_{n,k}^{\mathfrak{F}}(dD) \mathbf{U}_{n,k}^{\mathfrak{F}}(dD') \\ &= \int_{\mathbf{D}_{n,k}^{\mathfrak{F}}(X)} d_{\mathcal{B}}(D, \text{dgm}_k^{\mathfrak{F}}(X)) \mathbf{U}_{n,k}^{\mathfrak{F}}(dD) \\ &= E_{\mathbf{U}_{n,k}^{\mathfrak{F}}(X)} [d_{\mathcal{B}}(\mathbb{D}, \text{dgm}_k^{\mathfrak{F}}(X))] \\ &< \mathbf{diam}(X) \cdot C_X(n, \varepsilon) + \varepsilon. \end{aligned}$$

However, for any fixed  $\varepsilon$ ,  $C_X(n, \varepsilon) \rightarrow 0$  as  $n \rightarrow \infty$ . Thus,  $E_{\mathbf{U}_{n,k}^{\mathfrak{F}}(X)} [d_{\mathcal{B}}(\mathbb{D}, \text{dgm}_k^{\mathfrak{F}}(X))] \rightarrow 0$  and, with that,  $d_{\mathcal{GW},1}(\mathfrak{D}_{n,k}^{\mathfrak{F}}(X), *) \rightarrow 0$ .  $\square$

**Remark 6.4.** We can give an explicit upper bound for  $E_{\mathbf{U}_{n,k}^{\mathfrak{F}}(X)} [d_{\mathcal{B}}(\mathbb{D}, \text{dgm}_k^{\mathfrak{F}}(X))]$  in the case that  $\mu_X$  is Ahlfors regular. Given  $d \geq 0$ ,  $\mu_X$  is Ahlfors  $d$ -regular if there exists a constant  $C \geq 1$  such that

$$\frac{r^d}{C} \leq \mu_X(B_r(x)) \leq Cr^d$$

for all  $x \in X$ .

To get the upper bound, set  $\varepsilon = 4C^{1/d} \left(\frac{\ln n}{n}\right)^{1/d}$ . If  $\mu_X$  is Ahlfors  $d$ -regular,

$$f_X(\varepsilon/4) = \inf_{x \in X} \mu_X(B_{\varepsilon/4}(x)) \geq \frac{(\varepsilon/4)^d}{C} = \frac{\ln(n)}{n},$$

and

$$C_X(n, \varepsilon) = \frac{e^{-nf_X(\varepsilon/4)}}{f_X(\varepsilon/4)} \leq \frac{e^{-\ln(n)}}{\ln(n)/n} = \frac{1}{\ln(n)}.$$

Then,

$$\begin{aligned} E_{\mathbf{U}_{n,k}^{\mathfrak{F}}(X)} [d_{\mathcal{B}}(\mathbb{D}, \text{dgm}_k^{\mathfrak{F}}(X))] &< \mathbf{diam}(X) \cdot C_X(n, \varepsilon) + \varepsilon \\ &\leq \frac{\mathbf{diam}(X)}{\ln(n)} + 4C^{1/d} \left(\frac{\ln n}{n}\right)^{1/d}. \end{aligned}$$

## 7 Coordinates

The objects  $\mathbf{U}_{n,k}^{\mathfrak{F}}(X)$  can be complex, so it is important to find simple representations of them. Since these objects are probability measures on the space of persistence diagrams  $\mathcal{D}$ , we follow the statistical mechanics intuition and probe them via functions. In order to accomplish this, one should concentrate on families of functions  $\zeta_{\alpha} : \mathcal{D} \rightarrow \mathbb{R}$ , for  $\alpha$  in some index set  $A$ . One example of a family that is compatible with this is the so called *maximal persistence* of a persistence diagram:  $\zeta(D) = \max_{(t_b, t_d) \in D} (t_d - t_b)$ . In general, one may desire to obtain a class of *coordinates* [ACC16, Kal19] that are able to more or less canonically exhaust all the information contained in a given persistence diagram. A further desire is to design the class  $\{\zeta_{\alpha}\}_{\alpha \in A}$  in such a manner that it provides *stable information* about a given measure  $U \in \mathcal{P}_1(\mathcal{D})$ .

A first step in this direction is a stability result. To set up notation, let  $\mathfrak{F}$  be a filtration functor. Let  $n \geq 0$ ,  $k \geq 0$  be integers, and take an mm-space  $(X, d_X, \mu_X)$ . Consider a coordinate function  $\zeta : \mathcal{D} \rightarrow \mathbb{R}$ . The pushforward  $\zeta_{\#} \mathbf{U}_{n,k}^{\mathfrak{F}}(X)$  is a probability measure on  $\mathbb{R}$ . We denote its distribution function by  $H_X(t; n, k, \mathfrak{F}, \zeta) := \mathbf{U}_{n,k}^{\mathfrak{F}}(X)(\zeta^{-1}(-\infty, t])$  defined for  $t \in \mathbb{R}$ .

**Theorem 7.1.** *Let  $\zeta : \mathcal{D} \rightarrow \mathbb{R}$  be an  $L(\zeta)$ -Lipschitz coordinate function, and suppose  $\mathfrak{F}$  is a stable filtration functor. Write  $H_X(t) = H_X(t; n, k, \mathfrak{F}, \zeta)$  to simplify the notation. Then, for any two mm-spaces  $X$  and  $Y$ ,*

$$\int_{\mathbb{R}} |H_X(t) - H_Y(t)| dt \leq L(\zeta)L(\mathfrak{F}) \cdot d_{\mathcal{GW},1}(X, Y).$$

*Proof.* According to [Mém11, Lemma 6.1],

$$\int_{\mathbb{R}} |H_X(t) - H_Y(t)| dt \leq \inf_{\mu \in \mathcal{M}_U} \int_{\mathbf{D}_{n,k}^{\mathfrak{F}}(X) \times \mathbf{D}_{n,k}^{\mathfrak{F}}(Y)} |\zeta(D) - \zeta(D')| \mu(dD \times dD'),$$

where  $\mathcal{M}_U$  is the set of couplings between  $\mathbf{U}_{n,k}^{\mathfrak{F}}(X)$  and  $\mathbf{U}_{n,k}^{\mathfrak{F}}(Y)$ . Since  $\zeta$  is Lipschitz, the right side is bounded above by

$$\begin{aligned} & L(\zeta) \cdot \inf_{\mu \in \mathcal{M}_U} \int_{\mathbf{D}_{n,k}^{\mathfrak{F}}(X) \times \mathbf{D}_{n,k}^{\mathfrak{F}}(Y)} d_{\mathcal{B}}(D, D') \mu(dD \times dD') \\ &= L(\zeta) \cdot \inf_{\mu \in \mathcal{M}_U} \mathbf{diam}_{\mathcal{D},1}(\mathbf{D}_{n,k}^{\mathfrak{F}}(X) \times \mathbf{D}_{n,k}^{\mathfrak{F}}(Y)) \\ &= L(\zeta) \cdot d_{\mathcal{W},1}^{\mathcal{D}}(\mathbf{U}_{n,k}^{\mathfrak{F}}(X), \mathbf{U}_{n,k}^{\mathfrak{F}}(Y)) \\ &\leq L(\zeta)L(\mathfrak{F}) \cdot d_{\mathcal{G}\mathcal{W},1}(X, Y). \end{aligned}$$

Theorem 3.17 gives the last bound. □

## 8 Persistence sets of metric graphs

Let  $G$  be a metric graph; see [BBI01, Mug19, MO18] for a definition. The central question in this section is what features of  $G$  are detected by  $\mathbf{D}_{2k+2,k}^{\text{VR}}(G)$ . A first setting is the one when  $G$  is a tree.

**Lemma 8.1.** *Let  $k \geq 1$ . For any metric tree  $T$  and any  $X \subset T$  with  $|X| = n$ ,  $\text{PH}_k(X) = 0$  and, thus,  $\mathbf{D}_{n,k}^{\text{VR}}(T)$  is empty. In particular, if  $n = 2k + 2$ , then  $t_b(X) \geq t_d(X)$ .*

*Proof.* Any subset  $X \subset T$  is a tree-like metric space. By Theorem 2.1 of the appendix of [CCR13], the persistence module  $\text{PH}_k(X)$  is 0 for any  $k \geq 1$ . In particular, if  $n = 2k + 2$ , Theorem 4.4 implies that  $t_b(X) \geq t_d(X)$ . □

In other words, a metric graph  $G$  must have a cycle if  $\mathbf{D}_{n,k}^{\text{VR}}(G)$  is to be non-empty, and even if it does, not all configurations  $X \subset G$  with  $|X| = n$  produce persistence. As we will see in Example 8.4, even if there is no tree  $X \hookrightarrow T \hookrightarrow G$ ,  $X$  can still be a tree-like metric space. For this reason, it would be useful to have a notion of a minimal graph containing  $X$ . At least in the case  $n = 4$ , split metric decompositions provide a nice framework for our questions.

### 8.1 Split metric decompositions

We follow the exposition in [BD92]. Let  $(X, d_X)$  be a finite pseudo-metric space. Given a partition  $X = A \cup B$ , the *split metric*  $\delta_{A,B}$  is defined as the function

$$\delta_{A,B}(x, y) := \begin{cases} 0, & \text{if } x, y \in A \text{ or } x, y \in B, \\ 1, & \text{otherwise.} \end{cases}$$

Let

$$\beta_{\{a,a'\},\{b,b'\}} := \frac{1}{2} \left( \max [d_X(a, b) + d_X(a', b'), d_X(a, b') + d_X(a', b), d_X(a, a') + d_X(b, b')] - d_X(a, a') - d_X(b, b') \right),$$

and define the *isolation index*  $\alpha_{A,B}$  as

$$\alpha_{A,B} = \min \{ \beta_{\{a,a'\},\{b,b'\}} \mid a, a' \in A \text{ and } b, b' \in B \}.$$

Notice that both  $\alpha_{A,B}$  and  $\beta_{\{a,a'\},\{b,b'\}}$  are non-negative. If the isolation index  $\alpha_{A,B}$  is non-zero, then the unordered partition  $A, B$  is called a  $d_X$ -*split*. The main theorem regarding isolation indices and split metrics is the following.

**Theorem 8.2** ([BD92]). *Any (pseudo-)metric  $d_X$  on a finite space can be written uniquely as*

$$d_X = d_0 + \sum \alpha_{A,B} \delta_{A,B}$$

where  $d_0$  is a (pseudo-)metric that has no  $d_0$ -splits (also called *split-prime metric*), and the sum runs over all  $d_X$ -splits  $A, B$ .

In what follows, we may write  $\delta_{A,B}$  and  $\alpha_{A,B}$  as  $\delta_{a_1, \dots, a_n}$  and  $\alpha_{a_1, \dots, a_n}$ , respectively, when  $A = \{a_1, \dots, a_n\}$ , and  $X$  and  $B = X \setminus A$  are clear from the context.

Let's focus on the case in which  $X$  has 4 points. It has been shown that  $d_X$  has no split-prime component and, when  $A = \{a, a'\}$  and  $B = \{b, b'\}$ ,  $\alpha_{A,B} = \beta_{A,B}$ . Furthermore, there is at least one such partition for which  $d_X(a, a') + d_X(b, b')$  is maximal, which implies  $\alpha_{A,B} = 0$ . In that case,  $X$  can be isometrically embedded in the graph  $\Gamma_X$  shown in Figure 17. We now study the persistence diagram of  $X$ .

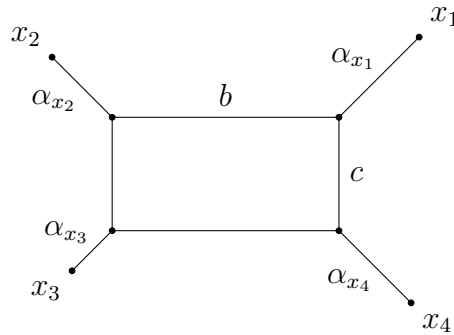


Figure 17: The graph  $\Gamma_X$  resulting from the split-metric decomposition of a metric space with 4 points. In this case,  $\alpha_{x_1, x_3} = 0$ ,  $b = \alpha_{x_1, x_4}$ ,  $c = \alpha_{x_1, x_2}$ , and  $d_X = \sum_{i=1}^4 \alpha_{x_i} \delta_{x_i} + \alpha_{x_1, x_2} \delta_{x_1, x_2} + \alpha_{x_1, x_4} \delta_{x_1, x_4}$ .

**Proposition 8.3.** *Let  $X \subset \Gamma_X$  be the metric space shown in Figure 17, and let  $a_i = \alpha_{x_i}$ ,  $b = \alpha_{x_1, x_4}$  and  $c = \alpha_{x_1, x_2}$ .*

1. If  $t_b(X) < t_d(X)$ , then  $t_b(X) = \max(d_{12}, d_{23}, d_{34}, d_{41})$  and  $t_d(X) = \min(d_{13}, d_{24})$ .

2.  $t_b(X) < t_d(X)$  if, and only if,

$$\begin{aligned} |a_2 - a_1| < b, \text{ and } |a_4 - a_3| < b, \\ |a_3 - a_2| < c, \text{ and } |a_1 - a_4| < c. \end{aligned} \tag{20}$$

3.  $t_d(X) - t_b(X) \leq \min(a, b)$ , regardless of whether  $t_b(X) < t_d(X)$  or not.

*Proof.* 1. The desired conclusion is equivalent to  $v_d(x_1) = x_3$  and  $v_d(x_2) = x_4$ . Suppose, though, that  $v_d(x_1) = x_4$  and  $v_d(x_2) = x_3$ . In particular, this means that  $d_{13} < d_{14}$  and  $d_{24} < d_{23}$ , and these inequalities are equivalent to

$$\begin{aligned} a_1 + (b + c) + a_3 &< a_1 + c + a_4 \\ a_2 + (b + c) + a_4 &< a_2 + c + a_3. \end{aligned}$$

After rearranging them, we get

$$b < a_4 - a_3 < -b,$$

a contradiction. The case  $v_d(x_1) = x_4$  and  $v_d(x_2) = x_3$  follows analogously, so  $v_d(x_1) = x_3$  and  $v_d(x_2) = x_4$ .

2. Notice that the inequalities  $d_{23} < d_{13}$  and  $d_{14} < d_{24}$  are equivalent to

$$\begin{aligned} a_2 + c + a_3 &< a_1 + (b + c) + a_3 \\ a_1 + c + a_4 &< a_2 + (b + c) + a_4, \end{aligned}$$

which, after rearranging terms, result in  $-b < a_2 - a_1 < b$ . Using similar combinations, we find that  $\max(d_{12}, d_{23}, d_{34}, d_{41}) < \min(d_{13}, d_{24})$  is equivalent to the system of inequalities in (20). If these hold, then  $t_b(X) = \max(d_{12}, d_{23}, d_{34}, d_{41}) < \min(d_{13}, d_{24}) = t_d(X)$ . Conversely, if  $t_b(X) < t_d(X)$ , then item 1 and the reasoning above imply (20).

3. If  $t_b(X) \geq t_d(X)$ , the bound is trivially satisfied. Suppose then, without loss of generality, that  $t_b(X) = d_{12}$ . Since  $a_3 + b + a_4 = d_{34} \leq d_{12} = a_1 + b + a_2$ , we have

$$\begin{aligned} t_d(X) - t_b(X) &= \min(d_{13}, d_{24}) - d_{12} \\ &\leq \frac{1}{2}[d_{13} + d_{24}] - d_{12} \\ &= \frac{1}{2}[a_1 + a_2 + a_3 + a_4 + 2(b + c)] - (a_1 + b + a_2) \\ &\leq \frac{1}{2}[a_1 + a_2 + (a_1 + a_2) + 2(b + c)] - (a_1 + a_2) - b \\ &= c. \end{aligned}$$

On the other hand,  $d_{14} \leq d_{12}$  and  $d_{23} \leq d_{12}$  give  $a_4 + c \leq a_2 + b$  and  $a_3 + c \leq a_1 + b$ . Then

$$\begin{aligned} t_d(X) - t_b(X) &\leq \frac{1}{2}[a_1 + a_2 + a_3 + a_4 + 2(b + c)] - (a_1 + b + a_2) \\ &\leq \frac{1}{2}[a_1 + a_2 + (a_1 + a_2) + 4b] - (a_1 + a_2) - b \\ &= b. \end{aligned}$$

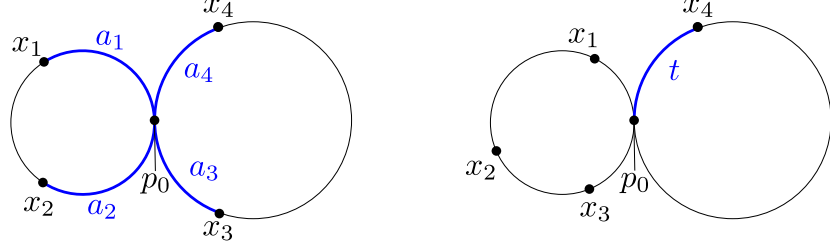


Figure 18: A graph formed by the wedge of two circles at 0. Left:  $\Gamma_X$  is a tree. Center: One circle contains three points, while the other only has one. Right: Both circles have two out of four points.

In summary,  $t_d(X) - t_b(X) \leq \min(a, b)$ . □

The following examples illustrate uses of Proposition 8.3.

**Example 8.4.** Let  $\lambda_1 \neq \lambda_2$  positive numbers. Let  $G = (\frac{\lambda_1}{\pi} \cdot \mathbb{S}^1) \vee (\frac{\lambda_2}{\pi} \cdot \mathbb{S}^1)$  be a wedge of two circles of diameters  $\lambda_1, \lambda_2$  at a common point  $p_0$ . The set  $\mathbf{D}_{4,1}^{\text{VR}}(\frac{\lambda_i}{\pi} \cdot \mathbb{S}^1)$  is the triangle in  $\mathbb{R}^2$  bounded by  $2(\lambda_i - t_b) \leq t_d$  and  $t_b < t_d \leq \lambda_i$  with vertices  $(\frac{1}{2}\lambda_i, \lambda_i)$ ,  $(\frac{2}{3}\lambda_i, \frac{2}{3}\lambda_i)$ , and  $(\lambda_i, \lambda_i)$  (see Remark 5.6). By functoriality of persistence sets, we have  $\mathbf{D}_{4,1}^{\text{VR}}(\frac{\lambda_1}{\pi} \cdot \mathbb{S}^1) \cup \mathbf{D}_{4,1}^{\text{VR}}(\frac{\lambda_2}{\pi} \cdot \mathbb{S}^1) \subset \mathbf{D}_{4,1}^{\text{VR}}(G)$ . We now show that equality holds.

Let  $X = \{x_1, x_2, x_3, x_4\} \subset G$ , and  $d_{ij} = d_G(x_i, x_j)$ . Define  $X_i = X \cap (\frac{\lambda_i}{\pi} \cdot \mathbb{S}^1)$ . If either  $X_i = \emptyset$ , then  $X$  is contained in the other  $\frac{\lambda_j}{\pi} \cdot \mathbb{S}^1$ , and  $\text{dgm}_1^{\text{VR}}(X) \in \mathbf{D}_{4,1}^{\text{VR}}(\frac{\lambda_j}{\pi} \cdot \mathbb{S}^1)$ . Suppose, then, that  $X_1$  and  $X_2$  are non-empty. Two cases follow.

First, assume  $X_2 = \{x_4\}$ , and set  $X' = \{p_0, x_1, x_2, x_3\}$ . Let  $t = d_G(p_0, x_4)$ . For  $i = 1, 2, 3$ ,  $d_{i4} = d_G(x_i, p_0) + t$ , so  $t_b(X') \leq t_b(X)$  and  $t_d(X') \leq t_d(X)$ . If  $t_b(X') < t_d(X')$ , suppose further that  $v_d(x_1) = x_3$  and  $v_d(x_2) = x_4$ . Then  $2\lambda_1 \leq 2t_b(X') + t_d(X') \leq 2t_b(X) + t_d(X)$  and  $t_d(X) \leq t_d(x_1) = d_{13} \leq \lambda_1$ , regardless of the position of  $x_4$ . In other words, if the point  $(t_b(X'), t_d(X')) \in \mathbf{D}_{4,1}^{\text{VR}}(\frac{\lambda_1}{\pi} \cdot \mathbb{S}^1)$ , then either  $t_b(X)$  is still smaller than  $t_d(X)$  and  $(t_b(X), t_d(X)) \in \mathbf{D}_{4,1}^{\text{VR}}(\frac{\lambda_1}{\pi} \cdot \mathbb{S}^1)$ , or  $t_b(X)$  becomes larger than  $t_d(X)$  and  $\text{dgm}_1^{\text{VR}}(X)$  is empty.

Even if  $t_b(X') \geq t_d(X')$ , it might be possible that  $t_b(X) < t_d(X)$ . However, several conditions must be met. First,  $d_{13}$  must be larger than  $d_{12}$  and  $d_G(x_1, p_0)$  in order to have  $v_d(x_1) = x_3$ . In that case,  $t_d(X) \leq d_{13}$ , so we also need  $t_b(X') < d_{13}$ . Also,  $t_b(X')$  cannot be  $d_G(x_i, p_0)$  because otherwise,  $t_b(X) = d_G(x_i, p_0) + t = t_b(X') + t \geq t_d(X') + t \geq t_d(X)$ . For that, the only option is  $t_b(X') = d_{12}$  (since  $d_{23} < d_G(x_2, p_0) \leq t_b(X')$ ). Then,

$$2\lambda_1 = d_{12} + d_{24} + d_{34} < 3d_{12},$$

so  $d_{12} > \frac{2\lambda_1}{3}$ , and we have

$$\begin{aligned} t_b(X) &\geq t_b(X') > \frac{2\lambda_1}{3}, \\ t_d(X) &\leq t_d(X') \leq \lambda_1. \end{aligned}$$

This point is also contained in  $\mathbf{D}_{4,1}^{\text{VR}}(\frac{\lambda_1}{\pi} \cdot \mathbb{S}^1)$ , so no new persistence is generated.

For the second case, let  $X_1 = \{x_1, x_2\}$  and  $X_2 = \{x_3, x_4\}$ . Let  $a_i = d_G(x_i, p_0)$ . Notice that  $d_G(x_i, x_j) = a_i + a_j$  for  $i \in \{1, 2\}$  and  $j \in \{3, 4\}$ . Then:

$$\begin{aligned} d_G(x_1, x_3) + d_G(x_2, x_4) &= d_G(x_1, x_4) + d_G(x_2, x_3) = a_1 + a_2 + a_3 + a_4, \\ d_G(x_1, x_2) + d_G(x_3, x_4) &\leq a_1 + a_2 + a_3 + a_4. \end{aligned}$$

In consequence,

$$\begin{aligned} \alpha_{x_1, x_3} &= \beta_{x_1, x_3} \\ &= \frac{1}{2} \left[ \max \left( d_G(x_1, x_3) + d_G(x_2, x_4), d_G(x_1, x_4) + d_G(x_2, x_3), d_G(x_1, x_2) + d_G(x_3, x_4) \right) \right. \\ &\quad \left. - d_G(x_1, x_3) - d_G(x_2, x_4) \right] \\ &= 0. \end{aligned}$$

Analogously,  $\alpha_{x_1, x_4} = 0 \leq \alpha_{x_1, x_2}$ . Then  $b = 0$  in Proposition 8.3 and item 3 gives that  $\text{dgm}_1^{\text{VR}}(X)$  is the empty diagram. Note, in particular, that  $\Gamma_X$  is a tree.

In summary, we've shown that if  $X_1$  and  $X_2$  are both non-empty, then either  $\text{dgm}_1^{\text{VR}}(X)$  is empty or it is in the union  $\mathbf{D}_{4,1}^{\text{VR}}(\frac{\lambda_1}{\pi} \cdot \mathbb{S}^1) \cup \mathbf{D}_{4,1}^{\text{VR}}(\frac{\lambda_2}{\pi} \cdot \mathbb{S}^1)$ . Thus,  $\mathbf{D}_{4,1}^{\text{VR}}(G) = \mathbf{D}_{4,1}^{\text{VR}}(\frac{\lambda_1}{\pi} \cdot \mathbb{S}^1) \cup \mathbf{D}_{4,1}^{\text{VR}}(\frac{\lambda_2}{\pi} \cdot \mathbb{S}^1)$ .

Example 8.4 shows that a configuration  $X \subset G$  produces persistence only if it is close to a cycle. That can happen when either  $X$  is contained in a circle  $\frac{\lambda_i}{\pi} \cdot \mathbb{S}^1$ , or only one point is outside of  $\frac{\lambda_i}{\pi} \cdot \mathbb{S}^1$ . In both cases, the graph  $\Gamma_X$  contains a cycle since both  $a$  and  $b$  are non-zero. If  $|X_1| = |X_2| = 2$ , on the other hand, then  $\Gamma_X$  is a tree. This might lead to conjecture that  $\mathbf{D}_{4,1}^{\text{VR}}(G)$  decomposes as the union of  $\mathbf{D}_{4,1}^{\text{VR}}(C)$ , where  $C \subset G$  is a cycle. However, the following examples show otherwise.

**Example 8.5.** Let  $G$  be a graph formed by attaching edges of length  $L$  to a circle  $\mathbb{S}^1$  at the points  $y_1 \prec y_2 \prec y_3 \prec y_4$ . Let  $X = \{x_1, x_2, x_3, x_4\} \subset G$ . If  $X \subset \mathbb{S}^1$ , then no new persistence is produced, so the points in  $X$  have to be in the attached edges. Also, if  $t_b(X)$  is to be smaller than  $t_d(X)$ , then each  $x_i$  must be on a different edge. For example, if  $x_1$  and  $x_2$  are on the edge attached to  $y_1$ , and  $x_3$  and  $x_4$  are on the edges adjacent to  $y_3$  and  $y_4$ , respectively, let  $X' = \{x_1, x_2, y_3, y_4\}$ . This  $X'$  consists of two points inside of a cycle and two points outside, so as we saw in Example 8.4 when  $|X_1| = |X_2| = 2$ ,  $X'$  is a tree-like metric space, and attaching edges at  $y_3$  and  $y_4$  doesn't change that. Thus,  $X$  is also a tree-like metric space.

Suppose, then, that each  $x_i$  is on the edge attached to  $y_i$ . Since the decomposition in Theorem 8.2 is unique, the isolation indices of the metrics of  $X$  and  $Y$  satisfy:

$$\begin{aligned} \alpha_{\{x_i\}, X \setminus \{x_i\}} &= \alpha_{\{y_i\}, Y \setminus \{y_i\}} + d_G(x_i, y_i), \\ \alpha_{\{x_i, x_j\}, \{x_h, x_k\}} &= \alpha_{\{y_i, y_j\}, \{y_h, y_k\}}, \end{aligned}$$

where  $\{i, j, h, k\} = \{1, 2, 3, 4\}$ . Suppose that  $\alpha_{\{y_1, y_3\}, \{y_2, y_4\}} = 0$ , and let

$$m = \min(\alpha_{\{y_1, y_2\}, \{y_3, y_4\}}, \alpha_{\{y_1, y_4\}, \{y_2, y_3\}}).$$

By Proposition 8.3,  $t_d(X) - t_b(X) \leq m$ , so

$$\mathbf{D}_{4,1}^{\text{VR}}(G) \subset \mathbf{D}_{4,1}^{\text{VR}}(\mathbb{S}^1) \cup \{(t_b, t_d) \mid t_b(Y) \leq t_b < t_d \leq t_b + m, \text{ and } t_b \leq t_b(Y) + 2L\}.$$

Observe that  $\mathbf{D}_{4,1}^{\text{VR}}(G)$  can have more points than  $\mathbf{D}_{4,1}^{\text{VR}}(C)$ . For example, if  $t_b(Y) < t_d(Y)$ , then the point  $(t_b(Y) + 2L, t_d(Y) + 2L) \in \mathbf{D}_{4,1}^{\text{VR}}(G)$ .

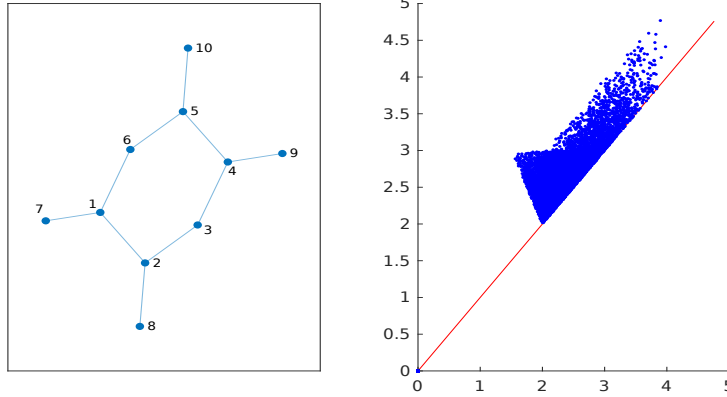


Figure 19: A cycle  $C$  with four edges of length  $L=1$  attached. This figure was obtained by sampling 100,000 configurations of 4 points from  $G$ . About 7.6% of those configurations produced a non-diagonal point.

**Remark 8.6.** It is curious to note that, in the last example,  $\text{VR}(G) \simeq \text{VR}(C)$ , but  $\mathbf{D}_{4,1}^{\text{VR}}(G) \neq \mathbf{D}_{4,1}^{\text{VR}}(C)$ . In other words,  $\mathbf{D}_{4,1}^{\text{VR}}$  detects a feature of  $G$  that the Vietoris-Rips complex doesn't. See Figure 19 for an example.

**Example 8.7.** Let  $G$  be the graph with edges of length 1 shown in Figure 20. Let  $C$  be the cycle that passes through the vertices 1, 2, 6, 5, 8, 7, 3, 4.  $C$  has length 8, but there is no point  $(2, 4) \in \mathbf{D}_{4,1}^{\text{VR}}(G)$ . The reason is that the shortest path between points in  $C$  is often not contained in  $C$ , and so  $C$  is not isometric to a circle. For example, the edge  $[1, 5]$  is not contained in  $C$  despite it being the shortest path from 1 to 5.

## 8.2 A family of metric graphs whose homotopy type can be characterized via $\mathbf{D}_{4,1}^{\text{VR}}$ .

Given an isometric embedding  $\frac{\lambda}{\pi} \cdot \mathbb{S}^1 \hookrightarrow G$ , the upper corner  $(\lambda/2, \lambda) \in \mathbf{D}_{4,1}^{\text{VR}}(\frac{\lambda}{\pi} \cdot \mathbb{S}^1)$  also appears in  $\mathbf{D}_{4,1}^{\text{VR}}(G)$ . Moreover,  $(\lambda/2, \lambda)$  is the only point in  $\mathbf{D}_{4,1}^{\text{VR}}(\frac{\lambda}{\pi} \cdot \mathbb{S}^1)$  that has  $t_d = 2t_b$ . Compare that to the recent examples in which there is a triangle in  $\mathbf{D}_{4,1}^{\text{VR}}(G)$ , coming from such an embedding, that is clearly distinguishable from the rest of the diagram. At this point,

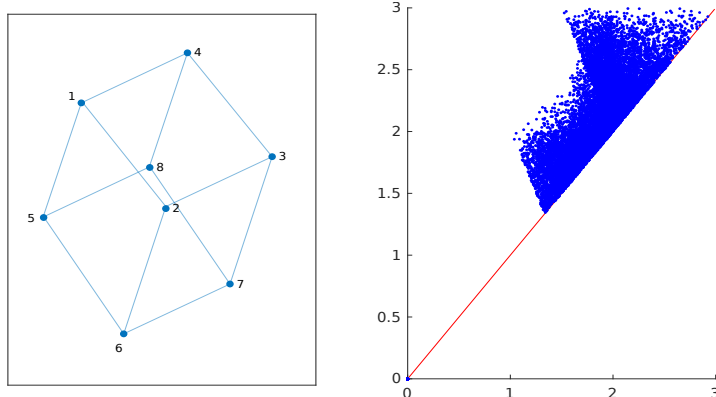


Figure 20: A graph  $G$  with a cycle not isometric to a circle. This figure was obtained by sampling 100,000 configurations of 4 points from  $G$ . About 13% of those configurations produced a non-diagonal point.

we can ask if there are conditions on  $G$  so that a point  $(t_b, t_d) \in \mathbf{D}_{4,1}^{\text{VR}}(G)$  with  $t_d = 2t_b$  must come from a configuration  $X \subset \frac{\lambda}{\pi} \cdot \mathbb{S}^1 \hookrightarrow G$ . It turns out that this is the right question, but the condition that  $G$  has to satisfy is elaborate. Before describing it, we prove a preliminary result.

**Lemma 8.8.** *Let  $k \geq 0$  and  $n = 2k+2$ , and take  $(X, d_X) \in \mathcal{M}$ . Suppose  $(\lambda/2, \lambda) \in \mathbf{D}_{n,k}^{\text{VR}}(X)$ . Then there exists a set  $Y = \{x_1, \dots, x_n\} \subset X$  with  $t_b(Y) = \lambda/2$ ,  $t_d(Y) = \lambda$  such that  $d_X(x_i, v_d(x_i)) = \lambda$  and  $d_X(x_i, x) = \lambda/2$  for every  $i$  and  $x \in Y$ ,  $x \neq v_d(x_i)$ .*

*Proof.* If  $(\lambda/2, \lambda) \in \mathbf{D}_{n,k}^{\text{VR}}(X)$ , there exists  $Y \subset X$  with  $|Y| = n$  such that  $t_b(Y) = \lambda/2$  and  $t_d(Y) = \lambda$ . For any  $i$  and  $x \in Y$ ,  $x \neq v_d(x_i)$ , the definition of  $t_b(Y)$  and  $t_d(Y)$  gives

$$\lambda \leq t_d(x_i) = d_X(x_i, v_d(x_i)) \leq d_X(x_i, x) + d_X(x, v_d(x_i)) \leq t_b(x_i) + t_b(v_d(x_i)) \leq \lambda.$$

Hence,  $d_X(x_i, v_d(x_i)) = \lambda$  and  $d_X(x_i, x) = d_X(x, v_d(x_i)) = \lambda/2$ . □

In particular, if  $(\lambda/2, \lambda) \in \mathbf{D}_{4,1}^{\text{VR}}(G)$  for a metric graph  $G$ , then there exists a “square”  $X \subset G$ . By square, we mean that if  $X = \{x_1, x_2, x_3, x_4\}$ , then  $d_G(x_i, x_{i+1}) = \lambda/2$  and  $d_G(x_i, x_{i+2}) = \lambda$ . It is tempting to suggest that  $X$  is contained in a cycle  $C \subset G$  isometric to  $\frac{\lambda}{\pi} \cdot \mathbb{S}^1$ , but this is not always the case. An example is shown in Figure 21. However, if  $G$  satisfies the hypothesis of Theorem 8.10, then at least we can ensure that  $X$  lies in a specific subgraph. Before that, we need one more preparatory result which was inspired by Theorem 3.15 in [AAG<sup>+</sup>20].

**Lemma 8.9.** *Let  $G = G_1 \cup_A G_2$  be a metric gluing of the graphs  $G_1$  and  $G_2$  such that  $A = G_1 \cap G_2$  is a closed path of length  $\alpha$ . Let  $\ell_j$  be the length of the shortest cycle contained in  $G_j$  that intersects  $A$ , and set  $\ell = \min(\ell_1, \ell_2)$ . Assume that  $\alpha < \frac{\ell}{2}$ . Then the shortest path  $\gamma_{uv}$  between any two points  $u, v \in A$  is contained in  $A$ . As a consequence, if  $\frac{\lambda}{\pi} \cdot \mathbb{S}^1 \hookrightarrow G$  is an isometric embedding, then  $\frac{\lambda}{\pi} \cdot \mathbb{S}^1$  is contained in either  $G_1$  or  $G_2$ .*

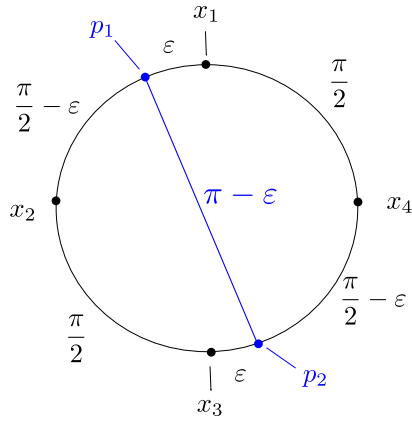


Figure 21: A graph  $G$  and a set  $X \subset G$  such that  $t_b(X) = \pi/2$  and  $t_d(X) = \pi$ . Notice that the outer black cycle  $C$  contains  $X$  but is not isometric to a circle. If it were, the shortest path in  $G$  between  $p_1$  and  $p_2$  would be contained in  $C$ , but that path is the blue edge of length  $\pi - \varepsilon$ .

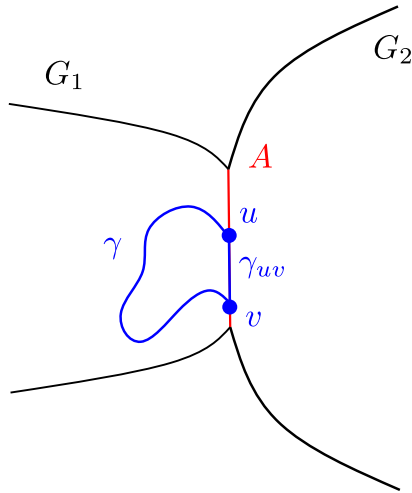


Figure 22: Any path in  $G_1$  between  $u$  and  $v$  has length greater than  $\alpha$ .

*Proof.* Let  $\gamma$  be any path that joins  $u$  and  $v$ , and is contained in either  $G_1$  or  $G_2$  but not in  $A$ ; see Figure 22. Then  $\gamma \cup \gamma_{uv}$  contains a cycle  $C$  that intersects  $A$ . Since  $\gamma_{uv} \subset A$ , its length is smaller than  $\alpha$ . Then

$$2\alpha < \ell \leq |\gamma| + |\gamma_{uv}| = |\gamma| + \alpha.$$

Thus,  $|\gamma| > \alpha \geq |\gamma_{uv}| = d_G(u, v)$ .

Now, a cycle  $C \subset G$  is isometric to  $\frac{\lambda}{\pi} \cdot \mathbb{S}^1$  if there is a shortest path between any  $x, x' \in C$  contained in  $C$ . If  $C \cap A$  has several connected components, then  $C$  can be decomposed as the union of paths in  $A$  and paths contained in  $G_1$  or  $G_2$ . If we pick two points  $u$  and  $v$  that lie in different connected components of  $C \cap A$ , then the shortest sub-path of  $C$  between them will contain a sub-path that lies either in  $G_1$  or  $G_2$ . By the previous paragraph, the sub-path contained in  $G_1$  or  $G_2$  has length larger than  $\alpha \geq d_G(u, v)$ . Thus, the shortest path between  $u$  and  $v$  lies outside of  $C$ , so  $C$  is not isometric to  $\frac{\lambda}{\pi} \cdot \mathbb{S}^1$ . Instead, the only possibility for  $C$  to be isometric to  $\frac{\lambda}{\pi} \cdot \mathbb{S}^1$  is that  $C \cap A$  is either empty or connected. This implies  $C \subset G_1$  or  $C \subset G_2$ .  $\square$

The next theorem is the main result of this section, and it is a generalization of Example 8.4. In that case,  $G = \frac{\lambda_1}{\pi} \mathbb{S}^1 \cup_{p_0} \frac{\lambda_2}{\pi} \mathbb{S}^1$ , and we showed that if  $X$  has  $t_b(X) < t_d(X)$  then in the worst case, only one point of  $X$  lies outside of either  $\frac{\lambda_1}{\pi} \mathbb{S}^1$  or  $\frac{\lambda_2}{\pi} \mathbb{S}^1$ . We cannot make such a strong statement in general, but the result can still be useful. The idea is similar to Lemma 8.9. We show that if a configuration  $X \subset G_1 \cup_A G_2$  with 4 points has the specific condition  $t_d(X) = 2t_b(X)$  (as opposed to just  $t_b(X) < t_d(X)$ ), then it is contained in either  $G_1$  or  $G_2$ .

**Theorem 8.10.** *Let  $G = G_1 \cup_A G_2$  be a metric gluing of the graphs  $G_1$  and  $G_2$  such that  $A = G_1 \cap G_2$  is a path of length  $\alpha$ . Let  $\ell_j$  be the length of the shortest cycle contained in  $G_j$  that intersects  $A$ , and set  $\ell = \min(\ell_1, \ell_2)$ . Assume that  $\alpha < \frac{\ell}{3}$ . If  $X = \{x_1, x_2, x_3, x_4\} \subset G$  satisfies  $t_b(X) = \lambda/2$  and  $t_d(X) = \lambda$ , then either  $X \subset G_1$  or  $X \subset G_2$ .*

*Proof.* Let  $\gamma_{ij}$  be a shortest path in  $G$  from  $x_i$  to  $x_j$ . Let  $X_1 = X \cap G_1$  and  $X_2 = X \cap G_2$ . We decompose a path  $\gamma$  as  $\gamma^{(1)} \cup \gamma^{(A)} \cup \gamma^{(2)}$ , where  $\gamma^{(i)} \subset G_i$ ,  $\gamma^{(A)} \subset A$  and each intersection  $\gamma^{(i)} \cap \gamma^{(A)}$  is a single point. We will break down the proof depending on the size of  $X_1$  and  $X_2$ .

**Case 0:** If either  $X_1$  or  $X_2$  is empty, the theorem holds immediately.

**Case 1:**  $X_1$  or  $X_2$  is a singleton.

Suppose that  $X_1 = \{x_1\}$  (see Figure 23). Let  $u = \gamma_{21}^{(1)} \cap A$  and  $v = \gamma_{14}^{(1)} \cap A$ . By Lemma 8.9,  $d_G(u, v) < |\gamma_{21}^{(1)}| + |\gamma_{14}^{(1)}|$ . However, if  $\gamma_{uv}$  is a shortest path between  $u$  and  $v$ , then  $\gamma'_{24} = \gamma_{21}^{(2)} \cup \gamma_{21}^{(A)} \cup \gamma_{uv} \cup \gamma_{14}^{(A)} \cup \gamma_{14}^{(2)}$  is a path between  $x_2$  and  $x_4$  such that

$$\begin{aligned} |\gamma'_{24}| &\leq |\gamma_{21}^{(2)}| + |\gamma_{21}^{(A)}| + |\gamma_{uv}| + |\gamma_{14}^{(A)}| + |\gamma_{14}^{(2)}| \\ &< |\gamma_{21}^{(2)}| + |\gamma_{21}^{(A)}| + |\gamma_{21}^{(1)}| + |\gamma_{14}^{(1)}| + |\gamma_{14}^{(A)}| + |\gamma_{14}^{(2)}| \\ &= |\gamma_{21}| + |\gamma_{14}| \\ &= \lambda. \end{aligned}$$

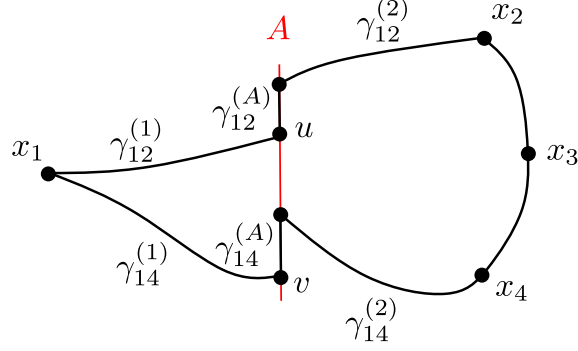


Figure 23: Case 1:  $x_1 \in G_1$  and  $x_2, x_3, x_4 \in G_2$ .

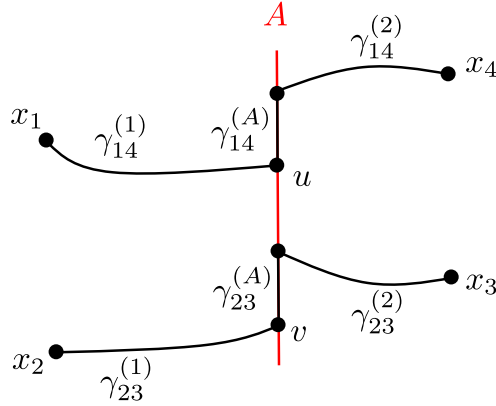


Figure 24: Case 3:  $X_1 = \{x_1, x_2\}$  and  $X_2 = \{x_3, x_4\}$ .

This contradicts the assumption that  $d_G(x_2, x_4) = \lambda$ .

**Case 2:**  $|X_1| = |X_2| = 2$ .

In this case, we have two ways to distribute the points of  $X$ , depending on whether we pair together the points that are at distance  $\lambda/2$  or  $\lambda$ . If we choose the second option, we can write  $X_1 = \{x_1, x_3\}$  and  $X_2 = \{x_2, x_4\}$ . The path  $\gamma_{12} \cup \gamma_{23} \cup \gamma_{31}$  is a cycle in  $G$  that intersects both  $G_1$  and  $G_2$ . Let  $u = \gamma_{12}^{(1)} \cap A$  and  $v = \gamma_{23}^{(1)} \cap A$ , and let  $\gamma_{uv} \subset A$  be a path between them. By Lemma 8.9,  $d_G(u, v) < |\gamma_{12}^{(2)}| + |\gamma_{12}^{(A)}| + |\gamma_{23}^{(2)}| + |\gamma_{23}^{(A)}|$ , so following the reasoning of Case 1,  $\gamma_{12}^{(1)} \cup \gamma_{uv} \cup \gamma_{23}^{(1)}$  is a path between  $x_1$  and  $x_3$  with length less than  $|\gamma_{12}| + |\gamma_{23}| = \lambda$ . This is again a contradiction.

**Case 3:**  $X_1 = \{x_1, x_2\}$  and  $X_2 = \{x_3, x_4\}$ . (See Figure 24)

Let  $u = \gamma_{14}^{(1)} \cap A$ , and  $v = \gamma_{23}^{(1)} \cap A$ . By the triangle inequality,

$$\lambda = d_G(x_1, x_3) \leq d_G(x_1, u) + d_G(u, v) + d_G(v, x_3). \quad (21)$$

Analogously,

$$\lambda \leq d_G(x_2, v) + d_G(v, u) + d_G(u, x_4). \quad (22)$$

On the other hand, since  $\gamma_{23}$  is the shortest path between  $x_2$  and  $x_3$  and it passes through  $v$ ,

$$\lambda/2 = d_G(x_2, x_3) = d_G(x_2, v) + d_G(v, x_3).$$

If there existed a path between  $v$  and  $x_3$  of length smaller than  $d_G(v, x_3)$ , then the concatenation of that path and  $\gamma_{23}^{(1)}$  would give a path between  $x_2$  and  $x_3$  shorter than  $\gamma_{23}$ . The same reasoning applies to  $x_2$  and  $v$ , so the above equality holds. By a similar argument, we get  $\lambda/2 = d_G(x_1, u) + d_G(u, x_4)$ . Adding these two equations gives

$$d_G(x_1, u) + d_G(x_2, v) + d_G(v, x_3) + d_G(u, x_4) = \lambda,$$

and combining this last equation with (21) and (22) produces, respectively,

$$d_G(x_2, v) + d_G(u, x_4) \leq d_G(u, v) \tag{23}$$

$$d_G(x_1, u) + d_G(v, x_3) \leq d_G(v, u). \tag{24}$$

Then, using 24 and 21, we obtain

$$\lambda \leq 2d_G(u, v).$$

Furthermore, since  $u, v \in A$ , we get  $\lambda/2 \leq d_G(u, v) \leq \alpha$ .

Now we further break down case 3 depending on whether  $\gamma_{12}$  and  $\gamma_{34}$  intersect  $A$  or not.

**Case 3.1:** Suppose that  $\gamma_{12}$  intersects  $A$ .

Write  $\gamma_{12} = \gamma_{12}^{(1)} \cup \gamma_{12}^{(A)} \cup \gamma_{12}^{(2)}$ , and let  $w_i = \gamma_{12}^{(i)} \cap \gamma_{12}^{(A)}$ . Let  $\gamma_{w_1}$  be a shortest path between  $u$  and  $w_1$ . By the triangle inequality,

$$|\gamma_{w_1}| = d_G(u, w_1) \leq d_G(u, x_1) + d_G(x_1, w_1) \leq d_G(x_1, x_4) + d_G(x_1, x_2) = \lambda.$$

If  $u \neq w_1$ , then  $\gamma_{14}^{(1)} \cup \gamma_{w_1} \cup \gamma_{12}^{(1)}$  is a cycle that intersects  $A$  of length at most  $2\lambda \leq 2\alpha$ . Then,  $\ell$  is smaller than  $2\alpha$  by definition. However, this is a contradiction because  $3\alpha < \ell$  by hypothesis. Thus,  $w_1 = u$ , and an analogous argument shows that  $w_2 = v$ . Since  $\gamma_{12}$  is a shortest path between  $x_1$  and  $x_2$ ,

$$\begin{aligned} \lambda/2 &= d_G(x_1, x_2) \\ &= d_G(x_1, w_1) + d_G(w_1, w_2) + d_G(w_2, x_2) \\ &= d_G(x_1, u) + d_G(u, v) + d_G(v, x_2) \\ &\geq d_G(u, v) \geq \lambda/2. \end{aligned}$$

Thus,  $x_1 = u$  and  $x_2 = v$ . In other words,  $X_1 \subset A \subset G_2$ , so  $X = X_1 \cup X_2 \subset G_2$ . Naturally, if  $\gamma_{34}$  intersected  $A$  instead of  $\gamma_{12}$ , then an analogous argument would give  $X \subset G_1$ .

**Case 3.2:** Neither  $\gamma_{34}$  nor  $\gamma_{12}$  intersect  $A$  (see Figure 25).

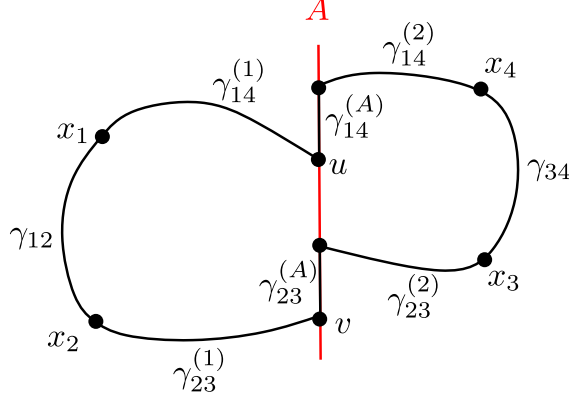


Figure 25: Case 3.2: The paths between points of  $X$  form a cycle in  $G$ .

Once more, let  $u = \gamma_{14}^{(1)} \cap A$ ,  $v = \gamma_{23}^{(1)} \cap A$ , and  $\nu = d_G(u, v)$ . Define the cycles  $C = \gamma_{12} \cup \gamma_{23} \cup \gamma_{34} \cup \gamma_{41}$ ,  $C_1 = \gamma_{12} \cup \gamma_{23}^{(1)} \cup \gamma_{uv} \cup \gamma_{41}^{(1)}$  and  $C_2 = \gamma_{34} \cup \gamma_{41}^{(2)} \cup \gamma_{41}^{(A)} \cup \gamma_{uv} \cup \gamma_{23}^{(A)} \cup \gamma_{23}^{(2)}$ . Set  $L = |C|$  and  $L_j = |C_j|$  for  $j = 1, 2$ . Clearly,  $L = 2\lambda$  and  $L_1 + L_2 - 2\nu = L = 2\lambda$ . For this reason, write  $\lambda = \frac{L_1 + L_2}{2} - \nu$ .

For brevity, let  $\delta_1 = d_G(x_1, u)$ ,  $\delta_2 = d_G(x_2, v)$ ,  $\delta_3 = d_G(x_3, v)$ , and  $\delta_4 = d_G(x_4, u)$ . By definition of  $u$  and  $v$ , we have

$$\lambda/2 = d_G(x_1, x_4) = d_G(x_1, u) + d_G(u, x_4) = \delta_1 + \delta_4, \quad (25)$$

and

$$\lambda/2 = d_G(x_2, x_3) = \delta_2 + \delta_3. \quad (26)$$

Additionally,

$$\begin{aligned} L_1 &= |\gamma_{12}| + |\gamma_{23}^{(1)}| + |\gamma_{uv}| + |\gamma_{14}^{(1)}| \\ &= d_G(x_1, x_2) + d_G(x_2, v) + d_G(u, v) + d_G(u, x_1) \\ &= \lambda/2 + \delta_2 + \nu + \delta_1, \end{aligned} \quad (27)$$

and

$$\begin{aligned} L_2 &= |\gamma_{34}| + |\gamma_{41}^{(2)} \cup \gamma_{41}^{(A)}| + |\gamma_{uv}| + |\gamma_{23}^{(A)} \cup \gamma_{23}^{(2)}| \\ &= d_G(x_3, x_4) + d_G(x_4, u) + d_G(u, v) + d_G(v, x_3) \\ &= \lambda/2 + \delta_4 + \nu + \delta_3. \end{aligned} \quad (28)$$

If we interpret the  $\delta_i$  as variables and  $L_1, L_2, \nu$ , and  $\lambda$  as constants, equations (25) - (28) form a system of 4 equations with 4 variables. It can be seen that the matrix of coefficients has rank 3, so the solution has one parameter. Thus, choosing  $\delta_4 = t$  gives the general

solution

$$\begin{aligned}
\delta_1 &= \lambda/2 - t \\
\delta_2 &= L_1 - \lambda - \nu + t \\
\delta_3 &= L_2 - \lambda/2 - \nu - t \\
\delta_4 &= t.
\end{aligned} \tag{29}$$

This means that there exists a particular number  $0 \leq t \leq \lambda/2$  such that the distances between points of  $X$  and  $u$  and  $v$  are given by the equations above. With this tool at hand, we now claim that at least one of the paths  $\gamma_1 := \gamma_{14}^{(1)} \cup \gamma_{uv} \cup \gamma_{23}^{(A)} \cup \gamma_{23}^{(2)}$  or  $\gamma_2 := \gamma_{14}^{(2)} \cup \gamma_{14}^{(A)} \cup \gamma_{uv} \cup \gamma_{23}^{(1)}$  has length less than  $\lambda$ . This would imply that either  $d_G(x_1, x_3)$  or  $d_G(x_2, x_4)$  is less than  $\lambda$ , violating the assumption that  $t_d(X) = \lambda$ .

An equivalent formulation of the claim is

$$\max_t (\min(|\gamma_1|, |\gamma_2|)) < \lambda. \tag{30}$$

If this inequality holds, then either  $|\gamma_1|$  or  $|\gamma_2|$  is smaller than  $\lambda$ , regardless of the value of  $t$ . Notice, though, that  $|\gamma_1| = \delta_1 + \nu + \delta_3$  and  $|\gamma_2| = \delta_4 + \nu + \delta_2$ . Using the equations in (29), we see that  $|\gamma_1| + |\gamma_2| = L_1 + L_2 - \lambda$  is a quantity independent of  $t$ . Thus, the maximum in (30) is achieved when  $|\gamma_1| = |\gamma_2|$ . This happens when  $t = \frac{1}{4}(L_2 - L_1 + \lambda)$ , and gives

$$|\gamma_1| = \frac{L_1 + L_2}{2} - \nu - \frac{\lambda}{2} = \frac{L_1 + L_2}{4} + \frac{\nu}{2}$$

The claim is that this quantity is less than  $\lambda = \frac{L_1 + L_2}{2} - \nu$ . Solving for  $\nu$  gives the equivalent inequality

$$\nu < \frac{L_1 + L_2}{6}.$$

Recall that  $\gamma_{uv} \subset A$ , the latter of which is a path of length  $\alpha < \frac{\ell}{3}$ , and that  $\ell$  is the length of the smallest cycle contained in either  $G_1$  or  $G_2$  that intersects  $A$ . Since  $C_i \subset G_i$ , we have

$$\nu \leq \alpha < \frac{\ell}{3} \leq \frac{L_1 + L_2}{6},$$

as desired. This forces  $d_G(x_1, x_3) \leq |\gamma_1| < \lambda$ , violating the assumption that  $t_d(X) = \lambda$ . This concludes the proof of Case 3.2, and gives the Theorem.  $\square$

To close up this section, we explore a consequence of Theorem 8.10. Once more, this application is inspired by [AAG<sup>+</sup>20], specifically Proposition 4.1. We will assume that all edges have length 1 for the sake of simplicity.

**Theorem 8.11.** *Let  $T_1, \dots, T_m$  be a set of trees, and for each  $k = 1, \dots, n$ , let  $C_k$  be a cycle of length  $L_k = 2\lambda_k$ . Suppose that all  $\lambda_k$  are distinct. Let  $G$  be a graph formed by iteratively attaching either a tree  $T_i$  or a cycle  $C_k$  along an edge or a vertex. Then, the number of points  $(\lambda/2, \lambda) \in \mathbf{D}_{4,1}^{\text{VR}}(G)$  is equal to the number of cycles  $C_k$  that were attached. Furthermore, if  $X \subset G$  is a set of 4 points such that  $t_b(X) = \lambda/2$  and  $t_d(X) = \lambda$ , then  $X$  is contained in a cycle  $C_k$  and  $L_k = 2\lambda$ .*

*Proof.* First, label the trees and the cycles as  $G_1, G_2, \dots, G_N$  depending on the order that they were attached. Consider a cycle  $C_k$  and denote it as  $G_m$ . Suppose that there is a path  $\gamma$  between  $x, x' \in C_k$  that intersects  $C_k$  only at  $x$  and  $x'$ . We claim that the edge  $[x, x']$  is in  $C_k$ . Otherwise, since we are only attaching graphs at an edge or a vertex, there are two different graphs attached to  $C_k$ , one at  $x$  and one at  $x'$ . However, if we follow  $\gamma$ , we will find a graph that was attached to the previous graphs at two disconnected segments. This contradicts the construction of  $G$ , so  $[x, x']$  is an edge of  $C_k$ . Thus,  $d_G(x, x') < |\gamma|$ . Moreover, the only paths between non-adjacent points  $x, x' \in C_k$  lie in  $C_k$ . Thus,  $C_k$  is isometric to a circle which, as a metric space, has  $\mathbf{diam}_G(C_k) = \lambda_k$ . Then  $(\lambda_k/2, \lambda_k) \in \mathbf{D}_{4,1}^{\text{VR}}(C_k) \subset \mathbf{D}_{4,1}^{\text{VR}}(G)$ .

Now, suppose that there is a point  $(\lambda/2, \lambda) \in \mathbf{D}_{4,1}^{\text{VR}}(G)$  generated by a set  $X \subset G$  with four points. Find the largest  $m$  such that  $X \cap G_m \neq \emptyset$ . By Theorem 8.10, either  $X \subset G_1 \cup \dots \cup G_{m-1}$ , or  $X \subset G_m$ . If  $X$  is not contained in  $G_m$ , we can keep using Theorem 8.10 to remove graphs until we find one that contains  $X$ . Notice that  $X$  cannot be contained in a tree  $T_i$  because of Lemma 8.1, so  $X \subset C_k$  for some  $k$ . Let  $\gamma_i$  be the shortest path between  $x_i$  and  $x_{i+1}$ . Then the sum  $d_G(x_1, x_2) + d_G(x_2, x_3) + d_G(x_3, x_4) + d_G(x_4, x_1)$  equals  $4(\lambda/2) = 2\lambda$  because  $t_b(X) = \lambda/2$ , but also  $L_k$  because the path  $\gamma_1 \cup \gamma_2 \cup \gamma_3 \cup \gamma_4$  is a cycle contained in  $C_k$ . Since  $L_k = 2\lambda_k$ ,  $\lambda = \lambda_k$ .  $\square$

Since the graphs described in Theorem 8.11 are pasted along a contractible space, we can detect the homotopy type of the graph.

**Corollary 8.12.** *Let  $G$  be a graph constructed as in Theorem 8.11. Then the first Betti number of  $G$  equals the number of points  $(\lambda/2, \lambda) \in \mathbf{D}_{4,1}^{\text{VR}}(G)$ .*

*Proof.* Attaching a tree to a graph doesn't change its homotopy type, while attaching a cycle  $C_k$  to  $G_1 \cup \dots \cup G_m$  at a contractible subspace induces  $(G_1 \cup \dots \cup G_m) \cup C_k \simeq (G_1 \cup \dots \cup G_m) \vee C_k$ . Thus, by induction,  $G = C_1 \vee \dots \vee C_n$ . Then  $\beta_1(G) = n$ , and by Theorem 8.11, the values of  $\lambda$  for which  $(\lambda/2, \lambda) \in \mathbf{D}_{4,1}^{\text{VR}}(G)$  are  $\lambda_1, \dots, \lambda_n$ .  $\square$

## 9 Discussion and Questions

Here we outline the open questions and conjectures collected so far.

- **Are there rich classes of compact metric spaces that can be distinguished with persistence sets?**

This question is a generalization of Theorem 8.11 and Corollary 8.12. The persistence set  $\mathbf{D}_{4,1}^{\text{VR}}$  can capture the number and length of cycles in a metric graph  $G$  that was constructed according to the instructions in Theorem 8.11. Are there other families of compact metric spaces where higher order diagrams  $\mathbf{D}_{n,k}^{\text{VR}}$  can detect relevant features? In other words, are there families  $\mathcal{C}$  of compact metric spaces such that

$$\sup_{n,k} d_{\mathcal{H}}^{\mathcal{D}}(\mathbf{D}_{n,k}^{\text{VR}}(X), \mathbf{D}_{n,k}^{\text{VR}}(Y))$$

is a metric when  $X, Y \in \mathcal{C}$ ?

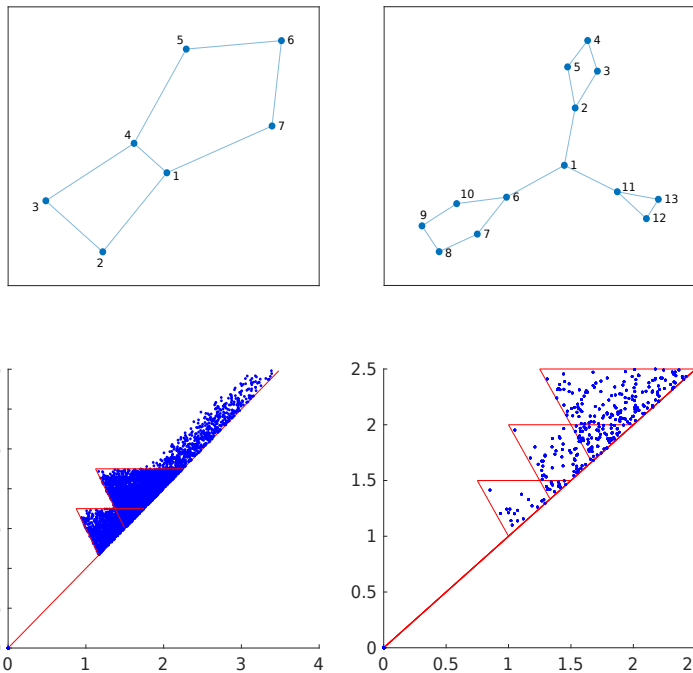


Figure 26: Two examples of admissible graphs  $G$  as in Corollary 8.12 and their persistence set  $\mathbf{D}_{4,1}^{\text{VR}}(G)$ . The red triangles are the boundaries of the sets  $\mathbf{D}_{4,1}^{\text{VR}}(C)$  for every cycle  $C \subset \mathbf{D}_{4,1}^{\text{VR}}(G)$ . Left: Two cycles of lengths  $\ell_1 = 3.5$  and  $\ell_2 = 4.5$  pasted over an edge of length  $\alpha = 0.5 < \frac{1}{3} \min(\ell_1, \ell_2)$ . Right: A tree of cycles. Each persistence set was found by sampling 100,000 uniform configurations from  $G$ .

- **Describe  $\mathbf{D}_{2k+2,k}^{\text{VR}}(\mathbb{S}_E^m)$  for all  $k$  and  $m$ :** Propositions 5.13 and 5.17 are a step in that direction. In fact, the latter implies that we only need to find  $\mathbf{D}_{2k+2,k}^{\text{VR}}(\mathbb{S}_E^{2k})$  to determine  $\mathbf{D}_{2k+2,k}^{\text{VR}}(\mathbb{S}_E^m)$  for all spheres with  $m \geq 2k + 1$ .
- **Stabilization of  $\mathbf{D}_{2k+2,k}^{\text{VR}}(\mathbb{S}_E^n)$ :** When  $k = 1$ , Corollary 5.18 shows that  $\mathbf{D}_{4,1}^{\text{VR}}(\mathbb{S}^m)$  stabilizes at  $m = 2$  instead of  $m = 3$ , as given by Proposition 5.17. The key to the reduction was the use of Ptolemy’s inequality as in Theorem 5.16. A natural follow up question, even if it is subsumed by the previous one, is when does  $\mathbf{D}_{2k+2,k}^{\text{VR}}(\mathbb{S}_E^m)$  really stabilize for general  $k$ .

## References

- [AA17] Michal Adamaszek and Henry Adams. The Vietoris-Rips complexes of a circle. *Pacific Journal of Mathematics*, 290(1):1–40, 2017.
- [AAG<sup>+</sup>20] Michał Adamaszek, Henry Adams, Ellen Gasparovic, Maria Gommel, Emilie Purvine, Radmila Sazdanovic, Bei Wang, Yusu Wang, and Lori Ziegelmeier. On homotopy types of Vietoris-Rips complexes of metric gluings. *Journal of Applied and Computational Topology*, 4(3):425–454, Sep 2020.
- [ACC16] Aaron Adcock, Erik Carlsson, and Gunnar Carlsson. The ring of algebraic functions on persistence bar codes. *Homology, Homotopy and Applications*, 18(1):381–402, 2016.
- [Ada14] Michał Adamaszek. Extremal problems related to Betti numbers of flag complexes. *Discrete Applied Mathematics*, 173:8–15, 2014.
- [AFN<sup>+</sup>18] Pankaj K Agarwal, Kyle Fox, Abhinandan Nath, Anastasios Sidiropoulos, and Yusu Wang. Computing the Gromov-Hausdorff distance for metric trees. *ACM Transactions on Algorithms (TALG)*, 14(2):1–20, 2018.
- [AMJ18] David Alvarez-Melis and Tommi S Jaakkola. Gromov-Wasserstein alignment of word embedding spaces. *arXiv preprint arXiv:1809.00013*, 2018.
- [AW20] Josh Alman and Virginia Vassilevska Williams. A refined laser method and faster matrix multiplication. *arXiv preprint arXiv:2010.05846*, 2020.
- [Bau19] Ulrich Bauer. Ripser: efficient computation of Vietoris-Rips persistence barcodes, 2019. Software available at <http://ripser.org/>.
- [BBBK08] Alexander M Bronstein, Michael Bronstein, Michael M Bronstein, and Ron Kimmel. *Numerical geometry of non-rigid shapes*. Springer, 2008.
- [BBI01] Dmitri Burago, Yuri Burago, and Sergei Ivanov. *A Course in Metric Geometry*, volume 33 of *Graduate Studies in Mathematics*. American Mathematical Society, 2001.

- [BCM<sup>+</sup>20] Andrew J Blumberg, Mathieu Carriere, Michael A Mandell, Raul Rabadan, and Soledad Villar. MREC: a fast and versatile framework for aligning and matching point clouds with applications to single cell molecular data. *arXiv preprint arXiv:2001.01666*, 2020.
- [BD92] Hans-Jürgen Bandelt and Andreas W.M Dress. A canonical decomposition theory for metrics on a finite set. *Advances in Mathematics*, 92(1):47–105, 1992.
- [BFW09] S. M. Buckley, K. Falk, and D. J. Wraith. Ptolemaic spaces and CAT(0). *Glasgow Mathematical Journal*, 51(2):301–314, 2009.
- [BGMP12] Andrew J Blumberg, Itamar Gal, Michael A Mandell, and Matthew Pancia. Robust statistics, hypothesis testing, and confidence intervals for persistent homology on metric measure spaces. *arXiv preprint arXiv:1206.4581*, 2012.
- [BGMP14] Andrew J Blumberg, Itamar Gal, Michael A Mandell, and Matthew Pancia. Robust statistics, hypothesis testing, and confidence intervals for persistent homology on metric measure spaces. *Foundations of Computational Mathematics*, 14(4):745–789, 2014.
- [BHPW20] Peter Bubenik, Michael Hull, Dhruv Patel, and Benjamin Whittle. Persistent homology detects curvature. *Inverse Problems*, 36(2):025008, jan 2020.
- [BK04a] Mireille Boutin and Gregor Kemper. On reconstructing  $n$ -point configurations from the distribution of distances or areas. *Adv. in Appl. Math.*, 32(4):709–735, 2004.
- [BK04b] Mireille Boutin and Gregor Kemper. On reconstructing  $n$ -point configurations from the distribution of distances or areas. *Advances in Applied Mathematics*, 32(4):709 – 735, 2004.
- [Car14] Gunnar Carlsson. Topological pattern recognition for point cloud data. *Acta Numerica*, 23:289–368, 2014.
- [CCM<sup>+</sup>20] Samir Chowdhury, Nathaniel Clause, Facundo Mémoli, Jose Ángel Sánchez, and Zoe Wellner. New families of stable simplicial filtration functors. *Topology and its Applications*, 279:107254, 2020.
- [CCR13] Joseph Minhow Chan, Gunnar Carlsson, and Raul Rabadan. Topology of viral evolution. *Proceedings of the National Academy of Sciences*, 110(46):18566–18571, 2013.
- [CCSG<sup>+</sup>09] F. Chazal, D. Cohen-Steiner, L. Guibas, F. Mémoli, and S. Oudot. Gromov-Hausdorff stable signatures for shapes using persistence. In *Proc. of SGP*, 2009.
- [CdS10] Gunnar Carlsson and Vin de Silva. Zigzag persistence. *Foundations of Computational Mathematics*, 10(4):367–405, August 2010.

- [CFL<sup>+</sup>14] Frédéric Chazal, Brittany Fasy, Fabrizio Lecci, Bertrand Michel, Alessandro Rinaldo, and Larry Wasserman. Subsampling methods for persistent homology, 2014.
- [CFL<sup>+</sup>15] Frédéric Chazal, Brittany Fasy, Fabrizio Lecci, Bertrand Michel, Alessandro Rinaldo, and Larry Wasserman. Subsampling methods for persistent homology. In *International Conference on Machine Learning*, pages 2143–2151. PMLR, 2015.
- [CM08] Gunnar Carlsson and Facundo Mémoli. Persistent clustering and a theorem of J. Kleinberg. *arXiv preprint arXiv:0808.2241*, 2008.
- [CM10a] Gunnar Carlsson and Facundo Mémoli. Characterization, stability and convergence of hierarchical clustering methods. *Journal of Machine Learning Research*, 11:1425–1470, 2010.
- [CM10b] Gunnar Carlsson and Facundo Mémoli. Characterization, stability and convergence of hierarchical clustering methods. *J. Mach. Learn. Res.*, 11:1425–1470, August 2010.
- [COS<sup>+</sup>98] Eugenio Calabi, Peter J Olver, Chehrzad Shakiban, Allen Tannenbaum, and Steven Haker. Differential and numerically invariant signature curves applied to object recognition. *International Journal of Computer Vision*, 26(2):107–135, 1998.
- [CSEH07] David Cohen-Steiner, Herbert Edelsbrunner, and John Harer. Stability of persistence diagrams. *Discrete & Computational Geometry*, 37(1):103–120, January 2007.
- [DSS<sup>+</sup>20] Pinar Demetci, Rebecca Santorella, Bjorn Sandstede, William Stafford Noble, and Ritambhara Singh. Gromov-Wasserstein optimal transport to align single-cell multi-omics data. *BioRxiv*, 2020.
- [EH10] Herbert Edelsbrunner and John Harer. *Computational Topology: An Introduction*. January 2010.
- [ELZ00] H. Edelsbrunner, D. Letscher, and A. Zomorodian. Topological persistence and simplification. In *Proc. 41st Ann. IEEE Sympos. Found Comput. Sci.*, pages 454–463, 2000.
- [Fro90a] P. Frosini. A distance for similarity classes of submanifolds of Euclidean space. *Bull. Austral. Math. Soc.*, 42:3:407–416, 1990.
- [Fro90b] P. Frosini. *Omotopie e invarianti metrici per sottovarietà di spazi euclidei (teoria della taglia)*. PhD thesis, University of Florence, Italy., 1990.

- [Fro99] Patrizio Frosini. Metric homotopies. *Atti Sem. Mat. Fis. Univ. Modena*, 47(2):271–292, 1999.
- [Ghr08] R. Ghrist. Barcodes: The persistent topology of data. *Bulletin-American Mathematical Society*, 45(1):61, 2008.
- [GM21] Mario Gómez and Facundo Mémoli. Github repo for: Curvature sets over persistence diagrams, 2021. <https://github.com/ndag/persistence-curv-sets>.
- [Gro87] M. Gromov. Hyperbolic groups. In *Essays in group theory*, volume 8 of *Math. Sci. Res. Inst. Publ.*, pages 75–263. Springer, New York, 1987.
- [Gro07] Misha Gromov. *Metric Structures for Riemannian and non-Riemannian Spaces*. Modern Birkhäuser Classics. Birkhäuser Boston Inc, Boston, MA, 2007.
- [Kah09] Matthew Kahle. Topology of random clique complexes. *Discrete Mathematics*, 309(6):1658–1671, 2009.
- [Kal19] Sara Kališnik. Tropical coordinates on the space of persistence barcodes. *Foundations of Computational Mathematics*, 19(1):101–129, Feb 2019.
- [Kat91] Mikhail Katz. On neighborhoods of the Kuratowski imbedding beyond the first extremum of the diameter functional. *Fundamenta Mathematicae*, 137(3):161–175, 1991.
- [KM21] Sakura Kawano and Jeremy K Mason. Classification of atomic environments via the Gromov-Hausdorff-Wasserstein distance. *Computational Materials Science*, 188:110144, 2021.
- [LMO20] Sunhyuk Lim, Facundo Memoli, and Osman Berat Okutan. Vietoris-Rips persistent homology, injective metric spaces, and the filling radius. *arXiv preprint arXiv:2001.07588*, 2020.
- [LMS21] Sunhyuk Lim, Facundo Mémoli, and Zane Smith. The Gromov-Hausdorff distance between spheres, 2021.
- [Mém05] Facundo Mémoli. *Estimation Of Distance Functions And Geodesics And Its Use For Shape Comparison And Alignment: Theoretical And Computational Results*. PhD thesis, Electrical and Computer Engineering Department, University of Minnesota, May 2005.
- [Mém07] Facundo Mémoli. On the use of Gromov-Hausdorff distances for shape comparison. In *Proceedings of Point Based Graphics 2007*, Prague, Czech Republic, 2007.
- [Mém11] Facundo Mémoli. Gromov-Wasserstein distances and the metric approach to object matching. *Foundations of Computational Mathematics*, 11(4):417–487, August 2011.

- [Mém12a] Facundo Mémoli. Curvature sets over persistence diagrams, 2012. Banff 2012: <http://webfiles.birs.ca/events/2012/5-day-workshops/12w5081/videos/watch/201210161051-Memoli.html>.
- [Mém12b] Facundo Mémoli. Some properties of Gromov-Hausdorff distances. *Discrete & Computational Geometry*, 48(2):416–440, September 2012.
- [Mém13a] Facundo Mémoli. Curvature sets over persistence diagrams, 2013. ACAT 2013. Bremen: [https://www.alta.uni-bremen.de/ACAT13/ACAT13\\_abstracts.pdf](https://www.alta.uni-bremen.de/ACAT13/ACAT13_abstracts.pdf).
- [Mém13b] Facundo Mémoli. Curvature sets over persistence diagrams, 2013. Bedlewo 2013: <http://bcc.impan.pl/13AppTop/>.
- [Mém14a] Facundo Mémoli. Curvature sets over persistence diagrams, 2014. IMA 2014: <https://www.ima.umn.edu/2013-2014/W10.7-11.13/14513>.
- [Mém14b] Facundo Mémoli. Curvature sets over persistence diagrams, 2014. SAMSI 2014: <https://www.samsi.info/programs-and-activities/research-workshops/2013-14-ldhd-topological-data-analysis-february-3-7-2014/>.
- [Mém14c] Facundo Mémoli. Curvature sets over persistence diagrams, 2014. SAMSI 2014: <https://people.math.osu.edu/memolitechera.1/talks/talk-dgh-rips.pdf>.
- [Mém17] Facundo Mémoli. A distance between filtered spaces via tripods. *arXiv preprint arXiv:1704.03965*, 2017.
- [MMS11] Nikola Milosavljević, Dmitriy Morozov, and Primoz Skraba. Zigzag persistent homology in matrix multiplication time. In *Proceedings of the Twenty-Seventh Annual Symposium on Computational Geometry*, SoCG '11, page 216–225, New York, NY, USA, 2011. Association for Computing Machinery.
- [MN18] Facundo Mémoli and Tom Needham. Distance distributions and inverse problems for metric measure spaces. *arXiv preprint arXiv:1810.09646*, 2018.
- [MNO21] F. Mémoli, T. Needham, and P. J. Olver. Generalized shape distributions and the Gromov-Wasserstein distance (in preparation). 2021.
- [MO18] Facundo Memoli and Osman Berat Okutan. Metric graph approximations of geodesic spaces, 2018.
- [MP20] Facundo Mémoli and Guilherme Vituri F. Pinto. Motivic clustering schemes for directed graphs. *arXiv preprint arXiv:2001.00278*, 2020.
- [MS04] Facundo Mémoli and Guillermo Sapiro. Comparing point clouds. In *SGP '04: Proceedings of the 2004 Eurographics/ACM SIGGRAPH symposium on Geometry processing*, pages 32–40, New York, NY, USA, 2004. ACM.

- [MS05] Facundo Mémoli and Guillermo Sapiro. A theoretical and computational framework for isometry invariant recognition of point cloud data. *Found. Comput. Math.*, 5(3):313–347, 2005.
- [MSW19] Facundo Mémoli, Zane Smith, and Zhengchao Wan. Gromov-Hausdorff distances on  $p$ -metric spaces and ultrametric spaces. *arXiv preprint arXiv:1912.00564*, 2019.
- [Mug19] Delio Mugnolo. What is actually a metric graph?, 2019.
- [MZ19] Facundo Mémoli and Ling Zhou. Persistent homotopy groups of metric spaces. *arXiv preprint arXiv:1912.12399*, 2019.
- [Olv01] P.J. Olver. Joint invariant signatures. *Foundations of computational mathematics*, 1(1):3–68, 2001.
- [PC<sup>+</sup>19] Gabriel Peyré, Marco Cuturi, et al. Computational optimal transport: With applications to data science. *Foundations and Trends<sup>®</sup> in Machine Learning*, 11(5-6):355–607, 2019.
- [PCS16] Gabriel Peyré, Marco Cuturi, and Justin Solomon. Gromov-Wasserstein averaging of kernel and distance matrices. In *International Conference on Machine Learning*, pages 2664–2672. PMLR, 2016.
- [Rob99] Vanessa Robins. Towards computing homology from finite approximations. In *Topology Proceedings 1999*, 1999.
- [Sch17] Felix Schmedl. Computational aspects of the Gromov-Hausdorff distance and its application in non-rigid shape matching. *Discrete & Computational Geometry*, 57(4):854–880, Jun 2017.
- [SMI<sup>+</sup>08] Gurjeet Singh, Facundo Memoli, Tigran Ishkhanov, Guillermo Sapiro, Gunnar Carlsson, and Dario L Ringach. Topological analysis of population activity in visual cortex. *Journal of vision*, 8(8):11–11, 2008.
- [SWB21] Elchanan Solomon, Alexander Wagner, and Paul Bendich. From geometry to topology: Inverse theorems for distributed persistence, 2021.
- [Val70a] J. E. Valentine. An analogue of Ptolemy’s theorem in spherical geometry. *The American Mathematical Monthly*, 77(1):47–51, 1970.
- [Val70b] Joseph E. Valentine. An analogue of Ptolemy’s theorem and its converse in hyperbolic geometry. 1970.
- [VCF<sup>+</sup>20] Titouan Vayer, Laetitia Chapel, Rémi Flamary, Romain Tavenard, and Nicolas Courty. Fused Gromov-Wasserstein distance for structured objects. *Algorithms*, 13(9):212, 2020.

- [Vil03] Cédric Villani. *Topics in optimal transportation*, volume 58 of *Graduate Studies in Mathematics*. American Mathematical Society, Providence, RI, 2003.
- [Wei11] Shmuel Weinberger. What is... persistent homology? *Notices of the AMS*, 58(1):36–39, 2011.
- [ZC04] Afra Zomorodian and Gunnar Carlsson. Computing persistent homology. In *SCG '04: Proceedings of the twentieth annual symposium on Computational geometry*, pages 347–356, New York, NY, USA, 2004. ACM.